

## CHAOS FROM SYMMETRY

*Navier Stokes equations, Beltrami fields and  
the Universal Classifying Crystallographic Group*<sup>1</sup>Pietro G. Fré<sup>a,c,d</sup> and Mario Trigiantè<sup>b,c,d</sup><sup>a</sup>*Dipartimento di Fisica, Università di Torino  
via P. Giuria 1, 10125 Torino, Italy*<sup>b</sup>*DISAT Politecnico di Torino,  
C.so Duca degli Abruzzi, 24, I-10129 Torino, Italy*<sup>c</sup>*INFN – Sezione di Torino*<sup>(d)</sup> *Arnold-Regge Center***Abstract**

The core of this paper is the group-theoretical approach, initiated in 2015 by one of the present authors in collaboration with Alexander Sorin brings into the classical field of mathematical fluid-mechanics a brand new vision, allowing for a more systematic classification and algorithmic construction of Beltrami flows on torii  $\mathbb{R}^3/\Lambda$  where  $\Lambda$  is a crystallographic lattice. Here this new hydro-theory is based on the focal idea of a Universal Classifying Group  $\mathcal{UC}_\Lambda$  is revised, reorganized, improved and extended. In particular, we construct the so far missing  $\mathcal{UC}_{\Lambda_{Hex}}$  for the hexagonal lattice and we advocate that, mastering the cubic and hexagonal instances of this group, we can cover all cases. The relation between the classification of Beltrami Flows with that of contact structures is enlightened. The recent developments about the framework of  $\mathfrak{b}$ -manifolds are considered and it is shown that the choice of the allowed critical surfaces for the  $\mathfrak{b}$ -deformation of a Beltrami field seems to be strongly related with the group-theoretical structure of the latter. This opens new directions of investigation about a group theoretical classification of critical surfaces. Apart from that the most promising research direction opened by the present work streams from the fact that the Fourier series expansion of a generic Navier-Stokes solution can be regrouped into an infinite sum of contributions  $\mathbf{W}_r$ , each associated with a spherical layer of quantized radius  $r$  in the momentum lattice. Each  $\mathbf{W}_r$  is the superposition of a Beltrami field  $\mathbf{W}_r^+$  plus an anti-Beltrami field  $\mathbf{W}_r^-$ . These latter have a priori exactly the same decomposition into irreps of the group  $\mathcal{UC}_\Lambda$  that are variously repeated on higher layers. This crucial property enables the construction of generic Fourier series with prescribed hidden symmetries as candidate solutions of the NS equations. Alternatively the Fourier series representation of known solutions can be analyzed from the point of view of such symmetries. As a further result of this research programme a complete and versatile system of MATHEMATICA Codes named **AlmafluidaNSPsystem** has been constructed and is now available through the site of the Wolfram Community. The exact solutions presented in this paper have to be considered as an illustration of the new conceptions and ideas that have emerged and of what can be further done utilizing the computer codes as an instrument. The main message streaming from our

---

<sup>1</sup>This article presents the new original results of an investigation performed within the framework of the Project ALMA FLUIDA, cofinanced by the Regione Toscana, in connection with the Consultancy Contract signed between the Company ITALMATIC Presse e Stampi and the DISAT of Torino Politecnico. It focuses on the theoretical aspects. The calculational **AlmafluidaNSPsystem** written in Wolfram MATHEMATICA language finalized to the explicit construction of Beltrami fields and to the analysis of their group theoretical structure is posted on the Wolfram Community site and can be downloaded from there.

constructions is that the more symmetric the Beltrami Flow the highest is the probability of the onset of chaotic trajectories.

# Contents

<b>1</b>	<b>Introduction</b>	<b>4</b>
<b>2</b>	<b>The Navier Stokes Equations and their elaboration</b>	<b>5</b>
2.1	Rewriting of the equations of hydrodynamics in a geometrical set up . . . . .	8
2.1.1	Foliations . . . . .	10
2.1.2	Arnold theorem . . . . .	10
2.2	The path leading to contact geometry . . . . .	11
<b>3</b>	<b>Geometrical Foundations</b>	<b>13</b>
3.1	Contact Geometry . . . . .	13
3.1.1	Contact structures . . . . .	13
3.1.2	Integrability and Frobenius Theorem . . . . .	15
3.1.3	Isotropic submanifolds of a contact manifold and non integrability . . . . .	15
3.1.4	Contact structures in $D = 3$ and hydro-flows . . . . .	17
3.1.5	Relation with Beltrami vector fields . . . . .	17
3.1.6	Darboux's theorem . . . . .	19
3.2	$\mathfrak{b}$ -Contact Geometry and Singular Beltrami Fields . . . . .	19
3.2.1	Symplectic and Poisson Manifolds . . . . .	20
3.2.2	Relation between symplectic and contact manifolds . . . . .	21
3.2.3	$\mathfrak{b}$ -Manifolds . . . . .	21
<b>4</b>	<b>Harmonic Analysis and the Algorithm</b>	<b>23</b>
4.1	Beltrami equation and harmonic analysis . . . . .	23
4.1.1	Harmonic analysis on the $T^3$ torus and the Universal Classifying Group . . . . .	24
4.1.2	The classical ABC flows . . . . .	26
4.2	The spectrum of the $\star\mathbf{d}$ operator on $T^3$ . . . . .	26
4.3	Fourier expansions and Beltrami chirality . . . . .	27
4.4	The algorithm to construct Arnold Beltrami Flows . . . . .	31
<b>5</b>	<b>Group Theory Foundations</b>	<b>33</b>
5.1	The cubic lattice and the octahedral point group $O_{24}$ . . . . .	33
5.1.1	Structure of the Octahedral Group $O_{24} \sim S_4$ . . . . .	34
5.1.2	Irreducible representations of the Octahedral Group . . . . .	35
5.1.3	$D_1$ : the identity representation . . . . .	35
5.1.4	$D_2$ : the quadratic Vandermonde representation . . . . .	36
5.1.5	$D_3$ : the two-dimensional representation . . . . .	36
5.1.6	$D_4$ : the three-dimensional defining representation . . . . .	36
5.1.7	$D_5$ : the three-dimensional unoriented representation . . . . .	36
5.2	The hexagonal lattice and the dihedral group $Dih_6$ . . . . .	37
5.2.1	The hexagonal lattice . . . . .	37
5.2.2	The point group $Dih_6$ . . . . .	38
5.2.3	Irreducible representations of the dihedral group $Dih_6$ and the character table . . . . .	39
5.2.4	$D_1$ : the identity representation . . . . .	41
5.2.5	$D_2$ : the second one-dimensional representation . . . . .	41

5.2.6	$D_3$ : the third one-dimensional representation . . . . .	41
5.2.7	$D_4$ : the fourth one-dimensional representation . . . . .	42
5.2.8	$D_5$ : the first two-dimensional representation . . . . .	42
5.2.9	$D_6$ : the second two-dimensional representation . . . . .	42
5.3	Extensions of the Point Group with translations and the Universal Classifying Group . . . . .	43
5.3.1	Group extensions . . . . .	43
5.3.2	The exact sequence for space groups and the inhomogeneous group $\mathfrak{I}p_\Lambda$ . . . . .	44
5.3.3	Frobenius congruences . . . . .	46
5.3.4	Frobenius congruences for the Octahedral Group $O_{24}$ . . . . .	47
5.3.5	The Universal Classifying Group for the cubic lattice: $G_{1536}$ . . . . .	49
5.3.6	Structure of the $G_{1536}$ group and derivation of its irreps . . . . .	50
5.3.7	Derivation of $G_{1536}$ irreps . . . . .	51
5.4	Classification of the 48 sublattices of the momentum lattice and the irreps of $G_{1536}$ . . . . .	52
5.4.1	Orbits of length 6 . . . . .	52
5.4.2	Orbits of length 8 . . . . .	52
5.4.3	Orbits of length 12 . . . . .	53
5.4.4	Orbits of length 24 . . . . .	54
5.4.5	Classification of the 48 types of orbits . . . . .	54
5.4.6	The 48 orbits type and the irreps of the Universal Classifying Group . . . . .	56
5.4.7	Classes of momentum vectors yielding orbits of length 6: $\{a,0,0\}$ . . . . .	56
5.4.8	Classes of momentum vectors yielding orbits of length 8: $\{a,a,a\}$ . . . . .	57
5.4.9	Classes of momentum vectors yielding orbits of length 12: $\{0,a,a\}$ . . . . .	57
5.4.10	Classes of momentum vectors yielding orbits of length 24: $\{a,a,b\}$ . . . . .	57
5.4.11	Classes of momentum vectors yielding point orbits of length 24 and $G_{1536}$ representations of dimensions 48: $\{a,b,c\}$ . . . . .	59
5.4.12	The interpretation of the 48 momentum classes as sublattices of the cubic lattice . . . . .	60
5.5	The universal classifying group $\mathfrak{U}_{72}$ for the Hexagonal Lattice $\Lambda_{Hex}$ . . . . .	60
5.5.1	Frobenius congruences for $Dih_6$ . . . . .	61
5.5.2	Structure and irreps of $\mathfrak{U}_{72}$ . . . . .	63
5.5.3	The auxiliary four dimensional representation of $\mathfrak{U}_{72}$ . . . . .	64
5.5.4	Irreducible representations and the character table of $\mathfrak{U}_{72}$ . . . . .	65
5.6	Classification of orbits of the point group $Dih_6$ in the momentum lattice . . . . .	65
5.6.1	Orbits of length 2 . . . . .	65
5.6.2	Orbits of length 6 . . . . .	66
5.6.3	Orbits of length 12 of type 1 . . . . .	67
5.6.4	Orbits of length 12 of type 2 . . . . .	67
5.6.5	Orbits of length 12 of type 3 . . . . .	69
5.6.6	Orbits of length 12 of type 4 . . . . .	70
<b>6</b>	<b>Group Theory and <math>\mathfrak{b}</math>-Beltrami fields</b> . . . . .	<b>70</b>
6.1	The Euler equations in a $\mathfrak{b}$ -three-manifold and the ABC model as a test ground . . . . .	70
6.1.1	The appropriate geometrical rewriting of Euler equations on general three-manifolds . . . . .	71
6.1.2	The $b$ -deformation of the ABC-model . . . . .	71
6.2	Group theoretical interpretation of the ABC flows . . . . .	73
6.2.1	The $(A, A, A)$ -flow invariant under $GS_{24}$ . . . . .	75

6.3	Chains of subgroups and the flows $(A, B, 0)$ , $(A, A, 0)$ and $(A, 0, 0)$ . . . . .	77
6.3.1	The $(A, B, 0)$ case and its associated chain of subgroups . . . . .	77
6.4	Temporary Conclusion . . . . .	80
6.4.1	A look at the streamlines of the $b$ -deformed $AB0$ -model . . . . .	81
<b>7</b>	<b>The Landscape Conception with Examples</b>	<b>82</b>
7.1	Beltrami equation and generalized steady flows . . . . .	82
7.2	The landscape conception . . . . .	83
7.3	Sketches of the cubic and hexagonal landscapes . . . . .	84
7.3.1	The cubic landscape . . . . .	84
7.3.2	An example of Chaos from symmetry from the cubic lattice . . . . .	84
7.3.3	The hexagonal landscape . . . . .	84
7.4	An example of chaos from symmetry in the hexagonal landscape . . . . .	85
7.4.1	Choice of the $\mathfrak{U}_{72}$ invariant subspace . . . . .	87
7.5	A vertical motion . . . . .	89
<b>8</b>	<b>Conclusions</b>	<b>90</b>

# 1 Introduction

The present paper is at the same time a research paper and partially a review one since its basic aim is the development of an entirely new and original theory of periodic incompressible hydro-flows that was initiated seven years ago by one of the present authors in collaboration with Aleksander S. Sorin [1]. The core of this new theory consists of the introduction in the context of three-dimensional crystallographic groups, of a new general and well defined concept, namely that of the **Universal Classifying Group**  $\mathfrak{U}\mathfrak{G}_\Lambda$ . As it will become clear in the course of our exposition (see in particular section 5)  $\mathfrak{U}\mathfrak{G}_\Lambda$  is essentially defined as the smallest finite group that contains, as possible subgroups, all the **space groups**  $\mathfrak{G}_\Lambda^{space}$  associated with the **point group**  $\mathfrak{P}_\Lambda$  of a specific lattice  $\Lambda$ . The reason why this group is relevant for hydro-flows is that solutions of Beltrami equation can be systematically constructed on the three torus  $\mathbb{R}^3/\Lambda$ , utilizing the decomposition into  $\mathfrak{P}_\Lambda$ -orbits of the dual momentum lattice  $\Lambda^*$ . The obtained solutions are the appropriate generalization to an exhaustive finite family of building blocks of the ABC models that pertain only to the smallest point group orbit of the cubic lattice (the six dimensional one) and are moreover a special truncation thereof. The fascinating discovery pointed out in [1] is that the classification of these building block Beltrami fields is naturally organized into irreducible representations of the group  $\mathfrak{U}\mathfrak{G}_\Lambda$  (see in particular section 5.4). Although it was already clear in 2015 that the unveiled hidden symmetry structure of Beltrami fields was a prominent new weapon in the study of hydro-flows, the development of this new group-based theory of hydrodynamics stopped at the level of the systematic construction of Beltrami fields for the cubic lattice, the other maximal lattice, the hexagonal one, being only touched upon, and, most significantly, the general scheme of utilization of the group theoretical weapon in the context of true solutions of Navier-Stokes equations being not envisaged.

The development of such a new theory is re-addressed in the present paper from scratch in view of three critical observations that open the road to a wealth of systematic new studies:

- A) On each spherical layer (or energy shell)  $SL_r$  of the momentum lattice (see in particular section 4.3) the contribution  $\mathbf{U}_r$  to the Fourier development of a generic Navier-Stokes velocity field  $\mathbf{U}$  is always partitioned into the sum of Beltrami field  $\mathbf{U}_r^+$  (eigenstate of the Beltrami operator with positive eigenvalue  $\pi r$ ) and an anti-Beltrami field  $\mathbf{U}_r^-$  (eigenstate of the Beltrami operator with negative eigenvalue  $-\pi r$ )
- B) The group theoretical structure of Beltrami and anti Beltrami fields is identical so that the decomposition into irreducible representations of the Universal Classifying group can be applied to the complete Fourier development of a generic velocity field.
- C) It appears from old results [2] which made no reference to the, at that time unknown,  $\mathfrak{U}\mathfrak{G}_\Lambda$  group structure, that the Beltrami modes are weakly interacting and that the so named Beltrami spectrum is almost conserved (see section 4.3)

Since paper [1] was mostly disregarded by the reference scientific community and, more relevantly, since the conceptual perspective is now deeply changed and the framing of derivations has been substantially improved and clarified, we decided to present the new results together with the old ones of [1] in a unified exposition, logically organized around the pivot of the new ideas presented above. Specifically the new results are:

1. The derivation of the Universal Class Group  $\mathfrak{U}_{72}$  for the hexagonal lattice case, the construction of its irreps and character table.
2. The development of the construction algorithm of Beltrami/anti-Beltrami fields for all the orbits of  $\Lambda_{hexag}^*$ .

3. The development of the decomposition algorithm of Beltrami/antiBeltrami fields into irreps of  $\mathfrak{U}_{72}$  and subgroups thereof.
4. The inspection of some examples of Beltrami flows, both in the cubic and hexagonal lattice case, that are endowed with large groups of hidden symmetries. These examples confirm the general idea of *Chaos from Symmetry* since the streamlines appear more chaotic wider is the hidden symmetry.

In view of the three critical observations exposed above, since the hidden symmetries of Beltrami fields can be extrapolated to generic Fourier expansions, the search for quasi chaotic trajectories or streamlines is now liable to be established in much more general setups.

Just only in order to further emphasize the role of the hidden symmetries, we have also considered the recent interesting results concerning the extension of Beltrami equation to so named *b*-manifolds. Our attention was captured by the result of [3] where *b*-deformation of the classical ABC-models was studied and it was shown that the deformation, by means of the introduction of two critical surfaces on the torus, can be done only if the parameter that is named *C* in our normalizations, vanishes. The previous group-theoretical analysis of the ABC models presented in [1] and repeated here for completeness was invoked in order to unveil the group theoretical meaning of the condition  $C = 0$ . We refer the reader to section 6 for all the details. The message is very clear and worth of systematic investigation. The ABC models, that for several decades have been the focus of a lot of attention, are just only, in their own functional definition, the tip of an iceberg. They encode half of the 6-parameter Beltrami field obtained from the lowest lying 6-dimensional orbit of the cubic lattice point group  $O_{24}$  which provides a precise irreducible representation of the relevant Universal Classifying Group. The splitting into two halves is obtained by decomposing this 6-dimensional irrep with respect to a proper subgroup that admits a three-dimensional irrep corresponding to the A,B,C parameters. The nullification of the C-parameter corresponds to choosing a further subgroup with respect to which C is a singlet. This reveals that *b*-deformations are in correspondence with subgroups of  $\mathfrak{UG}_\Lambda$ . Clarifying in a full-fledged manner such a correspondence is a research plan that some-one should address. From the point of view of the present article this is just an interesting side issue which by no means constitutes the goal and the core of the paper. Notwithstanding this, in order to present this lateral issue while keeping the paper readable for a mixed community of readers that hopefully, besides symplectic geometers includes also general relativists, supergravity/string theorists (as we are), group theorists and also fluid-mechanics experts working with CFD simulations, we had to provide some schematic but essential background on contact structures, symplectic manifolds and all that, in order to introduce the notion of *b*-deformations. This is done in section 3. Finally we should also mention that one of the main connected achievement of the present investigation project has been the construction in Wolfram MATHEMATICA language of the **AlmafluidaNSPsystem** published on the Wolfram community site at <https://community.wolfram.com/groups/-/m/t/2555905>. This code system is able to construct Beltrami and anti-Beltrami fields on any spherical momentum space layer, decompose them into irreps of any chosen hidden symmetry group, integrate the corresponding stream lines and plot them graphically. Hence this system provides the building blocks for further studies in the various theoretical directions emerged from the development of this new group-based theory of incompressible fluid-dynamics.

## 2 The Navier Stokes Equations and their elaboration

Our primary object of study is the fundamental equation of classical hydrodynamics of an *ideal, incompressible, viscous fluid* subject to some external forces, namely the Navier Stokes equation in three dimensional Euclidian

space  $\mathbb{R}^3$ , which, in our adopted notation, reads as follows:

$$\frac{\partial}{\partial t} \mathbf{u} + \mathbf{u} \cdot \nabla \mathbf{u} = -\nabla p + \nu \Delta \mathbf{u} + \mathbf{f} \quad ; \quad \nabla \cdot \mathbf{u} = 0 \quad (2.1)$$

In equation (2.1),  $\mathbf{u} = \mathbf{u}(x, t)$  denotes the local velocity field,  $p(\mathbf{x}, t)$  denotes the local pressure field,  $\nu$  is viscosity and  $\mathbf{f}$  is the external force, if it is introduced. The symbol  $\Delta = \sum_{i=1}^3 \frac{\partial^2}{\partial x_i^2}$  stands for the standard laplacian. In vector notation eq. (2.1) takes the following form:

$$\frac{\partial}{\partial t} u^i + u^j \partial_j u^i = -\partial^i p + \nu \Delta u^i + f^i \quad ; \quad \partial^\ell u_\ell = 0 \quad (2.2)$$

and admits some straightforward rewriting that, notwithstanding the kinder-garden arithmetic involved in its derivation, is at the basis of several profound and momentous theoretical developments which have kept the community of dynamical system theorists busy for already fifty years [4, 5, 6, 7, 8, 9, 10, 11, 12, 13, 14, 15, 16, 17].

Here we aim at extending to the case where  $\nu \neq 0$  previous results applying to the case of null viscosity, namely to Euler equation. The scope, however, is more ample since, as we already anticipated, we introduce a more direct reference to contact structures and to the recent developments occurred in this field of mathematics, where the notion of *singular contact structures* has been introduced [3, 18, 19, 20, 21, 22, 23, 24] to account, in particular for boundaries of a certain type (cylindrical ends), which are potentially momentous for some applications.

The core of our paper is the group-theoretical approach, initiated in [1] that brings into the classical field of mathematical fluid-mechanics a brand new vision allowing for a more systematic classification and algorithmic construction of the so named Beltrami flows, providing new insight into their properties. Combining the group theoretical classification of Beltrami (anti-Beltrami) fields and their generalized relation with *contact structures* possibly *admitting singularities* is one of the promising follow up of our work. The other, as we already stressed, is the general scheme for the construction of exact or approximate solutions of Navier Stokes equations with prescribed hidden symmetries and calculable Beltrami spectra.

The notion of Universal Classifying Group introduced in [1] and mentioned in the introduction is an intrinsic property of the considered crystallographic lattice  $\Lambda$  and of its point group  $\mathfrak{P}_\Lambda^{max}$ , which, by definition, is the maximal finite subgroup of  $SO(3)$  leaving the lattice  $\Lambda$  invariant.

The reason why lattices and crystallography are brought into the study of fluid dynamics is that we focus on *hydro-flows* that are confined within some bounded domain, as it happens in a large variety of cases of interest for technological applications like industrial autoclaves, pipelines, thermal machines of various kind, blood vessels in physiology, liquid helium micro-tubes in superconducting magnets, chemical reactors with mechanical agitation sytems and so on. The argument goes as follows. Solutions of partial differential equations (PDE.s) like the NS-equation in (2.1), that encode the characterizing feature of being confined to finite regions of space can be obtained essentially by means of two alternative strategies:

- A)** By brutally imposing boundary conditions that simulate the walls of the chamber, tube, box or whatever else contains the flowing fluid. This strategy is the most direct and suitable for numerical computer aided integration of the PDE.s but it is hardly viable in the search of exact analytic solutions of the same PDE.s with the ambition of establishing some rational taxonomy.
- B)** The use of periodic boundary conditions which amounts to restricting one's attention to a compact space  $\mathcal{M}_3$  without boundary ( $\partial \mathcal{M}_3 = 0$ ) as a mathematical model of the finite volume region of interest.

The use of alternative B) amounts to developing in some suitable Fourier series some functions (the velocity



components) that are not necessarily periodic but which, on a bounded support, coincide with periodic functions admitting a Fourier series development.

This being clarified a systematic way of imposing periodic boundary conditions is the identification of the  $\mathcal{M}_3$  manifold with a  $T^3$  torus obtained by modding  $\mathbb{R}^3$  with respect to a three dimensional lattice  $\Lambda \subset \mathbb{R}^3$ :

$$\mathcal{M}_3 = T_g^3 = \frac{\mathbb{R}^3}{\Lambda} \quad (2.3)$$

Abstractly the lattice  $\Lambda$  is a an abelian infinite group isomorphic to  $\mathbb{Z} \times \mathbb{Z} \times \mathbb{Z}$  which is embedded in some way into  $\mathbb{R}^3$ . Using eq.(2.3) the topological torus

$$T^3 \simeq S^1 \times S^1 \times S^1 \quad (2.4)$$

comes out automatically equipped with a flat constant metric. Indeed, according with (2.3) the flat Riemannian space  $T_g^3$  is defined as the set of equivalence classes with respect to the following equivalence relation:  $\mathbf{r}' \sim \mathbf{r}$  iff  $\mathbf{r}' - \mathbf{r} \in \Lambda$ . The metric  $g$  defined on  $\mathbb{R}^3$  is inherited by the quotient space and therefore it endows the topological torus (2.4) with a flat Riemannian structure. Seen from another point of view the space of flat metrics on  $T^3$  is just the coset manifold  $SL(3, \mathbb{R})/SO(3)$  encoding all possible symmetric matrices, alternatively all possible space lattices, each lattice being spanned by an arbitrary triplet of basis vectors.

**Lattices** To make the above statement precise let us consider the standard  $\mathbb{R}^3$  manifold and introduce a basis of three linearly independent 3-vectors that are not necessarily orthogonal to each other and of equal length:

$$\mathbf{w}_\mu \in \mathbb{R}^3 \quad \mu = 1, \dots, 3 \quad (2.5)$$

Any vector in  $\mathbb{R}$  can be decomposed along such a basis and we have:

$$\mathbf{r} = r^\mu \mathbf{w}_\mu \quad (2.6)$$

The flat, constant metric on  $\mathbb{R}^3$  is defined by:

$$g_{\mu\nu} = \langle \mathbf{w}_\mu, \mathbf{w}_\nu \rangle \quad (2.7)$$

where  $\langle, \rangle$  denotes the standard euclidian scalar product. The space lattice  $\Lambda$  consistent with the metric (2.7) is the free abelian group (with respect to the sum) generated by the three basis vectors (2.5), namely:

$$\mathbb{R}^3 \ni \mathbf{q} \in \Lambda \Leftrightarrow \mathbf{q} = q^\mu \mathbf{w}_\mu \quad \text{where} \quad q^\mu \in \mathbb{Z} \quad (2.8)$$

**Dual lattices** Any time we are given a lattice in the sense of the definition (2.8) we obtain a dual lattice  $\Lambda^*$  defined by the property:

$$\mathbb{R}^3 \ni \mathbf{p} \in \Lambda^* \Leftrightarrow \langle \mathbf{p}, \mathbf{q} \rangle \in \mathbb{Z} \quad \forall \mathbf{q} \in \Lambda \quad (2.9)$$

A basis for the dual lattice is provided by a set of three *dual vectors*  $\mathbf{e}^\mu$  defined by the relations<sup>2</sup>:

$$\langle \mathbf{w}_\mu, \mathbf{e}^\nu \rangle = \delta_\mu^\nu \quad (2.10)$$

---

<sup>2</sup>In the sequel for the scalar product of two vectors we utilize also the equivalent shorter notation  $\mathbf{a} \cdot \mathbf{b} = \langle \mathbf{a}, \mathbf{b} \rangle$

so that

$$\forall \mathbf{p} \in \Lambda^* \quad \mathbf{p} = p_\mu \mathbf{e}^\mu \quad \text{where} \quad p_\mu \in \mathbb{Z} \quad (2.11)$$

According with such a definition it immediately follows that the original lattice is always a subgroup of the dual lattice and necessarily a normal one, due to the abelian character of both the larger and smaller group:

$$\Lambda \subset \Lambda^* \quad (2.12)$$

## 2.1 Rewriting of the equations of hydrodynamics in a geometrical set up

Let us then begin with the rewriting of eq.(2.2) which is the starting point of the entire adventure. The first step to be taken in our raising conceptual ladder is that of promoting the fluid trajectories, defined as the solutions of the following first order differential system<sup>3</sup>:

$$\frac{d}{dt}x^i(t) = u^i(x(t), t) \quad (2.14)$$

to smooth maps:

$$\mathcal{S} : \mathbb{R}_t \rightarrow \mathcal{M}_g \quad (2.15)$$

from the time real line  $\mathbb{R}_t$  to a smooth Riemannian manifold  $\mathcal{M}_g$  endowed with a metric  $g$ . The classical case corresponds to  $\mathcal{M} = \mathbb{R}^3$ ,  $g_{ij}(x) = \delta_{ij}$ , but any other Riemannian three-manifold might be used and there exist also generalizations to higher dimensions. Adopting this point of view, the velocity field  $\mathbf{u}(x, t)$  is turned into a time evolving vector field on  $\mathcal{M}$  namely into a smooth family of sections of the tangent bundle  $\mathcal{TM}$ :

$$\forall t \in \mathbb{R} : u^i(x, t) \partial_i \equiv \mathbf{U}(t) \in \Gamma(\mathcal{TM}, \mathcal{M}) \quad (2.16)$$

Next, using the Riemannian metric, which allows to raise and lower tensor indices, with any  $\mathbf{U}(t)$  we can associate a family of sections of the cotangent bundle  $\mathcal{T}^*\mathcal{M}$  defined by the following time evolving one-form:

$$\forall t \in \mathbb{R} : \Omega^{[\mathbf{U}]}(t) \equiv g_{ij} u^i(x, t) dx^j \in \Gamma(\mathcal{T}^*\mathcal{M}, \mathcal{M}) \quad (2.17)$$

Utilizing the exterior differential and the contraction operator acting on differential forms, we can evaluate the Lie-derivative of the one-form  $\Omega^{[\mathbf{U}]}(t)$  along the vector field  $\mathbf{U}$ . Applying definitions (see for instance [25], chapter five, page 120 of volume two) we obtain:

$$\mathcal{L}_{\mathbf{U}}\Omega^{[\mathbf{U}]}(t) \equiv \mathbf{i}_{\mathbf{U}} \cdot d\Omega^{[\mathbf{U}]} + d(\mathbf{i}_{\mathbf{U}} \cdot \Omega^{[\mathbf{U}]}) = \left( u^\ell \partial_\ell u^i + g^{ik} \partial_k \underbrace{\|\mathbf{U}\|^2}_{g_{mn} u^m u^n} \right) g_{ij} dx^j \quad (2.18)$$

---

<sup>3</sup>In mathematical hydrodynamics people distinguish two notions, that of trajectories, which are the solutions of the differential equations (2.14) and that of streamlines. Streamlines are the instantaneous curves that at any time  $t = t_0$  admit the velocity field  $u^i(x, t_0)$  as tangent vector. Introducing a new parameter  $\tau$ , streamlines at time  $t_0$ , are the solutions of the differential system:

$$\frac{d}{d\tau}x^i(\tau) = u^i(\mathbf{x}(\tau), t_0) \quad (2.13)$$

In the case of steady flows where the velocity field is independent from time, trajectories and streamlines coincide.

and the Navier Stokes equation can be rewritten in the the following index-free reformulation

$$-d\left(p + \frac{1}{2} \|U\|^2\right) = \partial_t \Omega^{[U]} + i_U \cdot d\Omega^{[U]} - \nu \Delta_g \Omega^{[U]} - \mathbf{f} \quad (2.19)$$

Where  $\Delta_g$  is the Laplace-Beltrami operator on 1-forms, written in an index free notation as it follows:

$$\Delta_g = \delta d + d\delta \quad ; \quad \delta \equiv \star_g d\star_g \quad (2.20)$$

where with  $\star_g$  we have denoted the Hodge duality operation in the background of the metric  $g$ .

Eq.(2.19) is one of the possible formulations of classical Bernoulli theorem. To begin with, consider inviscid fluids ( $\nu = 0$ ) with no external forces ( $\mathbf{f} = 0$ ). Then equation eq.(2.19) becomes:

$$-d\left(p + \frac{1}{2} \|U\|^2\right) = \partial_t \Omega^{[U]} + i_U \cdot d\Omega^{[U]} \quad (2.21)$$

and from eq.(2.19) we immediately conclude that

$$H_B = p + \frac{1}{2} \|U\|^2 \quad (2.22)$$

is constant along the trajectories defined by eq.(2.14). Turning matters around we can say that in **steady flows** of inviscid free fluids, where

$$\partial_t \Omega^{[U]} = 0 \quad (2.23)$$

the fluid trajectories necessarily lay on the level surfaces  $H_B(x) = h \in \mathbb{R}$  of the function:

$$H : \mathcal{M} \rightarrow \mathbb{R} \quad (2.24)$$

defined by (2.22) and hereafter named, as it is traditional in Fluid Mechanics, the **Bernoulli function**.

An identical conclusion can be reached in the case of non-vanishing viscosity if the steady flow condition (2.23) is replaced by:

$$\partial_t \Omega^{[U]} = \nu \Delta_g \Omega^{[U]} + \mathbf{f} \quad (2.25)$$

For instance if at time  $t = t_0$ , the 1-form  $\Omega^{[U]}$  is the superposition of a collection of  $N$  eigenstates of the Laplace-Beltrami operator:

$$\Omega^{[U]}|_{t=t_0} = \sum_{i=1}^N \omega_i \quad ; \quad \Delta_g \omega_i = \lambda_i \omega_i \quad (2.26)$$

choosing a subset of such forms, say those from  $i = 1$  to  $i = M < N$ , one can solve the condition (2.25) by setting the driving force as follows:

$$\mathbf{f} = -\nu \sum_{i=1}^M \lambda_i \omega_i \quad (2.27)$$

and the 1-form flow as follows:

$$\Omega^{[U]} = \sum_{i=1}^M \omega_i + \sum_{i=M+1}^N \omega_i \exp[-\lambda_i t] \quad (2.28)$$

For viscid fluids, flows satisfying eq.(2.25) will be referred to as **generalized steady flows**. It follows that in the case of steady and generalized steady flows the fluid trajectories necessarily lay on the level surfaces  $H_B(x) = h \in \mathbb{R}$  of the Bernoulli function (2.24) defined by (2.22).

### 2.1.1 Foliations

Then if  $H_B(\mathbf{x})$  has a non trivial  $x$ -dependence, locally, in open charts  $\mathcal{U}_n \subset \mathcal{M}_n$  of the considered  $n$ -dimensional manifold, it defines a natural foliation of such charts  $\mathcal{U}_n$  into a smooth family of  $(n - 1)$ -manifolds (all diffeomorphic among themselves) corresponding to the level surfaces.

The global topological and analytic structure of level surfaces of the Bernoulli function is the object of interesting recent mathematical studies (see for instance [26]) that we avoid addressing since the focus of the present discussion is only local and heuristic since the 3-dimensional manifolds eventually considered in this paper are just flat, non singular torii  $\mathbb{R}^3/\Lambda$  where  $\Lambda$  is a lattice. Then in the mentioned open charts, as already advocated, the trajectories, *i.e.* the solutions of eq.(2.14), lay on these surfaces. In other words the dynamical system encoded in eq.(2.14) is effectively  $(n - 1)$ -dimensional admitting  $H$  as an additional conserved hamiltonian. In the classical case  $n = 3$  this means that the differential system (2.14) is actually two-dimensional, namely non-chaotic and in some instances even integrable<sup>4</sup>. Consequently we reach the conclusion that no chaotic trajectories (or streamlines) can exist in those domains where the Bernoulli function  $H_B(x)$  has a non trivial  $x$ -dependence: the only window open for lagrangian chaos occurs in those domains where  $H_B$  is a constant function. Looking at eq.s(2.19-2.21) we realize that the previous argument implies that in steady and generalized steady flows, chaotic trajectories can occur only if velocity field satisfies the following condition:

$$i_{\mathbf{U}} \cdot d\Omega^{[\mathbf{U}]} = 0 \quad (2.29)$$

This weak condition (2.29) is certainly satisfied if the velocity field  $\mathbf{U}$  satisfies the following strong condition that is named **Beltrami equation**:

$$d\Omega^{[\mathbf{U}]} = \lambda \star_g \Omega^{[\mathbf{U}]} \Leftrightarrow \star_g d\Omega^{[\mathbf{U}]} = \lambda \Omega^{[\mathbf{U}]} \quad (2.30)$$

where  $\star_g$ , as already specified, denotes the Hodge duality operator in the metric  $g$ :

$$\star_g \Omega^{[\mathbf{U}]} = \epsilon_{\ell mn} g^{\ell k} \Omega_k^{[\mathbf{U}]} dx^m \wedge dx^n = u^\ell dx^m \wedge dx^n \epsilon_{\ell mn} \quad (2.31)$$

$$\star_g d\Omega^{[\mathbf{U}]} = \epsilon_{\ell mn} g^{mp} g^{nq} \partial_p (g_{qr} u^r) dx^\ell \quad (2.32)$$

### 2.1.2 Arnold theorem

The heuristic argument which leads to consider velocity fields that satisfy *Beltrami condition* (2.30) as the unique steady candidates compatible with chaotic trajectories was transformed by Arnold into a rigorous theorem [9] which, under the strong hypothesis that  $(\mathcal{M}, g)$  is a closed, compact Riemannian three-manifold, states the following:

**Theorem 2.1** *Assume that a region  $D \subset \mathcal{M}$  of the considered **three-dimensional** Riemannian manifold  $(\mathcal{M}, g)$  is bounded by a compact analytic surface and that the velocity field  $\mathbf{U}$  does not satisfy Beltrami equation everywhere in  $D$ , namely  $\Omega^{[\mathbf{U}]} \neq \lambda \star_g d\Omega^{[\mathbf{U}]}$ , where  $\lambda \in \mathbb{R}$  is a real number. Then the region of the flow can be partitioned by an analytic submanifold into a finite number of cells, in each of which the flow is constructed in a standard way. Namely the cells are of two types: those fibered into tori invariant under the flow and those fibered into surfaces invariant under the flow, diffeomorphic to the annulus  $\mathbb{R} \times \mathbb{S}^1$ . On each of these tori the flow lines are either all closed or all dense, and on each annulus all the flow lines are closed.*

<sup>4</sup>Here we rely on a general result established by the theorem of Poincaré-Bendixson [27, 28] on the limiting orbits of planar differential systems whose corollary is generally accepted to establish that two-dimensional continuous systems cannot be chaotic.

As one sees, in steady flows, when the velocity vector field of the fluid is not a Beltrami field, then streamlines either lie on surfaces that have the topology of torii or on surfaces that are cylindrical. In both cases chaotic streamlines are excluded.

*Chaotic trajectories or streamlines* are of particular interest, both from the point of view of theory and of applications, since, in many scenarios, chaotic flows are desirable in order either to homogenize the heat exchange between the fluid and some external objects immersed in the flow, as it happens in *autoclaves*, or to promote the mixing of two different fluids, like it happens in *chemical reactors*. The examples are multiple and the mentioned ones are just an illustration.

On the other hand the chaotic trajectories are desirable in all these applications at *small scales* while on *larger scales* the fluid should appear as moving steadily in some given direction. The intrinsic non linearity of the NS equation forbids the linear combination of solutions as new solutions and the superposition of different regimes at different scales is a very difficult mathematical problem that requires specialized analysis.

The desire to investigate the on-set of chaotic trajectories in steady (or generalized steady) flows of incompressible fluids motivated the interest of the dynamical system community in Beltrami vector fields defined by the condition (2.30). Furthermore, in view of the above powerful theorem proved by Arnold, the focus of attention concentrated on the mathematically very interesting case of compact three-manifolds. Within this class, the most easily treatable case is that of flat compact manifolds without boundary, so that the most popular playground turned out to be the three torus  $T^3$ , whose possible role in applications has already been emphasized. Certainly many physical contexts for fluid dynamics do not correspond to the idealized situation of a motion in a compact manifold or, said differently, periodic boundary conditions are not the most appropriate to be applied either in a river, or in the atmosphere or in the charged plasmas environing a compact star, yet the message conveyed by Arnold theorem that Beltrami vector fields play a distinguished role in chaotic behavior is to be taken seriously into account and gives an important hint. In view of what we are going to discuss in section 2.2 this hint is properly developed by considering the one-to-one relation between Beltrami fields and contact structures on three-manifolds that is now extended to contact structures with singularities.

## 2.2 The path leading to contact geometry

Beltrami vector fields are intimately related with the mathematical notion of *contact geometry and contact topology*. As we have seen from our sketch of Arnold Theorem, the main obstacle to the onset of chaotic trajectories has a distinctive geometrical flavor: trajectories are necessarily ordered and non-chaotic if the manifold where they take place has a foliated structure  $\Sigma_h \times \mathbb{R}_h$ , the two dimensional level sets  $\Sigma_h$  being invariant under the action of the velocity vector field  $U$ . In this case each streamline lays on some surface  $\Sigma_h$ . Equally adverse to chaotic trajectories is the case of *gradient flows* where there is a foliation provided by the level sets of some function  $H(x)$  and the velocity field  $U = \nabla H$  is just the gradient of  $H$ . In this case all trajectories are orthogonal to the leaves  $\Sigma_h$  of the foliation and their well aligned tangent vectors are parallel to its normal vector.

In conclusion in presence of a foliation (or a local foliation) we have the following decomposition of the tangent space to the manifold  $\mathcal{M}$  at any point  $p \in \mathcal{M}$

$$T_p \mathcal{M} = T_p^\perp \Sigma_h \oplus T_p^\parallel \Sigma_h \tag{2.33}$$

and no chaotic trajectories are possible in a region  $\mathfrak{S} \subset \mathcal{M}$  where  $U(p) \in T_p^\perp \Sigma_h$  or  $U(p) \in T_p^\parallel \Sigma_h$  for  $\forall p \in \mathfrak{S}$  (see fig.1).

This matter of fact motivates an attempt to capture the geometry of the bundle of subspaces orthogonal

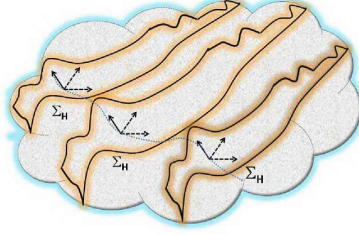


Figure 1: *Schematic view of the foliation of a three dimensional manifold  $\mathcal{M}$ . The family of two-dimensional surfaces  $\Sigma_h$  are typically the level sets  $H(\mathbf{x}) = h$  of some function  $H : \mathcal{M} \rightarrow \mathbb{R}$ . At each point of  $p \in \Sigma_h \subset \mathcal{M}$  the dashed vectors span the tangent space  $T_p^{\parallel} \Sigma_h$ , while the solid vector span the normal space to the surface  $T_p^{\perp} \Sigma_h$ . Equally adverse to chaotic trajectories is the case where the velocity field  $U$  lies in  $T_p^{\perp} \Sigma_h$  (gradient flow) or in  $T_p^{\parallel} \Sigma_h$*

to the lines of flow by introducing an intrinsic topological indicator that distinguishes necessarily non-chaotic flows from possibly chaotic ones. Let us first consider the extreme case of a gradient flow where  $\Omega^{[U]} = dH$  is an exact form. For such flows we have:

$$\Omega^{[U]} \wedge d\Omega^{[U]} = \Omega^{[U]} \wedge \underbrace{ddH}_{=0} = 0 \quad (2.34)$$

Secondly let us consider the opposite case where the velocity field  $U$  is orthogonal to a gradient vector field  $\nabla H$  so that the integral curves of  $U$  lay on the level surfaces  $\Sigma_h$ . Furthermore let us assume that  $U$  is self similar on neighboring level surfaces. We can characterize this situation in a Riemannian manifold  $(\mathcal{M}, g)$  by the following two conditions:

$$i_{\nabla H} \Omega^{[U]} \Leftrightarrow g(U, \nabla H) = 0 \quad ; \quad [U, \nabla H] = 0 \quad (2.35)$$

The first of eq.s(2.35) is obvious. To grasp the second it is sufficient to introduce, in the neighborhood of any point  $p \in \mathcal{M}$ , a local coordinate system composed by  $(h, x^{\parallel})$  where  $h$  is the value of the function  $H$  and  $x^{\parallel}$  denotes some local coordinate system on the level set  $\Sigma_h$ . The situation we have described corresponds to assuming that:

$$U \simeq U^{\parallel}(x^{\parallel}) \partial_{\parallel} \quad ; \quad \partial_h U^{\parallel}(x^{\parallel}) = 0 \quad (2.36)$$

Under the conditions spelled out in eq.(2.35) we can easily prove that:

$$i_{\nabla H} d\Omega^{[U]} = 0 \quad (2.37)$$

Indeed from the definition of the Lie derivative we obtain:

$$i_{\nabla H} d\Omega^{[U]} = \underbrace{\mathcal{L}_{\nabla H} \Omega^{[U]}}_{= \Omega^{[U, \nabla H]} = 0} - d \left( \underbrace{i_{\nabla H} \Omega^{[U]}}_{=0} \right) \quad (2.38)$$

Since we have both  $i_{\nabla H}\Omega^{[U]} = 0$  and  $i_{\nabla H}d\Omega^{[U]} = 0$  it follows that also in this case:

$$\Omega^{[U]} \wedge d\Omega^{[U]} = 0 \quad (2.39)$$

Therefore in order not to exclude chaotic trajectories one has to assume that

$$\Omega^{[U]} \wedge d\Omega^{[U]} \neq 0 \quad (2.40)$$

and the above condition is what leads us to *contact geometry*.

### 3 Geometrical Foundations

In this section we just summarize some definitions and theorems of basic differential geometry that we shall later utilize or quote, for their conceptual relevance in the development of our original arguments.

#### 3.1 Contact Geometry

Contact Geometry is both an old and a relatively new chapter of Mathematics, since it springs from some classical results of analysis that date back to Darboux, Goursat, Lie and other XIX century maitres, yet it has been vigorously developed in the last two decades from a relatively small community of mathematicians. To say it in short, *Contact Geometry* is a mathematical theory aiming at providing an intrinsic geometrical-topological characterization of *non integrability*.

Contact Geometry deals exclusively with real *Differential Manifolds*  $\mathcal{M}_{2n+1}$  of *odd-dimension* and on the other hand it has a symbiotic relation with *Symplectic Manifolds*  $\mathcal{S}_{2n+2}$  and  $\mathcal{S}_{2n}$  in the two adjacent even dimensions, upper and lower.

In the present concise summary we closely follow the excellent review [29].

##### 3.1.1 Contact structures

We consider an odd dimensional differential manifold  $\mathcal{M}_{2n+1}$  its tangent bundle  $\mathcal{T}\mathcal{M}_{2n+1} \xrightarrow{\pi} \mathcal{M}_{2n+1}$  whose space of sections  $\Gamma[\mathcal{T}\mathcal{M}_{2n+1}, \mathcal{M}_{2n+1}]$  is composed by vector fields, whose local description is in terms of first order differential operators  $\mathbf{X} = X^\mu(x) \frac{\partial}{\partial x^\mu}$  and the cotangent bundle  $\mathcal{T}^*\mathcal{M}_{2n+1} \xrightarrow{\pi^*} \mathcal{M}_{2n+1}$  whose space of sections  $\Gamma[\mathcal{T}^*\mathcal{M}_{2n+1}, \mathcal{M}_{2n+1}]$  is composed by differential 1-forms  $\omega = \omega_\mu(x) dx^\mu$ . A hyperplane bundle is a reduction of the tangent bundle where the fibres over each point constitute a codimension one vector subspace of the tangent space in the same point, the transition functions being accordingly derived:

$$\begin{aligned} \mathcal{HY} \xrightarrow{\mathcal{P}} \mathcal{M} \quad ; \quad \forall p \in \mathcal{M}, \mathcal{P}^{-1}(p) \subset \pi^{-1}(p) \quad \text{where} \quad \mathcal{TM} \xrightarrow{\pi} \mathcal{M} \\ \dim_{\mathbb{R}} \mathcal{M} = m \quad ; \quad \dim_{\mathbb{R}} \pi^{-1}(p) = m \quad ; \quad \dim_{\mathbb{R}} \mathcal{P}^{-1}(p) = m - 1 \end{aligned} \quad (3.1)$$

A simple way of constructing a hyperplane bundle is by means of the choice of a section of the cotangent bundle namely of some 1-form  $\omega \in \Gamma[\mathcal{T}^*\mathcal{M}, \mathcal{M}]$ . Then the hyperplane sub-bundle  $\mathcal{HY}^\omega \subset \mathcal{TM}$  of the tangent bundle is implicitly defined by stating what is the space of its sections  $\Gamma[\mathcal{HY}^\omega, \mathcal{M}]$ , namely mentioning all the possible vector fields that are sections of  $\mathcal{HY}^\omega$ . Utilizing a precise mathematical language let  $\mathbf{X} \in \Gamma[\mathcal{TM}, \mathcal{M}]$  be a vector field, we write

$$\mathbf{X} \in \Gamma[\mathcal{HY}^\omega, \mathcal{M}] \quad \text{iff} \quad \mathbf{X} \in \ker \omega \quad \text{i.e.} \quad \omega(\mathbf{X}) \equiv 0 \quad (\text{everywhere}) \quad (3.2)$$

**Definition 3.1** Given a manifold  $\mathcal{M}_{2n+1}$  of odd dimension, a **contact structure** on  $\mathcal{M}_{2n+1}$  is a rank  $2n$  sub-bundle  $\xi \xrightarrow{\mathcal{P}} \mathcal{M}_{2n+1}$  of the tangent bundle  $\mathcal{T}\mathcal{M}_{2n+1} \xrightarrow{\pi} \mathcal{M}_{2n+1}$  that can be identified with the hyperplane bundle  $\mathcal{H}\mathcal{Y}^\alpha$  where the 1-form  $\alpha$  satisfies the following condition:

$$\alpha \wedge \underbrace{d\alpha \wedge \dots \wedge d\alpha}_{n\text{-times}} \neq 0 \quad (\text{everywhere on } \mathcal{M}_{2n+1}) \quad (3.3)$$

The 1-form  $\alpha$  is named a **contact form**.

**Definition 3.2** A **contact manifold** is a pair  $(\mathcal{M}_{2n+1}, \xi)$  of an odd dimensional manifold and a contact structure  $\xi \xrightarrow{\mathcal{P}} \mathcal{M}_{2n+1}$ .

Few relevant observations are in order in relation with the above two definitions. The first is that the same contact structure can be defined by several different contact forms  $\alpha, \alpha', \dots$ . Indeed all multiples of a given contact form  $\alpha$  through a scalar, nowhere vanishing, function  $\lambda : \mathcal{M}_{2n+1} \rightarrow \mathbb{R}$  define the same contact structure. Secondly it is quite possible that the same odd-dimensional manifold  $\mathcal{M}_{2n+1}$  can admit more than one contact structure. The classification of these latter, modulo trivial diffeomorphisms, is an interesting and relevant mathematical problem. It is therefore mandatory to single out the notion of **contactomorphism**.

**Definition 3.3** Let  $(\mathcal{M}, \xi)$  and  $(\mathcal{N}, \chi)$  be two contact-manifolds and let:

$$\varphi : \mathcal{M} \longrightarrow \mathcal{N} \quad (3.4)$$

be a diffeomorphism of the former on the latter manifold (obviously  $\mathcal{M}$  and  $\mathcal{N}$  must have the same dimension in order for  $\varphi$  to possibly exist). Let  $\alpha$  be a contact form defining  $\xi$  and let  $\beta$  be a contact form defining  $\chi$ . The considered diffeomorphism  $\varphi$  is named a **contactomorphism** if and only if:

$$\varphi^*(\beta) = \lambda \alpha \quad (3.5)$$

where  $\varphi^*$  is the pull-back map and

$$\lambda : \mathcal{M} \longrightarrow \mathbb{R} \quad (3.6)$$

is a nowhere vanishing real function on the contact manifold  $\mathcal{M}$ . If a contactomorphism exists between them, the two considered contact manifolds are named **contactomorphic**.

In the above definition the manifold  $\mathcal{M}$  and  $\mathcal{N}$  might be the same. In this case what we are actually considering is the transformation by means of a diffeomorphism of a contact structure into another one by means of a contactomorphism.

**Definition 3.4** Given two contact structures  $\xi$  and  $\chi$  on the same manifold  $\mathcal{M}_{2n+1}$  they are to be identified as the same if there exists a contactomorphism that maps one into the other.

In conclusion the relevant mathematical problem is that of classifying contact structures on  $\mathcal{M}_{2n+1}$  modulo contactomorphisms.



### 3.1.2 Integrability and Frobenius Theorem

We refrain here from providing a detailed discussion of Frobenius theorem about integrability. We shall limit ourselves to sketch the basic concepts underlying its formulation. One just begins with the observation that every vector field  $\mathbf{X}$  on a manifold  $\mathcal{M}$  of whatever dimension defines its own integral curves  $\mathcal{I}_{\mathbf{X}}$ , namely those curves that at any of their points admit the local value of the vector field  $\mathbf{X}$  as tangent vector. Since any point  $p \in \mathcal{M}$  lies on some integral curve  $\mathcal{I}_{\mathbf{X}}$ , we are guaranteed that a single vector field induces a *foliation* of the manifold  $\mathcal{M}$  into one-dimensional submanifolds. It is more tricky to establish whether a sub-bundle of the tangent bundle  $\mathcal{E} \rightarrow \mathcal{M}$  of rank  $r > 1$  induces or not a foliation of  $\mathcal{M}$ . In this case, to say it in a not-completely rigorous, yet intuitive and qualitatively correct way, by *foliation* we mean the covering of the manifold with a family of *leaves*, namely of sub-manifolds diffeomorphic among themselves,  $\mathcal{F}_{\boldsymbol{\nu}} \subset \mathcal{M}$  of dimension equal to the rank  $r$  of the sub-bundle  $\mathcal{E}$ , each of which can be thought as the level set hypersurface for  $r$  functions  $u_i(p)$  ( $i = 1, \dots, r$ ) that originate from the integration of a basis of sections  $\mathbf{X}_i$  of the sub-bundle  $\mathcal{E} \rightarrow \mathcal{M}$ .

$$\begin{aligned} \mathcal{F}_{\boldsymbol{\nu}} &= \{p \in \mathcal{M} \mid u_i(p) = \nu_i\} \quad ; \quad \boldsymbol{\nu} \equiv \{\nu_1, \dots, \nu_r\} \quad ; \quad \nu_i = \text{real constants} \\ \nabla u_i(p) &= \mathbf{X}_i \big|_p \end{aligned} \tag{3.7}$$

When the above situation is realized one says that the sub-bundle  $\mathcal{E} \rightarrow \mathcal{M}$  is **integrable**.

**Frobenius theorem** establishes the necessary condition for such integrability.

**Theorem 3.1** *Let  $\mathcal{M}$  be a manifold and  $\mathcal{E} \rightarrow \mathcal{M}$  a sub-bundle of its tangent bundle of rank  $r > 1$ . The necessary and sufficient condition for  $\mathcal{E}$  to be integrable is that:*

$$\forall \mathbf{X}, \mathbf{Y} \in \Gamma[\mathcal{E}, \mathcal{M}] \quad : \quad [\mathbf{X}, \mathbf{Y}] \in \Gamma[\mathcal{E}, \mathcal{M}] \tag{3.8}$$

In the case where  $\mathcal{E} \rightarrow \mathcal{M}$  is an hyperplane bundle defined by a 1-form  $\omega$  Frobenius integrability condition can also be formulated as:

$$\omega \wedge d\omega = 0 \tag{3.9}$$

This shows that a contact structure defined by a contact form is the exact opposite of an integrable sub-bundle. Indeed one might show that it corresponds to maximal non-integrability.

### 3.1.3 Isotropic submanifolds of a contact manifold and non integrability

We begin with the following

**Definition 3.5** *Let  $(\mathcal{M}_{2n+1}, \xi)$  be a contact manifold and  $\mathcal{L} \subset \mathcal{M}_{2n+1}$  a submanifold. Consider the tangent bundle of such a submanifold  $\mathcal{TL} \xrightarrow{\pi_{\mathcal{T}}} \mathcal{L}$  and the contact structure bundle  $\xi \xrightarrow{\pi_{\xi}} \mathcal{M}$ . The submanifold  $\mathcal{L}$  is named **isotropic** if and only if*

$$\forall p \in \mathcal{L} \quad : \quad \pi_{\mathcal{T}}^{-1}(p) \subset \pi_{\xi}^{-1}(p) \tag{3.10}$$

*Equivalently, if the contact structure  $\xi$  is defined by the contact-form  $\alpha$ , the sub-manifold  $\mathcal{L}$  is **isotropic** if any vector field  $\mathbf{X}$  tangent to  $\mathcal{L}$ , is also in  $\ker \alpha$ :*

$$\mathbf{X} \in \Gamma[\mathcal{TL}, \mathcal{L}] \quad \Rightarrow \quad \alpha(\mathbf{X}) = 0 \tag{3.11}$$

We introduce the additional definition

**Definition 3.6** Let  $(\mathcal{M}_{2n+1}, \xi)$  be a contact manifold and  $\widetilde{\mathcal{M}}_{2m+1} \subset \mathcal{M}_{2n+1}$  an odd dimensional submanifold of codimension  $2(n-m) \geq 0$ . Let  $\alpha$  be the contact one form defining the contact structure  $\xi$  and  $\iota$  the inclusion map:

$$\iota : \widetilde{\mathcal{M}}_{2m+1} \longrightarrow \mathcal{M}_{2n+1} \quad (3.12)$$

Then  $(\widetilde{\mathcal{M}}_{2m+1}, \chi)$  is named a **contact submanifold** of  $(\mathcal{M}_{2n+1}, \xi)$  if the contact structure  $\chi$  on  $\widetilde{\mathcal{M}}_{2m+1}$  is defined by the **contact-form**  $\iota^* \alpha$ , in other words if:

$$\chi = \ker \iota^* \alpha \quad (3.13)$$

The main reason why contact geometry is relevant for chaotic flows in fluid dynamics streams from the following

**Theorem 3.2** Let  $(\mathcal{M}_{2n+1}, \xi)$  be a contact manifold in  $2n + 1$ -dimensions and  $\mathcal{L} \subset \mathcal{M}_{2n+1}$  an isotropic submanifold. Then  $\dim \mathcal{L} \leq n$ .

In order to prove theorem 3.2 we need first the following

**Lemma 3.1** Let  $(\mathcal{M}_{2n+1}, \xi)$  be a contact manifold whose contact structure  $\xi$  is defined as  $\ker \alpha$ , in terms of the contact 1-form  $\alpha$ . Because of the defining condition 3.3 it follows that  $d\alpha|_{\xi} \neq 0$  and for every point  $p \in \mathcal{M}_{2n+1}$  the  $2n$ -dimensional fibre  $\xi_p \subset T_p \mathcal{M}_{2n+1}$  is a vector-space equipped with a skew-symmetric 2-form of maximal rank (no-zero eigenvalues) exactly provided by the restriction to  $\xi_p$  of  $d\alpha$  i.e.  $d\alpha|_{\xi_p}$ . Hence the contact structure is a symplectic bundle with respect to the 2-form  $d\alpha|_{\xi}$ .

**Proof 3.2.1** In order to prove the theorem, consider the inclusion map:  $\iota : \mathcal{L} \longrightarrow \mathcal{M}_{2n+1}$  and consider the pull-back of the contact form on the isotropic manifold. By definition of isotropy  $\iota^* \alpha = 0$ . Hence we have also  $\iota^* d\alpha = 0$ . At each point  $p \in \mathcal{L}$ , the tangent space  $\mathcal{T}_p \mathcal{L}$  is a subspace of the symplectic space  $\xi_p$  on which the symplectic 2-form vanishes  $d\alpha|_{\xi_p}$ . From elementary linear algebra it follows that such a subspace has at most

one-half of the dimension of  $\xi_p$ . Indeed it suffices to put the skew 2-form in canonical form:  $\left( \begin{array}{c|c} \mathbf{0}_{n \times n} & \mathbf{1}_{n \times n} \\ \hline -\mathbf{1}_{n \times n} & \mathbf{0}_{n \times n} \end{array} \right)$

and the statement becomes evident. This proves the theorem ■.

What are the consequences of this theorem? It states that if we have a contact structure  $\xi$ , induced by a contact form  $\alpha$ , then we can exclude a foliation of the contact manifold into hypersurfaces  $\Sigma_h \subset \mathcal{M}_{2n+1}$  of codimension 1:

$$\mathcal{M}_{2n+1} \simeq \Sigma_h \times \mathbb{R}_h \quad (3.14)$$

such that for each  $h \in \mathbb{R}$  the tangent bundle of  $\Sigma_h$  is comprised within the contact structure. Indeed if that happened each leave  $\Sigma_h$  of the foliation would be an isotropic submanifold of dimension  $2 \times n$  which is what the theorem forbids.

**Definition 3.7** An isotropic submanifold  $\mathcal{L} \subset \mathcal{M}_{2n+1}$  of maximal possible dimension, namely  $n$ , of a contact manifold in dimensions  $2n + 1$ , is named a **Legendrian submanifold**.

Furthermore

**Definition 3.8** Associated with a contact form  $\alpha$  one has the so called **Reeb vector field**  $\mathbf{R}_\alpha$ , defined by the two conditions:

$$\begin{aligned} \alpha(\mathbf{R}_\alpha) &= \lambda(\mathbf{x}) = \text{nowhere vanishing function on } \mathcal{M}_{2n+1} \\ \forall \mathbf{X} \in \Gamma[\mathcal{T}\mathcal{M}_{2n+1}, \mathcal{M}_{2n+1}] &: d\alpha(\mathbf{R}_\alpha, \mathbf{X}) = 0 \end{aligned} \quad (3.15)$$

If the contact manifold  $\mathcal{M}_{2n+1}$  is equipped with a Riemannian metric  $g$ , then the contact 1-form  $\alpha$  and its Reeb field  $\mathbf{R}_\alpha$  are related one to the other by the raising and lowering of indices. Suppose that we start from the Reeb field:

$$\mathbf{R} = R^\mu \frac{\partial}{\partial x^\mu} \quad (3.16)$$

The corresponding  $\alpha$  is obtained by setting:

$$\alpha = \Omega^{[\mathbf{R}]} \equiv g_{\mu\nu} R^\mu dx^\nu \quad (3.17)$$

and the contact structure condition (3.3) is turned into the following condition on the Reeb field components:

$$\epsilon^{\lambda\mu_1\nu_1\mu_2\nu_2\dots\mu_n\nu_n} R_\lambda \partial_{\mu_1} R_{\nu_1} \partial_{\mu_2} R_{\nu_2} \dots \partial_{\mu_n} R_{\nu_n} \neq 0 \quad \text{nowhere vanishes} \quad (3.18)$$

On the contrary, if one begins with the contact form  $\alpha$ , the components of the Reeb field are obtained by setting:

$$R_\alpha^\mu = g^{\mu\nu} \alpha_\nu \quad (3.19)$$

Note that the nowhere vanishing function  $\lambda$  mentioned in the definition 3.8 is just the squared norm of the Reeb field or of the contact form which coincide:

$$\lambda = \|\mathbf{R}\|^2 = \|\Omega^{[\mathbf{R}]}\|^2 \equiv g_{\mu\nu} R^\mu R^\nu \quad (3.20)$$

### 3.1.4 Contact structures in $D = 3$ and hydro-flows

Let us now consider the case relevant for fluid dynamics, namely that of three dimensional contact manifolds  $(\mathcal{M}_3, \xi_\alpha)$ , where, in the notation  $\xi_\alpha$ , we mention the contact form  $\alpha$  defining the contact structure. The consequence of theorem 3.2 is that in such contact manifolds, the Legendrian submanifolds are all 1-dimensional, namely they are *curves* or, as it is customary to name them in the present context, *knots*.

Hence in three dimensions there are two kind of knots, the **Legendrian knots** whose tangent vector belongs to  $\ker \alpha$  and the **transverse knots** whose tangent vector is parallel to the Reeb field at each point of the trajectory.

Furthermore in  $D=3$  the condition (3.18) becomes:

$$\epsilon^{\lambda\mu\nu} R_\lambda \partial_\mu R_\nu \neq 0 \quad (3.21)$$

**The standard contact structure on  $\mathbb{R}^3$ .** The flat Euclidian space in three dimensions whose coordinates we denote as  $x, y, z$  is endowed with a standard contact structure that admits the following contact form:

$$\alpha_s = dz + x dy \quad (3.22)$$

A picture of the local planes defining the contact structure (3.22) is shown in fig.2.

### 3.1.5 Relation with Beltrami vector fields

As we see the main reason to introduce the contact form conception is that, so doing one liberates the notion of a vector field capable to generate chaotic trajectories from the use of any metric structure. A vector field  $U$  is potentially interesting for chaotic regimes if it is a Reeb field for at least one contact form  $\alpha$ . In this way the

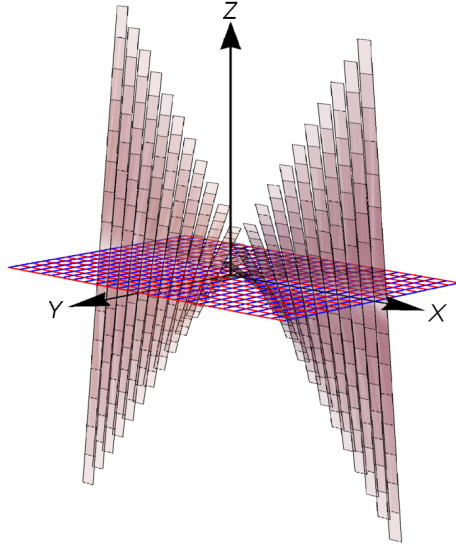


Figure 2: *Schematic view of the standard contact structure  $\mathbb{R}^3$*

mathematical theorems about the classification of contact structures modulo diffeomorphisms (theorems that are metric-free and of topological nature) provide new global methods to capture the topology of hydro-flows.

Instead if we work in a Riemannian manifold endowed with a metric  $(\mathcal{M}, g)$  we can always invert the procedure and define the contact form  $\alpha$  that can admit  $U$  as a Reeb vector field by identifying

$$\alpha = \Omega^{[U]} \quad (3.23)$$

In this way the first of the two conditions (3.15) is automatically satisfied:  $i_U \Omega^{[U]} = \|U\|^2 > 0$ . It remains to be seen whether  $\Omega^{[U]}$  is indeed a contact form, namely whether  $\Omega^{[U]} \wedge d\Omega^{[U]} \neq 0$  and whether the second condition  $i_U d\Omega^{[U]} = 0$  is also satisfied. Both conditions are automatically fulfilled if  $U$  is a Beltrami field, namely if it is an eigenstate of the operator  $\star_g d$  as advocated in eq.(2.30). Indeed the implication  $i_U d\Omega^{[U]} = 0$  of Beltrami equation was shown in eq. (2.29), while from the Beltrami condition it also follows:

$$\Omega^{[U]} \wedge d\Omega^{[U]} = \Omega^{[U]} \wedge \star_g \Omega^{[U]} = \|U\|^2 \text{Vol} \neq 0 \quad ; \quad \text{Vol} \equiv \frac{1}{3!} \times \epsilon_{ijk} dx^i \wedge dx^j \wedge dx^k \quad (3.24)$$

In this way the conceptual circle closes and we see that all Beltrami vector fields can be regarded as Reeb fields for a bona-fide contact form. Since the same contact structure (in the topological sense) can be described by different contact forms, once Beltrami fields have been classified it remains the task to discover how many inequivalent contact structures they actually describe. Yet it is reasonable to assume that every contact structure has a contact form representative that is derived from a Beltrami Reeb field. Indeed a precise correspondence is established by a theorem proved in [17]:

**Theorem 3.3** *Any rotational Beltrami vector field on a Riemannian 3-manifold is a Reeb field for some contact form. Conversely any Reeb field associated to a contact form on a 3-manifold is a rotational Beltrami field for some Riemannian metric. Rotational Beltrami field means an eigenfunction of the  $\star_g d$  operator corresponding to a non-vanishing eigenvalue  $\lambda$ .*

### 3.1.6 Darboux's theorem

We finally mention, without providing its proof that can be found in [29], a classical theorem named after Darboux, which shows that the standard contact structure on  $\mathbb{R}^3$  displayed in eq.(3.22) and graphically shown in fig.2 is not just a choice, rather it corresponds to the canonical local form of any contact structure on any contact manifold.

**Theorem 3.4** *Let  $(\mathcal{M}_{2n+1}, \xi)$  be an  $(2n + 1)$ -dimensional contact manifold and  $\alpha$  a contact 1-form defining  $\xi = \ker \alpha$ . Let  $p \in \mathcal{M}_{2n+1}$  be any point of the manifold and  $U \subset \mathcal{M}_{2n+1}$  an open neighborhood of  $p$ . Then we can always find a local homomorphism:  $\varphi : U \rightarrow \mathbb{R}^{2n+1}$  such that, naming  $\{y_0, x_i, y_i\}, (i = 1, \dots, n)$  the coordinates on  $\varphi(U) \subset \mathbb{R}^{2n+1}$  we obtain:*

$$\alpha|_U = dy_0 + \sum_{i=1}^n x_i dy_i \quad (3.25)$$

In the case  $n = 1$  eq.(3.25) reproduces eq.(3.22). Hence for all three-dimensional contact manifolds  $\mathcal{M}_3$  that in (3.22) is the universal local form of the contact 1-form  $\alpha$ .

## 3.2 $\mathfrak{b}$ -Contact Geometry and Singular Beltrami Fields

As we emphasized in the introduction, the main difficulty in solving NS or Euler equations comes from the non-linearity of the transport term which forbids the generic linear superposition of solutions, a limited superposition being possible, within the landscape approach to be discussed in section 7, with Beltrami fields belonging to the same spherical layer. As we stressed, Beltrami fields are essential, via their relation with contact structures, in order to create the possibility of chaotic streamlines at small scales, yet they are defined on compact manifolds without boundary, in particular on torii, while the geometry of physical systems of relevance for applications is certainly not that of torii, rather that of finite portions of  $\mathbb{R}^3$  delimited by boundaries, like finite 3D cylinders. Furthermore at larger scales, the fluids of interest for applications should present a non-chaotic behavior similar to that of the Poiseuille flow (see for instance [30]). How could we try to reconcile the two conflicting needs? A new window of opportunity opens up with the relatively new set up of Beltrami fields in  $\mathfrak{b}$ -manifolds, which can be viewed as compact manifolds with boundaries. In this section we make a short review of this new approach which, as already stressed, we desire to combine with our group theoretical classification of Beltrami fields. Essentially we collect the main definitions and concepts developed in particular by Victor Guillemin, Eva Miranda, Robert Cardona, Daniel Peralta Salas and other collaborators in [3, 18, 19, 20, 21, 22], having, as main goal, that of discussing the example of the  $\mathfrak{b}$ -modified ABC flow<sup>5</sup> presented in [18]. Such a discussion will be done, in view of the underlying group theoretical structures, in section 6.1.

In order to introduce the  $\mathfrak{b}$ -generalization of contact manifolds we have first to set the stage by recalling essential facts and definitions about symplectic manifolds and Poisson structures.

---

<sup>5</sup>see section 4.1.2 for the definition of ABC flows

### 3.2.1 Symplectic and Poisson Manifolds

We begin with

**Definition 3.9** A symplectic manifold is a pair  $(\mathcal{SM}_{2n+2}, \omega)$  of a smooth manifold  $\mathcal{SM}_{2n+2}$  in even dimension  $2n + 2$  and a 2-form  $\omega$  which is closed and non degenerate of maximal rank:

$$d\omega = 0 \quad ; \quad \omega \wedge \omega \wedge \cdots \wedge \omega \neq 0 \quad \text{everywhere on } \mathcal{SM}_{2n+2} \quad (3.26)$$

On a symplectic manifold we have a naturally defined antisymmetric quadratic form on the space of sections of the tangent bundle, *i.e.* on the vector fields:

$$\begin{aligned} \omega & : \quad \Gamma[\mathcal{TSM}_{2n+2}, \mathcal{SM}_{2n+2}] \times \Gamma[\mathcal{TSM}_{2n+2}, \mathcal{SM}_{2n+2}] \longrightarrow C^{(\infty)}(\mathcal{SM}_{2n+2}) \\ \forall X, Y \in \Gamma[\mathcal{TSM}_{2n+2}, \mathcal{SM}_{2n+2}] & \quad , \quad \omega(X, Y) \in C^{(\infty)}(\mathcal{SM}_{2n+2}) \end{aligned} \quad (3.27)$$

Poisson manifolds are instead defined as follows.

**Definition 3.10** A Poisson manifold  $(\mathcal{PM}_m, \{, \})$  is the pair of a smooth manifold  $\mathcal{PM}_m$  of dimension  $m$  and a Poisson bracket  $\{, \}$  which is a binary operation on the space of smooth functions on the manifold:

$$\{, \} : C^{(\infty)}(\mathcal{PM}_m) \times C^{(\infty)}(\mathcal{PM}_m) \longrightarrow C^{(\infty)}(\mathcal{PM}_m) \quad (3.28)$$

satisfying the following three properties:

- 1) *Antisymmetry*  $\{f, g\} = -\{g, f\}, \quad \forall f, g \in C^{(\infty)}(\mathcal{PM}_m)$
- 2) *Jacobi Identity*  $\{f, \{g, h\}\} + \{g, \{h, f\}\} + \{h, \{f, g\}\} = 0, \quad \forall f, g, h \in C^{(\infty)}(\mathcal{PM}_m)$
- 3) *Leibniz rule*  $\{f, g \cdot h\} = \{f, g\}h + g\{f, h\}, \quad \forall f, g, h \in C^{(\infty)}(\mathcal{PM}_m)$

The first two properties mentioned in the definition 3.10 guarantee that the space of functions on the Poisson manifold becomes a Lie algebra once equipped with the Poisson bracket. On the other hand the third property implies that to each function  $f \in C^{(\infty)}$  the Poisson bracket associates a derivation of the commutative algebra of functions on the manifold, namely, by definition a vector field  $\mathbf{X}_f$ , named the **hamiltonian vector field** of  $f$ .

Locally, in any coordinate patch  $\{x_1, \dots, x_j\}$ , the Poisson bracket takes the following form:

$$\{f, g\} = \pi^{ij}(x) \frac{\partial f}{\partial x^i} \frac{\partial g}{\partial x^j} \quad ; \quad \pi^{i,j}(x) = -\pi^{j,i}(x) \quad (3.29)$$

where the contravariant antisymmetric tensor  $\pi^{ij}(x)$  is usually called a **bivector**. The hamiltonian vector field  $\mathbf{X}_f$  is then easily identified:

$$\mathbf{X}_f = \pi^{ij} \partial_i f \partial_j \quad (3.30)$$

Let us now suppose that the dimension of the Poisson manifold is even  $m = 2n + 2$  and that the bivector  $\pi^{ij}(x)$  is an everywhere invertible matrix. Setting:  $\omega = \pi_{k\ell}^{-1} dx^k \wedge dx^\ell$  we obtain a symplectic 2-form of maximal rank which is closed as a consequence of the Jacobi identities satisfied by the bivector. In this way the Poisson manifold is recognized to be a symplectic manifold. In particular we can set:

$$\{f, g\} = \omega(\mathbf{X}_f, \mathbf{X}_g) \quad (3.31)$$

**Definition 3.11** Let  $(\mathcal{SM}_{2n+2}, \omega)$  be a symplectic manifold. A Liouville vector field is a vector field that leaves the symplectic form  $\omega$  invariant, namely:

$$\omega = \mathcal{L}_X \omega \equiv i_X d\omega + d(i_X \omega), \quad (3.32)$$

where  $\mathcal{L}_X$  denotes the Lie derivative along the vector field.

### 3.2.2 Relation between symplectic and contact manifolds

Let us consider a symplectic manifold  $(\mathcal{SM}_{2n+2}, \omega)$  and let us assume that it admits at least one Liouville vector field  $\mathbf{L}$ . Let moreover  $\Sigma_{\mathbf{L}} \subset \mathcal{SM}_{2n+2}$  be a hypersurface transverse to the Liouville vector field  $\mathbf{L}$ . Then we realize that  $\Sigma_{\mathbf{L}}$  is a contact manifold with contact form  $\alpha = i_{\mathbf{L}}\omega$ . If  $\Sigma_{\mathbf{L}}$  is transverse to  $\mathbf{L}$  the form  $\alpha$  vanishes on  $\mathbf{L}$  and no-where vanishes on  $T\Sigma_{\mathbf{L}}$ . To verify that it is indeed a contact form we just have to compute:

$$\alpha \wedge \underbrace{d\alpha \wedge \cdots \wedge d\alpha}_{n\text{-times}} = i_{\mathbf{L}}\omega \wedge \underbrace{di_{\mathbf{L}}\omega \wedge \cdots \wedge di_{\mathbf{L}}\omega}_{n\text{-times}} = i_{\mathbf{L}}\omega \wedge \underbrace{\omega \wedge \cdots \wedge \omega}_{n\text{-times}} = \frac{1}{n+1} i_{\mathbf{L}} \left( \underbrace{\omega \wedge \cdots \wedge \omega}_{(n+1)\text{-times}} \right) = \text{Vol}_{\Sigma_{\mathbf{L}}} \quad (3.33)$$

The last equation is true because  $\omega^{n+1}$  is the volume form of the ambient symplectic manifold and the hypersurface  $\Sigma_{\mathbf{L}}$  is by hypothesis transverse to the Liouville vector field.

Conversely given a contact manifold  $(\mathcal{M}_{2n+1}, \xi)$  with contact form  $\alpha$  and Reeb field  $\mathbf{R}$ , any hypersurface  $\Sigma \subset \mathcal{M}_{2n+1}$  which is transverse to the Reeb field  $\mathbf{R}$  automatically acquires the structure of a symplectic manifold with symplectic form  $\tilde{\omega} = d\alpha|_{\Sigma}$ .

Hence we can have odd-dimensional contact manifolds that sit in between two symplectic manifolds of adjacent dimensions as shown in the following diagram:

$$\begin{array}{ccccc} (\mathcal{SM}_{2n}, \tilde{\omega} = d\alpha) & \xhookrightarrow{\quad} & (\mathcal{M}_{2n+1}, \alpha = i_{\mathbf{L}}\omega) & \xhookrightarrow{\quad} & (\mathcal{SM}_{2n+2}, \omega) \\ \downarrow & & \downarrow & & \downarrow \\ \text{symplectic} & & \text{contact} & & \text{symplectic} \\ \text{transverse to Reeb field} & & \text{transverse to Liouville field} & & \end{array} \quad (3.34)$$

The scheme described in eq.(3.34) reminds that occurring with Sasaki manifolds that sit in between two Kähler manifolds which, indeed, are special instances of symplectic manifolds, the symplectic form being the Kähler 2-form.

### 3.2.3 $\mathfrak{b}$ -Manifolds

Having recalled for reader's ease the above concepts and definitions we come to our main goal that is the definition of  $\mathfrak{b}$ -manifolds. Following [19, 3] we set:

**Definition 3.12** A  $\mathfrak{b}$ -manifold is a pair  $(\mathcal{M}, \Sigma)$  where  $\mathcal{M}$  is a differentiable manifold and  $\Sigma \subset \mathcal{M}$  is a hypersurface, namely a submanifold of codimension one.

Given two  $\mathfrak{b}$ -manifolds  $(\mathcal{M}, \Sigma)$  and  $(\mathcal{N}, \Pi)$  one defines as follows a smooth  $\mathfrak{b}$ -map between them.

**Definition 3.13** *A smooth map*

$$f : \mathcal{M} \longrightarrow \mathcal{N} \quad (3.35)$$

is a  $\mathfrak{b}$ -map:

$${}^b f : (\mathcal{M}, \Sigma) \longrightarrow (\mathcal{N}, \Pi) \quad (3.36)$$

if  $f$  is transverse to  $\Pi$  and  $f^{-1}(\Pi) = \Sigma$

With this setup one can re-establish all the basic ingredients of differential geometry in the  $\mathfrak{b}$ -version. We begin with vector fields.

**Definition 3.14** *A  $\mathfrak{b}$ -vector field on  $\mathfrak{b}$ -manifold  $(\mathcal{M}_{m+1}, \Sigma_m)$  is a vector field  ${}^b \mathbf{X}$  which is tangent to the hypersurface  $\Sigma_m$  in all  $p \in \Sigma_m$*

In an open neighborhood  $U \subset \mathcal{M}_{m+1}$  that contains the point  $p \in \Sigma$  we can choose the coordinates in the following way. Let  $\sigma(x_0, x_1, \dots, x_m)$  be the function whose vanishing defines the surface  $\Sigma_m$  in that neighborhood. We can trade one of the standard coordinates  $x_i$ , say  $x_0$ , for the value  $s = \sigma(x_0, \dots, x_{m+1})$  of the function, regarding the remaining ones  $\mathbf{x} = \{x_1, \dots, x_m\}$  as coordinates on the hypersurface  $\Sigma$ . Using such coordinate frame a vector field parallel to the surface is of the form:

$${}^b \mathbf{X} = s X_0(\mathbf{x}) \frac{\partial}{\partial s} + \sum_{i=1}^m X^i(s, \mathbf{x}) \frac{\partial}{\partial x^i} \quad (3.37)$$

One can easily check that under standard commutation the  $\mathfrak{b}$ -vector fields form a Lie subalgebra of the Lie algebra of vector fields. They can be considered the sections of a new vector-bundle on  $\mathcal{M}_{m+1}$  that we name the  $\mathfrak{b}$ -tangent bundle:  ${}^b T\mathcal{M}_{m+1} \xrightarrow{\pi} \mathcal{M}_{m+1}$ . This being established the road easily climbs down. We obtain the the  $\mathfrak{b}$ -cotangent bundle by usual duality.

In practice as shown in [21] the  $\mathfrak{b}$  de-Rham complex is structured as follows. A  $k$ -form  ${}^b \omega \in {}^b \Omega^k(\mathcal{M})$ , namely a section of the  $k$ -th external power of the cotangent bundle  ${}^b T^* \mathcal{M}$  can always be written as:

$${}^b \omega = \frac{ds}{s} \wedge \alpha + \beta \quad ; \quad \alpha \in \Omega^{k-1}(\mathcal{M}) \quad ; \quad \beta \in \Omega^k(\mathcal{M}) \quad (3.38)$$

Furthermore in [21] it is stated and shown that although  $\alpha, \beta$  are not unique in the bulk of the manifold they are unique at every point  $p \in \Sigma$  on the distinguished surface or boundary.

This provides an algorithmic tool to perform the  $b$ -deformation of any given Riemannian metric on a given manifold  $\mathcal{M}$ .

Relevant to our goals is the  $\mathfrak{b}$ -generalization of the definition of contact manifolds.

**Definition 3.15** *Let  $(\mathcal{M}, \Sigma)$  be a  $(2n + 1)$ -dimensional,  $\mathfrak{b}$ -manifold. A  $\mathfrak{b}$ -contact structure is the kernel of a  $\mathfrak{b}$ -one-form  $\alpha \in {}^b T^* \mathcal{M}$  that satisfies the condition:*

$$\alpha \wedge d\alpha \wedge \dots \wedge d\alpha \neq 0 \quad (3.39)$$

In this case  $\alpha$  is a  $\mathfrak{b}$ -contact form and  $\xi = \ker \alpha$  is a  $\mathfrak{b}$ -contact structure.

As in the un-deformed case we can introduce the  $\mathfrak{b}$ -Reeb field as that particular  $\mathfrak{b}$ -vector field  $\mathbf{R}$  which satisfies the two conditions:

$$i_{\mathbf{R}} \cdot d\alpha = 0 \quad ; \quad \alpha(\mathbf{R}) = 1 \quad (3.40)$$



As we are going to see in section 6.1, the use of  $\mathfrak{b}$ -deformations can introduce modified Beltrami fields that are parallel to certain boundaries. The open deep question that is touched upon and put into evidence in chapter 6 is that the choice of an allowed distinguished surface  $\Sigma$  seem to depend on the group structure of the Beltrami field one wants to  $\mathfrak{b}$ -deform. Up to the knowledge of the authors this aspect was not so far discussed in the literature. It appears to be a very momentous question worth an in depth investigation.

## 4 Harmonic Analysis and the Algorithm

### 4.1 Beltrami equation and harmonic analysis

In the present section which is partly based on a corresponding section of [1], partly new, we stress that all the arguments presented above have been instrumental to enlighten the role of Beltrami vector fields from various viewpoints related with hydrodynamics and lagrangian chaos. Let us now consider from a more general point of view Beltrami equation (2.30). The one here at stake is the case  $p = 1$  of an eigenvalue equation that can be written in any  $(2p + 1)$ -dimensional Riemannian manifold  $(\mathcal{M}_p, g)$ , namely:

$$\star_g d\omega^{(p)} = \lambda \omega^{(p)} \quad (4.1)$$

The eigenfunctions of the  $\star_g d$  operator are 1-forms for  $p = 1$ , namely in three-dimensions, but they are higher differential forms in higher odd dimensions. Another particularly interesting case is that of 7-manifolds where the eigenfunctions of  $\star_g d$  are three-forms and can be related with a  $G_2$ -structure of the manifold [31, 32, 33]. On the other hand the relation encoded in theorem 3.3 between eq.(4.1) and contact structures, as they are defined in current mathematical literature, is true only for  $p = 1$  and it is lost for higher  $p$ . Indeed contact structures are always defined in terms of a contact one-form  $\alpha$  and by the condition:

$$\alpha \wedge \underbrace{d\alpha \wedge d\alpha \dots d\alpha}_{p\text{-times}} \neq 0 \quad (4.2)$$

Hence the problem of determining the spectrum and the eigenfunctions of the operator  $\star_g d\omega^{(p)}$  is a general one and can be addressed in the same way in all odd-dimensions, yet its relation with flows and contact-structures is peculiar to  $d = 3$  and has not a general significance. In any case it is absolutely clear that once the correspondence of theorem 3.3 has been established, the classification of Beltrami fields is reduced to a classical problem of differential geometry whose solution can be derived within a time honored framework which makes no reference to trajectories and contact structures.

The framework we refer to is that of *harmonic analysis* on compact Riemannian manifolds  $(\mathcal{M}, g)$  and its application to the spectral analysis of Laplace-Beltrami operators (for reviews see the book [34] and the articles [35, 36, 37, 38, 39]). As thoroughly discussed in the quoted references there are, on a Riemann manifold  $(\mathcal{M}, g)$ , several invariant differential operators, generically named Laplace-Beltrami some of which are of second order, some other of first order. They act on the sections of vector bundles  $E \rightarrow \mathcal{M}$  of different rank, for instance the tangent bundle, the bundle of  $p$ -forms, the bundle of symmetric two tensors, the spinor bundle etc. Among the first order operators the most important ones are the Dirac operator acting on sections of the spinor bundle and the  $\star_g d$ -operator acting on  $p$ -forms in a  $(2p + 1)$ -dimensional manifold. The spectrum of all Laplace-Beltrami operators is sensitive both to the topology and to the metric of the underlying manifold. Each eigenspace is organized into irreducible representations of the isometry group  $G$  of the metric  $g$  and the eigenfunctions assigned to a particular representation are generically named *harmonics*.

Here comes an important distinction in relation with the nature of the group  $G$ . If  $G$  is a Lie group and if the manifold  $\mathcal{M}$  is homogeneous under its action, than  $\mathcal{M} \sim G/H$  where  $H \subset G$  is the stability subgroup of some reference point  $p_0 \in \mathcal{M}$ . In this case harmonic analysis reduces completely to group-theory and the spectrum of any Laplace-Beltrami operator can be derived in pure algebraic terms without ever using any differential operations. In the case  $G$  is not a Lie group and/or  $\mathcal{M}$  is not homogeneous under its action, then matters become more complicated and *ad hoc* techniques have to be utilized case by case to analyze the spectrum of invariant operators.

#### 4.1.1 Harmonic analysis on the $T^3$ torus and the Universal Classifying Group

The reasons to compactify Arnold-Beltrami flows on a  $T^3$  have already been discussed and we do not resume the issue. We just observe that  $\mathbb{R}^3$  is a non-compact coset manifold so that harmonic analysis over  $\mathbb{R}^3$  is a complicated matter of functional analysis. After compactification, namely after imposing periodic boundary conditions, things drastically simplify.

Firstly, as we explained above the compactification is obtained by quotienting  $\mathbb{R}^3$  with respect to a discrete subgroup of the translation group which constitutes a lattice (see eq.(2.3)).

Secondly we implement the programme of harmonic analysis by presenting a general algorithm to construct solutions of the Beltrami equation which utilizes as main ingredient the orbits under the action of the point group  $\mathfrak{P}_\Lambda$  of three-vectors in the momentum lattice  $^*\Lambda$  that is just the dual of the lattice  $\Lambda$ . In the language of crystallography the point group is just the discrete subgroup  $\mathfrak{P}_\Lambda \subset SO(3)$  of the rotation group which maps the lattice  $\Lambda$  and its dual  $^*\Lambda$  into themselves:

$$\mathfrak{P}_\Lambda \Lambda = \Lambda \quad ; \quad \mathfrak{P}_\Lambda ^*\Lambda = ^*\Lambda \quad (4.3)$$

In the case of the cubic lattice, that is the main example studied in paper [1] we have  $\mathfrak{P}_{\text{cubic}} = O_{24}$  where  $O_{24} \sim S_4$  is the proper octahedral group of order  $|O_{24}| = 24$ . In the case of the hexagonal lattice which was only briefly touched upon in [1] and which instead we analyze in depth in the present work, the point group is the dihedral group  $Dih_6$  of order  $|Dih_6| = 12$ .

Thirdly, as it was originally conceived and introduced for the first time in [1], a general argument, inspired by the logic that crystallographers used to derive and classify space groups, leads to introduce a large finite group  $\mathfrak{UG}_\Lambda$ , named by the authors of [1] the *Universal Classifying Group for the Lattice*  $\Lambda$ , made out of discretized rotations and translations that are defined by the structure of  $\Lambda$ . All eigenfunctions of the  $\star_g$ -operator can be organized into a finite number of classes and each class decomposes in a specific unique way into the irreducible representations of  $\mathfrak{UG}_\Lambda$ . Hence all Arnold-Beltrami vector fields are in correspondence with the irreps of  $\mathfrak{UG}_\Lambda$ . Knowing the branching rules of such irreps with respect to its various subgroups  $H_i \subset \mathfrak{UG}_\Lambda$  and selecting the identity representation one obtains Arnold-Beltrami vector fields invariant with respect to those  $H_i$  for which we are able to find an identity irrep  $D_1$  in the branching rules. In this way we can classify all Arnold Beltrami flows and also uncover their *hidden symmetries*.

Such a conclusion was already reached in [1].

As we recalled above, the authors of [1] considered in an extensive way the case of the cubic lattice and constructed the corresponding Universal Classifying Group  $\mathfrak{UG}_{\text{cubic}} = G_{1536}$ . This latter is a finite group of order  $|G_{1536}| = 1536$  which was studied in full detail in [1]. All of its 37 irreducible representations were derived and the associated character table was also constructed. A large class of its subgroups  $H_i \subset G_{1536}$  were also singled out and each of them was studied systematically, by constructing their irreps and character tables. This allowed the derivation of all the *branching rules* of the 37 irreps of  $G_{1536}$  with respect to the considered

subgroups which were displayed in dedicated tables in the appendices of [1]. In the present paper one of the goals is that of providing the same group theoretical lore for the case of the hexagonal lattice which in [1] was only briefly touched upon and sketched.

Since the crystallographic lattices are more than two one might think that covering these two cases is only part of the work. It is not so. Mastering the Universal Classifying Groups for the cubic and hexagonal lattices is sufficient to provide the entire picture. Indeed the crystallographic lattices in D=3 subdivide just in two classes:

**A)** The lattices whose basis vectors  $\mathbf{w}_\lambda$  provide an orthogonal basis (although not necessarily orthonormal):

$$(\mathbf{w}_\lambda, \mathbf{w}_\mu) = a_\lambda^2 \delta_{\lambda\mu} \quad (4.4)$$

where  $\delta_{\lambda\mu}$  is the Kronecker delta and  $a_\lambda$  is the lattice spacing in direction  $\lambda = 1, 2, 3$ .

**B)** The lattices whose basis vectors  $\mathbf{w}_\lambda$  are arranged as follows:

$$\begin{aligned} (\mathbf{w}_1, \mathbf{w}_1) = (\mathbf{w}_2, \mathbf{w}_2) &= a^2 \quad ; \quad (\mathbf{w}_3, \mathbf{w}_3) = b^2 \\ (\mathbf{w}_1, \mathbf{w}_2) &= a^2 \cos \left[ \frac{2\pi}{3} \right] \\ (\mathbf{w}_1, \mathbf{w}_3) = (\mathbf{w}_2, \mathbf{w}_3) &= 0 \end{aligned} \quad (4.5)$$

$a$  being the lattice spacing in each horizontal plane spanned by  $\mathbf{w}_{1,2}$  which is endowed with a hexagonal tessellation and  $b$  the lattice spacing in the third vertical direction.

The point groups pertaining to the lattices of class A) are:

$$\mathfrak{P}_{\Lambda_A} = (C_2, C_4, \text{Dih}_2, \text{Dih}_4, T_{12}, O_{24}) \quad (4.6)$$

where  $C_n$  denotes the cyclic group of order  $n$ ,  $\text{Dih}_m$  denotes the dihedral group of order  $m$  and  $T_{12}$  is the tetrahedral group, while  $O_{24}$  is the already mentioned octahedral group. All the point groups in the list (4.6) are subgroups of the maximal one  $O_{24}$ .

The point groups pertaining to the lattices of class B) are:

$$\mathfrak{P}_{\Lambda_B} = (C_3, C_6, \text{Dih}_3, \text{Dih}_6) \quad (4.7)$$

All the point groups in the list (4.7) are subgroups of the maximal one  $\text{Dih}_6$ .

This fact has the important consequence that the Universal Classifying Group for the cubic lattice contains as subgroups the Universal Classifying Groups for all the other lattices of class A), while the Universal Classifying group for the hexagonal lattice contains as subgroups all the Universal Classifying Groups for the lattices of class B). Since, as we explain below, the construction of Beltrami fields is organized into irreps of such classifying groups, once we have the algorithm for the largest group we have also that for all its subgroups.

In the case of the cubic lattice, the main result of [1] was the proof that the  $O_{24}$  orbits in the cubic lattice arrange into 48 equivalence classes, the parameters of the corresponding Beltrami vector fields filling all the 37 irreducible representations of  $G_{1536}$ .

### 4.1.2 The classical ABC flows

The following vector field:

$$\mathbf{u}(x, y, z) = \mathcal{V}^{(ABC)}(x, y, z) \equiv \begin{pmatrix} C \cos(2\pi y) + A \sin(2\pi z) \\ A \cos(2\pi z) + B \sin(2\pi x) \\ B \cos(2\pi x) + C \sin(2\pi y) \end{pmatrix} \quad (4.8)$$

which satisfies the Beltrami condition with eigenvalue  $\lambda = 1$  and which contains three real parameters  $A, B, C$  defines what is known in the literature by the name of an ABC-flow (Arnold-Beltrami-Childress) and during the last half century it was the target of fantastically numerous investigations.

Main motivation of the paper [1] was to understand the principles underlying the construction of the ABC-flows in order to use systematically such principles to construct and classify all other Arnold-like Beltrami flows, deriving also, as a bonus, their hidden discrete symmetries. For instance symmetries of Beltrami flows have proved to be crucial in connection with their use in modeling *magneto-hydrodynamic fast dynamos*[40],[14],[13],[15]. By this words it is understood the mechanism that in a steady flow of charged particles generates a large scale magnetic field whose magnitude might be exponentially increasing with time. No analytic results do exist on fast dynamos and all studies have been so far numerical, yet while dealing with these latter, crucial simplifications occur and optimization algorithms become available if the steady flow possesses a large enough group  $G_{\text{sim}} \subset \mathcal{UG}_\Lambda$  of symmetries. In this case the magnetic field can be developed into irreducible representations of  $G_{\text{sim}}$  and this facilitates the numerical determination of growing rates of different modes. It is important to stress that the linearized dynamo equations for the magnetic field  $\mathbf{B}$  coincide with the linearized equations for perturbations around a steady flow. Therefore the same development of perturbations into irreps of  $G_{\text{sim}}$  is of great relevance also for the study of fluid instabilities.

As already stressed a much shorter sketch of the Hexagonal Lattice was provided in [1] in order to emphasize the generality of the applied methods, yet the authors did not address the construction of the Universal Classifying Group which is one of the tasks addressed in the present paper.

## 4.2 The spectrum of the $\star d$ operator on $T^3$

The main issue of paper [1] was the construction of vector fields defined over the three-torus  $T^3$  that are eigenstates of the  $\star_g d$  operator, namely solutions of the following equation:

$$\star_g d\Omega^{(n;I)} = m_{(n)} \Omega^{(n;I)} \quad ; \quad \Omega^{(n;I)} [V_{(m;J)}] = \delta_m^n \delta_J^I \quad (4.9)$$

where  $d$  is the exterior differential, and  $\star_g$  is the Hodge-duality operator which, differently from the exterior differential, can be defined only with reference to a given metric  $g$ . By  $\Omega^{(n;I)}$  we denote a one-form:

$$\Omega^{(n;I)} = \Omega_\mu^{(n;I)} dx^\mu \quad (4.10)$$

which is declared to be dual to the vector field we are interested in:

$$\begin{aligned} V_{(m;J)} &= V_{(m;J)}^\mu \partial_\mu \\ \Omega^{(n;I)} [V_{(m;J)}] &\equiv \Omega_\mu^{(n;I)} V_{(m;J)}^\mu = \delta_m^n \delta_J^I \end{aligned} \quad (4.11)$$

and by means of the composite index  $(n; I)$  we make reference to the quantized eigenvalues  $m_{(n)}$  of the  $\star_g d$  operator (ordered in increasing magnitude  $|m_{(n)}|$ ) and to a basis of the corresponding eigenspaces

$$\star_g d\Omega^{(n)} = m_{(n)}\Omega^{(n)} \quad \Rightarrow \quad \Omega^{(n)} = \sum_{I=1}^{d_n} c_I \Omega^{(n;I)} \quad (4.12)$$

the symbol  $d_n$  denoting the degeneracy of  $|m_{(n)}|$  and  $c_I$  being constant coefficients.

Indeed, since  $T^3$  is a compact manifold, the eigenvalues  $m_{(n)}$  form a discrete set. Their values and their degeneracies are a property of the metric  $g$  introduced on it. Here we outline the general procedure to construct the eigenfunctions of  $\star_g d$ , to calculate the eigenvalues and to determine their degeneracies. What follows is an elementary and straightforward exercise in harmonic analysis.

In tensor notation, equation (4.9) has the following appearance:

$$\frac{1}{2} g_{\mu\nu} \epsilon^{\nu\rho\sigma} \partial_\rho \Omega_\sigma = m \Omega_\mu \quad (4.13)$$

The equation written above was named Beltrami equation since it was already considered by the great italian mathematician Eugenio Beltrami in 1881 [41], who presented one of its periodic solutions previously constructed by Gromeka in 1881. Such a solution was inherited by Arnold and it is essentially the basis of his Hydrodynamical Model. We will see that Arnold Model just corresponds to the lowest eigenfunction of the  $\star_g d$ -operator in the case of the cubic lattice. Many more similar models can be constructed choosing higher eigenvalues, choosing irreducible representation of the point group in their eigenspaces or changing the lattice.

Introducing the basis vectors of the dual lattice  $\Lambda^*$  we can write:

$$\Omega = \Omega_\mu dr^\mu = \Omega_\mu e_i^\mu dx^i = \Omega_i dx^i \quad (4.14)$$

where  $e_i^\mu$  are the components of the vectors  $\mathbf{e}^\mu$  in a standard orthogonal basis of  $\mathbb{R}^3$  and

$$x^i = w_\mu^i r^\mu \quad (4.15)$$

are a new set of euclidian coordinates obtained from the original ones  $r^\mu$  by means of the components  $w_\mu^i$  of the basis vectors  $\mathbf{w}_\mu$  of the space lattice  $\Lambda$ . Recalling that:

$$\partial_\mu = \frac{\partial}{\partial r^\mu} = w_i^\mu \partial_i = w_i^\mu \frac{\partial}{\partial x^i} \quad (4.16)$$

with a little bit of straightforward algebra we can rewrite eq.(4.9) in the equivalent universal way:

$$\frac{1}{2} \epsilon_{ijk} \partial_j \Omega_k = \mu \Omega_i \quad ; \quad \mu = \frac{m}{\det w} \quad (4.17)$$

where by  $\det w$  we denote the determinant of the  $3 \times 3$  matrix  $w_\mu^i$ .

### 4.3 Fourier expansions and Beltrami chirality

It is now the appropriate moment to point out that the first order Beltrami operator is a chirality operator that splits the ordinary Fourier spectrum of any vector field defined over the three torus in two disjoint sectors of **positive** and **negative Beltramicity**, respectively.

This statement is easily understood by means of the following elementary discussion. Given a Riemannian three-manifold  $(\mathcal{M}, g)$ , the Laplace–Beltrami operator on one-forms is given by:

$$\Delta_g = \star_g d \star_g d \quad (4.18)$$

namely it is the square of the Beltrami operator  $\mathfrak{B}_g \equiv \star_g d$ . Hence any eigenstate  $\Omega^{[U]}$  of the Beltrami operator with eigenvalue  $\mu$  is automatically an eigenstate of the Laplace–Beltrami operator  $\Delta_g$  with eigenvalue  $\mu^2$ :

$$\mathfrak{B}_g \Omega^{[U]} = \mu \Omega^{[U]} \quad \Rightarrow \quad \Delta_g \Omega^{[U]} = \mu^2 \Omega^{[U]} \quad (4.19)$$

Inverting the argument one expects that the eigenspace of  $\Delta_g$  corresponding to an eigenvalue  $E = \mu^2 > 0$ , that is a linear vector space, can be partitioned in two vector subspaces, respectively spanned by the solutions of Beltrami equation with eigenvalue  $\mu = \pm\sqrt{E}$ . This is precisely what it happens for the one-form duals of vector fields defined on torii  $T^3 = \mathbb{R}^3/\Lambda$  where  $\Lambda$  is a lattice.

Let us name  $U_i(\mathbf{x})$  a generic vector field on  $T^3$ , its most general form is necessarily provided by the standard Fourier expansion that we write as follows<sup>6</sup>:

$$\begin{aligned} U_i(\mathbf{x}) &= \sum_{\mathbf{k} \in \Lambda^*} Y_i(\mathbf{k} | \mathbf{x}) \\ Y_i(\mathbf{k} | \mathbf{x}) &= v_i(\mathbf{k}) \cos(2\pi \mathbf{k} \cdot \mathbf{x}) + \omega_i(\mathbf{k}) \sin(2\pi \mathbf{k} \cdot \mathbf{x}) \end{aligned} \quad (4.20)$$

The condition that the momenta  $\mathbf{k}$  included in the Fourier expansion should belong to the dual lattice guarantees that each mode  $Y_i(\mathbf{x})$  is periodic with respect to the space lattice  $\Lambda$  and, a fortiori, such is the vector field  $U_i(\mathbf{x})$ . Indeed, by means of the very definition of the dual lattice (2.9) it follows that:

$$\forall \mathbf{q} \in \Lambda : \quad Y_i(\mathbf{x} + \mathbf{q}) = Y_i(\mathbf{x}) \quad (4.21)$$

If  $U_i(\mathbf{x})$  is supposed to be the velocity field of a fluid, then, in force of Navier-Stokes or Euler equations, it must be divergenceless  $\partial^i U_i = 0$  and this requires that we impose such a condition on each mode, namely  $\partial^i Y_i(\mathbf{k} | \mathbf{x}) = 0$ . Imposing this constraint on the general ansatz (4.20) we obtain:

$$\mathbf{k} \cdot \mathbf{v}(\mathbf{k}) = 0 \quad ; \quad \mathbf{k} \cdot \boldsymbol{\omega}(\mathbf{k}) = 0 \quad (4.22)$$

which reduces the 6 parameters per mode contained in the general ansatz (4.20) to 4 per mode. At the same time we can easily verify that the vector field:

$$\mathbf{Y}_{\mathbf{k}}(\mathbf{x}) \equiv Y_i(\mathbf{k} | \mathbf{x}) \frac{\partial}{\partial x^i} \quad (4.23)$$

is dual to a 1-form  $\Omega^{[Y_{\mathbf{k}}]}$  that is an eigenstate of the Laplace-Beltrami operator with the explicit eigenvalue displayed in the following formula:

$$\Delta_g \Omega^{[Y_{\mathbf{k}}]} = \mu^2 \Omega^{[Y_{\mathbf{k}}]} \quad (4.24)$$

$$\mu^2 = \pi^2 \langle \mathbf{k}, \mathbf{k} \rangle \quad (4.25)$$

---

<sup>6</sup>Take note that the latin indices  $i, j, ..$  refer to the standard euclidian metric of  $\mathbb{R}^3$  in whose basis the components of the momentum vectors lying in the dual lattice  $\Lambda^*$  are not necessarily integer valued.

Let us now set:

$$r = \sqrt{\langle \mathbf{k}, \mathbf{k} \rangle} \quad \Rightarrow \quad \mu^2 = \pi^2 r^2 \quad (4.26)$$

The degeneracy of each Laplace-Beltrami eigenvalue  $\pi^2 r^2$  is geometrically provided by counting the number of intersection points of the dual lattice  $\Lambda^*$  with a sphere whose center is in the origin and whose radius is  $r$ . For a generic lattice the number of solutions of equation (4.26) namely the number of intersection points of the lattice with the sphere is either 0 (the sphere does not intersect the lattice) or just two:  $\pm \mathbf{k}$  (the sphere intersects the lattice in two points), so that the typical degeneracy of each eigenvalue is just 2. On the other hand, if the lattice  $\Lambda$  is one of the Bravais lattices admitting a non trivial point group  $\mathfrak{P}_\Lambda$ , then the number of solutions of eq.(4.26) is larger, since all lattice vectors  $\mathbf{k}$  that sit in one orbit of  $\mathfrak{P}_\Lambda$  have the same norm and therefore are located on the same spherical layer. Hence we ought to consider the spherical layers of radius  $r_k = \sqrt{\mathbf{k}^2}$  defined as the intersection of a sphere of such a radius with the momentum lattice:

$$\text{SL}_{r_k} \equiv \mathbb{S}_{r_k} \cap \Lambda^* \quad (4.27)$$

The set of available radii for which the corresponding spherical layer is not an empty set is an infinite increasing sequence of rational numbers:

$$0 < r_1 < r_2 < \dots < r_k < \dots \infty \quad (4.28)$$

whose explicit form depends on the chosen lattice  $\Lambda$ . In each spherical layer  $\text{SL}_{r_k}$  we find a certain finite number of points:

$$|\text{SL}_{r_k}| \equiv \# \text{ of points in } \text{SL}_{r_k} \quad (4.29)$$

which in the average steadily increases with  $r_k$ , yet it strongly fluctuates on the short range (see section 7 for more details on this point). Indeed, in a rather capricious way, depending on the choice of the primary lattice  $\Lambda$  and, hence, of the point group  $\mathfrak{P}_\Lambda$ , each spherical layer  $\text{SL}_{r_k}$  decomposes into a certain number  $n_{r_k} \in \mathbb{N}$  of orbits:

$$\text{SL}_{r_k} = \bigcup_{i=1}^{n_{r_k}} \mathcal{O}_i^{\ell_i}(r_k) \quad (4.30)$$

where  $i$  is an enumeration index and  $\ell_i$  is the length of the orbit  $\mathcal{O}_i^{\ell_i}(r_k)$ , namely the number of elements it contains. Each point groups admits a finite number of orbit types of a characteristic length, whose maximal value is the order of the point group  $|\mathfrak{P}_\Lambda|$ . Actually the orbits are in one-to-one correspondence with the possible stability subgroups  $\mathcal{H}_i \subset \mathfrak{P}_\Lambda$  of moment vectors and the orbit lengths are just the orders of these corresponding subgroups which, by Lagrange theorem, are divisors of the order of the point group. Since, by definition, orbits are disjoint sets we have:

$$|\text{SL}_{r_k}| = \sum_{j=1}^{n_{r_k}} \ell_j \quad (4.31)$$

In view of this discussion the general Fourier series of eq.(4.20) can be reorganized in the following way:

$$\mathbf{U}(\mathbf{x}) = \sum_{q=1}^{\infty} \underbrace{\sum_{\mathbf{k} \in \text{SL}_{r_q}} \mathbf{Y}_{\mathbf{k}}(\mathbf{x})}_{\mathbf{W}_{r_q}(\mathbf{x})} \quad (4.32)$$

The vector field  $\mathbf{W}_{r_k}(\mathbf{x})$  is the most general divergenceless one associated with the spherical layer  $\text{SL}_{r_k}$  and,

according with the counting provided above, in principle it contains a number of parameters that is  $4 \times |\text{SL}_{r_k}|$  since there are 4 parameters for each momentum vector  $\mathbf{k}$ . There is however a subtlety. Necessarily both  $\pm\mathbf{k}$  are located on the same layer since they have the same norm. For each of these momentum pairs the number of parameters appearing in  $\mathbf{W}_{r_k}(x)$  is not 8 rather it is 4, since  $\cos(\mathbf{k}\cdot\mathbf{x}) = \cos(-\mathbf{k}\cdot\mathbf{x})$  and  $\sin(\mathbf{k}\cdot\mathbf{x}) = -\sin(-\mathbf{k}\cdot\mathbf{x})$ . Hence the total number of parameters appearing in  $\mathbf{W}_{r_k}(\mathbf{x})$  is:

$$N_{r_k} \equiv \# \text{ of parameters in } \mathbf{W}_{r_k}(\mathbf{x}) = 2|\text{SL}_{r_k}| \quad (4.33)$$

Hence to each layer we can associate an eigenstate of the Laplace Beltrami operator  $\Delta_g$  of eigenvalue<sup>7</sup>  $\mu_{r_k}^2 = \pi^2 r_k^2$

$$\Delta_g \mathbf{W}_{r_k}(\mathbf{x}|\mathbf{F}) = \mu_{r_k}^2 \mathbf{W}_{r_k}(\mathbf{x}|\mathbf{F}) \quad (4.34)$$

where by  $\mathbf{F}$  we have denoted the  $N_{r_k}$ -component vector of free parameters appearing in the vector field  $\mathbf{W}_{r_k}$ . Note that, as it appears from eq.(4.33),  $N_{r_k}$  is always a multiple of 2. This is relevant because the parameter space can be split into two subspaces each of dimension  $|\text{SL}_{r_k}|$  by imposing the additional Beltrami/anti-Beltrami condition, mode by mode. Indeed we can explicitly implement equation (4.17) and we get the following two conditions:

$$\mu v_i(\mathbf{k}) = \pi \epsilon_{ijl} k_j \omega_l(\mathbf{k}) \quad (4.35)$$

$$\mu \omega_i(\mathbf{k}) = -\pi \epsilon_{ijl} k_j v_l(\mathbf{k}) \quad (4.36)$$

The two equations are self consistent if and only if the eigenvalue  $\mu$  is such that  $\mu^2 = \pi^2 \langle \mathbf{k}, \mathbf{k} \rangle$ . Hence we can choose either  $\mu = \pi r_k$  or  $\mu = -\pi r_k$  and in each case we obtain a solution of the algebraic equations depending on 2 parameters. This amounts to stating that the general contribution  $\mathbf{W}_{r_k}$  of the spherical layer  $\text{SL}_{r_k}$  to the general Fourier series is split in a Beltrami plus an anti-Beltrami part:

$$\mathbf{W}_{r_k}(\mathbf{x}|\mathbf{F}) = \mathbf{W}_{r_k}^+(\mathbf{x}|\mathbf{F}^+) + \mathbf{W}_{r_k}^-(\mathbf{x}|\mathbf{F}^-) \quad (4.37)$$

such that:

$$\star_g d\Omega[\mathbf{w}_{r_k}^\pm] = \pm \pi r_k \Omega[\mathbf{w}_{r_k}^\pm] \quad (4.38)$$

We can introduce an  $L^2$  functional space on each spherical shell  $\text{SL}_{r_k}$  by defining the scalar product of any two eigenvector field  $A(\mathbf{x})$  and  $B(\mathbf{x})$  of the Laplace Beltrami operator  $\Delta_g$  with the same eigenvalue  $\pi^2 r_k^2$ :

$$(\mathbf{A}, \mathbf{B}) \equiv \int_{FC} d^3\mathbf{x} \mathbf{A}(\mathbf{x}) \cdot \mathbf{B}(\mathbf{x}) \quad ; \quad |\mathbf{A}|^2 = (\mathbf{A}, \mathbf{A}) \quad (4.39)$$

where by  $FC$  we denote the fundamental cell (namely the torus) of  $\mathbb{R}^3$  modulus the lattice  $\Lambda$ . It is easy to see that with respect to such a product Beltrami and anti-Beltrami fields are always orthogonal to each other. Relying on this observation the authors of [2] introduced the Beltrami index of a stationary Navier-Stokes solution  $\mathbf{U}$  by means of the following formula:

$$\beta_{r_k}[\mathbf{U}] = \frac{|U_{r_k}^+|^2 - |U_{r_k}^-|^2}{|U_{r_k}^+|^2 + |U_{r_k}^-|^2} \quad (4.40)$$

---

<sup>7</sup>Originally we defined the Laplace-Beltrami operator on the 1-forms, but its definition trivially extends, by lowering the indices with the metric, to the corresponding vector field



and partially proved, partially conjectured from the results of computer simulations a set of properties of this chiral spectral index. The word chiral is utilized because a space reflection  $\mathbf{x} \rightarrow -\mathbf{x}$  transforms Beltrami fields into anti Beltrami ones and viceversa. What was not even envisaged in the very interesting papers [2] and [42] is the group theoretical structure underlying Beltrami (and anti-Beltrami) fields appearing in the Fourier expansions of Navier-Stokes solutions. Indeed that group theoretical structure, based on the new conception of the *Universal Classifying Group* was unveiled only in 2015 in [1], starting from the observation by Arnold of a hidden roto-translation symmetry in the AAA model, which isomorphic, as a group, to the relevant point group  $O_{24}$ .

As stated in the introduction, the ultimate goal of the research plan initiated by the present paper, is that of complementing the spectral analysis of papers [2, 42] with the insights provided by a systematic use of the group theoretical structure inherent to the *Universal Classifying Group*  $\mathfrak{UC}_\Lambda$ . Indeed, in view of the decomposition (4.30) of the spherical layer into orbits of the point group, the general field  $\mathbf{W}_{r_k}(\mathbf{x}|\mathbf{F})$  can be seen as the sum of as many vector fields as there are orbits in the layer:

$$\mathbf{W}_{r_k}(\mathbf{x}|\mathbf{F}) = \sum_{i=1}^{n_{r_k}} \mathbf{Y}_{[\mathcal{O}_i]}(\mathbf{x}|\mathbf{F}^{[i]}) \quad (4.41)$$

and each vector field associated with an orbit  $\mathcal{O}_i$  can be split into its Beltrami and anti-Beltrami part. It follows that the construction of Beltrami (or by reflection anti-Beltrami) vector fields provides the building blocks to represent any Navier-Stokes flow in a compact torus  $\mathbb{T}^3 = \mathbb{R}^3/\Lambda$ . The completely new lore introduced in this paper on the basis of the results of [1] is that the orbit building blocks to be described in the next subsection can be further analyzed and organized into irreducible representations of the Universal Classifying Group fully discussed in section 5. It is in view of this powerful group theoretical weapon that the spectral analysis of [2] has to be reconsidered.

#### 4.4 The algorithm to construct Arnold Beltrami Flows

What we described in the previous subsection provides a well defined algorithm to construct a series of Arnold Beltrami flows that can be summarized in a few clear-cut steps and it is quite suitable for a systematic computer aided implementation.

The steps are the following ones:

- a) Choose a Bravais Lattice  $\Lambda$  with a non trivial proper point group  $\mathfrak{P}_\Lambda$ .
- b) Construct the character table and the irreducible representations of  $\mathfrak{P}_\Lambda$ .
- c) Analyze the structure of orbits of  $\mathfrak{P}_\Lambda$  on the lattice  $\Lambda$  and determine the number of lattice points contained in each spherical layer  $SL_{r_k}$  of the dual lattice  $\Lambda^*$  of quantized radius  $r_k$ , that as we already remarked is always even  $|SL_{r_k}| = 2P_{r_k}$
- d) Construct the most general solution of the Beltrami equation with eigenvalue  $\mu_k = \pi r_k$  by using the individual harmonics discussed in the previous section. The corresponding anti-Beltrami field is immediately determined by a reflection  $\mathbf{x} \rightarrow -\mathbf{x}$

$$V_i(\mathbf{x}) = \sum_{\mathbf{x} \in \mathfrak{S}_n} Y_i(\mathbf{k}|\mathbf{x}) \quad (4.42)$$

Hidden in each harmonic  $Y_i(\mathbf{k}|\mathbf{x})$  there are two parameters that are the remainder of the six parameters  $v_i(\mathbf{k})$  and  $\omega_i(\mathbf{k})$  after conditions (4.22,4.35,4.36) have been imposed. This would amount to a total of

$4P_{r_k}$  parameters, yet, for the already discussed reason, the number of independent parameters is always reduced to  $2P_{r_k}$ . Hence, at the end of the construction encoded in eq. (4.42), we have a Beltrami vector depending on a set of  $2P_{r_k}$  parameters that we can call  $F_I$  and consider as the  $2P_{r_k}$ -components of a vector  $\mathbf{F}$ . Ultimately we have an object of the following form:

$$\mathbf{V}(\mathbf{x} | \mathbf{F}) \quad (4.43)$$

which under the point group  $\mathfrak{P}_\Lambda$  necessarily transforms in the following way:

$$\forall \gamma \in \mathfrak{P}_\Lambda : \quad \gamma^{-1} \cdot \mathbf{V}(\gamma \cdot \mathbf{x} | \mathbf{F}) = \mathbf{V}(\mathbf{x} | \mathfrak{R}[\gamma] \cdot \mathbf{F}) \quad (4.44)$$

where  $\mathfrak{R}[\gamma]$  are  $2P_{r_k} \times 2P_{r_k}$  matrices that form a representation of  $\mathfrak{P}_\Lambda$ . Eq.(4.44) is necessarily true because any rotation  $\gamma \in \mathfrak{P}_\Lambda$  permutes the elements of  $SL_{r_k}$  among themselves.

- e) Decompose the representation  $\mathfrak{R}[\gamma]$  into irreducible representations of  $\mathfrak{P}_\Lambda$ . Each irreducible subspace  $\mathbf{f}_p$  of the  $2P_{r_k}$  parameter space  $\mathbf{F}$  defines an Arnold–Beltrami Flow:

$$\frac{d}{dt} \mathbf{x}(t) = \mathbf{V}(\mathbf{x}(t) | \mathbf{f}_p) \quad (4.45)$$

which is worth to analyze.

An obvious question which arises in connection with such a constructive algorithm is the following: how many Arnold–Beltrami flows are there? At first sight it seems that there is an infinite number of such systems since we can arbitrarily increase the radius of the spherical layer and on each new layer it seems that we have new models. Let us however observe that if on two different spherical layers  $SL_{r_1}$  and  $SL_{r_2}$  there are two orbits of lattice vectors  $\mathcal{O}_1$  and  $\mathcal{O}_2$  that have the same order

$$\ell = |\mathcal{O}_1| = |\mathcal{O}_2| \quad (4.46)$$

and furthermore all vectors  $\mathbf{k}_{(n_2)} \in \mathcal{O}_2$  are simply proportional to their analogues in orbit  $\mathcal{O}_1$ :

$$\mathbf{k}_{(n_2)} = \lambda \mathbf{k}_{(n_1)} \quad ; \quad \lambda \in \mathbb{Z} \quad (4.47)$$

then we can conclude that:

$$\mathbf{V}_{(n_2)}(\mathbf{x} | \mathbf{f}_p) = \mathbf{V}_{(n_1)}(\lambda \mathbf{x} | \mathbf{f}_p) \quad (4.48)$$

By redefining the coordinate fields  $\lambda \mathbf{x} = \mathbf{x}'$  and rescaling time  $t$  the two differential systems (4.45) respectively constructed from layer  $n_1$  and layer  $n_2$  can be identified.

As it was demonstrated in [1] analyzing the case of the cubic lattice and the orbits of the octahedral group there is always a finite number of  $\mathfrak{P}_\Lambda$ -orbit type on each lattice  $\Lambda$ . There is a maximal orbit  $\mathcal{O}_{max}$  that has order equal to the order of the point group :

$$|\mathcal{O}_{max}| = |\mathfrak{P}_\Lambda| \quad (4.49)$$

and there are a few shortened orbits  $\mathcal{O}_i$  ( $i = 1, \dots, s$ ) that have a smaller order:

$$\ell_i = |\mathcal{O}_i| < |\mathfrak{P}_\Lambda| \quad (4.50)$$

The fascinating property is that for the shortened orbits, which seem to play an analogue role in this context to that of BPS states in another context, property (4.47) is always true. The vectors pertaining to the same orbit  $\mathcal{O}_i$  in different spherical layers are always the same up to a multiplicative factor. Hence from the shortened orbits it was shown in [1] that one always obtains a finite number of Arnold–Beltrami flows. It remained the case of the maximal orbit for which property (4.47) is not necessarily imposed. How many independent flows do we obtain considering all the layers? The answer to the posed question is hidden in number theory. Indeed one has to analyze how many different type of triplets of integer numbers satisfy Diophantine equations of the Fermat type. In section 5.4 we review the answer obtained in [1] providing a systematic classification of such triplets for the cubic lattice.

Actually that classification is a classification of sublattices of the cubic lattice and each sublattice is associated with irreducible representations of the Universal Classifying Group  $\mathfrak{UC}_\Lambda$ .

Such result demonstrated that there is a finite number of Arnold–Beltrami flows and each of them can be promoted to a definite type of exact solutions of the Navier-Stokes equations depending on a finite number of parameters that acquire a dependence on the momenta and are, in this way, identified with Fourier coefficients in a Fourier series expansion of the initial conditions.

## 5 Group Theory Foundations

In order to make the present paper self-consistent and better highlight the interpretation of several of the results obtained in [1], that here are clarified in a more systematic way and extended from the cubic to the hexagonal case, we review the main group theoretical ingredients utilized in [1] to derive the *Universal Classifying Group*, whose very notion in the present paper is made more precise in view of *exact sequences* and *finite group cohomology*.

Skipping generalities we just remind the reader of what was already presented in eq.s(4.6,4.7), namely that in three dimensions the available *Lattice Point Groups*  $\mathfrak{P}_\Lambda$  are either the cyclic groups  $C_h \sim \mathbb{Z}_h$  with  $h = 2, 3, 4, 6$  or the dihedral groups  $Dih_h$  with  $h = 2, 3, 4, 6$  or the tetrahedral group  $T_{12} \sim A_4$  or the octahedral group  $O_{24} \sim S_4$ .

### 5.1 The cubic lattice and the octahedral point group $O_{24}$

The case of the cubic lattice was analyzed in depth in [1]. We review and repeat here a good deal of the results of that paper for three reasons:

1. We need to revise the conventions and the notations in order to make clear how the upgrading to the complete Navier-Stokes equations is achieved in practice.
2. Since a large part of the results to be obtained, classified and visualized necessarily depends on the use of MATHEMATICA codes that derive from those developed in 2014-2015 by means of a systematic reorganization of the routines and subroutines and by a transcription from MATHEMATICA 5.2 to MATHEMATICA 12, it is of vital importance to utilize a well defined and already established set of conventions and nomenclature.
3. The cubic lattice case constitutes the paradigm for the development of the same lore in the case of the hexagonal lattice which is a goal of the present paper.

Hence, within the general frame presented above, let us review the cubic lattice case.

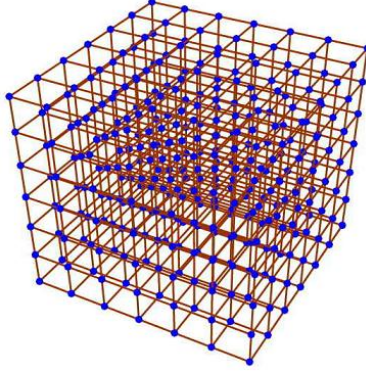


Figure 3: *A view of the self-dual cubic lattice*

The self-dual cubic lattice (momentum and space lattice at the same time) is displayed in fig.3. The basis vectors of the cubic lattice  $\Lambda_{cubic}$  are :

$$\mathbf{w}_1 = \{1, 0, 0\} \quad ; \quad \mathbf{w}_2 = \{0, 1, 0\} \quad ; \quad \mathbf{w}_3 = \{0, 0, 1\} \quad (5.1)$$

which implies that the metric is just the Kronecker delta:

$$g_{\mu\nu} = \delta_{\mu\nu} \quad (5.2)$$

and the basis vectors  $\mathbf{e}^\mu$  of the dual lattice  $\Lambda_{cubic}^*$  coincide with those of the lattice  $\Lambda$ . Hence the cubic lattice is self-dual:

$$\mathbf{w}_\mu = \mathbf{e}^\mu \quad \Rightarrow \quad \Lambda_{cubic} = \Lambda_{cubic}^* \quad (5.3)$$

The subgroup of the proper rotation group which maps the cubic lattice into itself is the octahedral group  $O_{24}$  whose order is 24. In the next subsection we recall its structure.

### 5.1.1 Structure of the Octahedral Group $O_{24} \sim S_4$

Abstractly the octahedral Group  $O_{24} \sim S_4$  is isomorphic to the symmetric group of permutations of 4 objects. It is defined by the following generators and relations:

$$T, S \quad : \quad T^3 = \mathbf{e} \quad ; \quad S^2 = \mathbf{e} \quad ; \quad (ST)^4 = \mathbf{e} \quad (5.4)$$

On the other hand  $O_{24}$  is a finite, discrete subgroup of the three-dimensional rotation group and any  $\gamma \in O_{24} \subset SO(3)$  of its 24 elements can be uniquely identified by its action on the coordinates  $x, y, z$ , as it is

displayed below:

<b>e</b>	$1_1 = \{x, y, z\}$		$4_1 = \{-x, -z, -y\}$	
$C_3$	$2_1 = \{-y, -z, x\}$	$C_2$	$4_2 = \{-x, z, y\}$	
	$2_2 = \{-y, z, -x\}$		$4_3 = \{-y, -x, -z\}$	
	$2_3 = \{-z, -x, y\}$		$4_4 = \{-z, -y, -x\}$	
	$2_4 = \{-z, x, -y\}$		$4_5 = \{z, -y, x\}$	
	$2_5 = \{z, -x, -y\}$		$4_6 = \{y, x, -z\}$	
	$2_6 = \{z, x, y\}$			
	$2_7 = \{y, -z, -x\}$		$C_4$	$5_1 = \{-y, x, z\}$
	$2_8 = \{y, z, x\}$			$5_2 = \{-z, y, x\}$
$C_4^2$	$3_1 = \{-x, -y, z\}$	$5_3 = \{z, y, -x\}$		
	$3_2 = \{-x, y, -z\}$	$5_4 = \{y, -x, z\}$		
	$3_3 = \{x, -y, -z\}$	$5_5 = \{x, -z, y\}$		
				$5_6 = \{x, z, -y\}$

(5.5)

As one sees from the above list the 24 elements are distributed into 5 conjugacy classes mentioned in the first column of the table, according to a nomenclature which is standard in the chemical literature on crystallography. The relation between the abstract and concrete presentation of the octahedral group is obtained by identifying in the list (5.5) the generators  $T$  and  $S$  mentioned in eq. (5.4). Explicitly we have:

$$T = 2_8 = \begin{pmatrix} 0 & 1 & 0 \\ 0 & 0 & 1 \\ 1 & 0 & 0 \end{pmatrix} ; \quad S = 4_6 = \begin{pmatrix} 0 & 1 & 0 \\ 1 & 0 & 0 \\ 0 & 0 & -1 \end{pmatrix} \quad (5.6)$$

All other elements are reconstructed from the above two using the multiplication table of the group which we omit for brevity. This observation is important in relation with representation theory. Any linear representation of the group is uniquely specified by giving the matrix representation of the two generators  $T = 2_8$  and  $S = 4_6$ . In the sequel this will be extensively utilized in the compact codification of the reducible representations that emerge in our calculations.

### 5.1.2 Irreducible representations of the Octahedral Group

There are five conjugacy classes in  $O_{24}$  and therefore according to theory there are five irreducible representations of the same group, that we name  $D_i$ ,  $i = 1, \dots, 5$ . Let us briefly describe them.

#### 5.1.3 $D_1$ : the identity representation

The identity representation which exists for all groups is that one where to each element of  $O$  we associate the number 1

$$\forall \gamma \in O_{24} : D_1(\gamma) = 1 \quad (5.7)$$

Obviously the character of such a representation is:

$$\chi_1 = \{1, 1, 1, 1, 1\} \quad (5.8)$$

### 5.1.4 $D_2$ : the quadratic Vandermonde representation

The representation  $D_2$  is also one-dimensional. It is constructed as follows. Consider the following polynomial of order six in the coordinates of a point in  $\mathbb{R}^3$  or  $T^3$ :

$$\mathfrak{V}(x, y, z) = (x^2 - y^2)(x^2 - z^2)(y^2 - z^2) \quad (5.9)$$

As one can explicitly check under the transformations of the octahedral group listed in eq.(5.5) the polynomial  $\mathfrak{V}(x, y, z)$  is always mapped into itself modulo an overall sign. Keeping track of such a sign provides the form of the second one-dimensional representation whose character is explicitly calculated to be the following one:

$$\chi_1 = \{1, 1, 1, -1, -1\} \quad (5.10)$$

### 5.1.5 $D_3$ : the two-dimensional representation

The representation  $D_3$  is two-dimensional and it corresponds to a homomorphism:

$$D_3 : O_{24} \rightarrow \text{SL}(2, \mathbb{Z}) \quad (5.11)$$

which associates to each element of the octahedral group a  $2 \times 2$  integer valued matrix of determinant one. The homomorphism is completely specified by giving the two matrices representing the two generators:

$$D_3(T) = \begin{pmatrix} 0 & 1 \\ -1 & -1 \end{pmatrix} ; \quad D_3(S) = \begin{pmatrix} 0 & 1 \\ 1 & 0 \end{pmatrix} \quad (5.12)$$

The character vector of  $D_2$  is easily calculated from the above information and we have:

$$\chi_3 = \{2, -1, 2, 0, 0\} \quad (5.13)$$

### 5.1.6 $D_4$ : the three-dimensional defining representation

The three dimensional representation  $D_4$  is simply the defining representation, where the generators  $T$  and  $S$  are given by the matrices in eq.(5.6).

$$D_4(T) = T ; \quad D_4(S) = S \quad (5.14)$$

From this information the characters are immediately calculated and we get:

$$\chi_3 = \{3, 0, -1, -1, 1\} \quad (5.15)$$

### 5.1.7 $D_5$ : the three-dimensional unoriented representation

The three dimensional representation  $D_5$  is simply that one where the generators  $T$  and  $S$  are given by the following matrices:

$$D_5(T) = \begin{pmatrix} 0 & 1 & 0 \\ 0 & 0 & 1 \\ 1 & 0 & 0 \end{pmatrix} ; \quad D_5(S) = \begin{pmatrix} 0 & 1 & 0 \\ 1 & 0 & 0 \\ 0 & 0 & 1 \end{pmatrix} \quad (5.16)$$

From this information the characters are immediately calculated and we get:

$$\chi_5 = \{3, 0, -1, 1, -1\} \quad (5.17)$$

The table of characters is summarized in eq.(1).

Class Irrep	$\{\mathbf{e}, 1\}$	$\{C_3, 8\}$	$\{C_4^2, 3\}$	$\{C_2, 6\}$	$\{C_4, 6\}$
$D_1, \chi_1 =$	1	1	1	1	1
$D_2, \chi_2 =$	1	1	1	-1	-1
$D_3, \chi_3 =$	2	-1	2	0	0
$D_4, \chi_4 =$	3	0	-1	-1	1
$D_5, \chi_5 =$	3	0	-1	1	-1

Table 1: Character Table of the proper Octahedral Group

## 5.2 The hexagonal lattice and the dihedral group $Dih_6$

We come next to a discussion of the hexagonal lattice. Since in this section all considered representations are relative to the point group we simplify the notation mentioning the irreps only as  $D_1, \dots, D_6$  without writing in square brackets the group.

### 5.2.1 The hexagonal lattice

The basis vectors of the hexagonal space lattice  $\Lambda_{Hex}$  are the following ones :

$$\mathbf{w}_1 = \{\sqrt{2}, 0, 0\} \quad ; \quad \mathbf{w}_2 = \left\{-\frac{1}{\sqrt{2}}, \sqrt{\frac{3}{2}}, 0\right\} \quad ; \quad \mathbf{w}_3 = \{0, 0, \sqrt{2}\} \quad (5.18)$$

which implies that the metric is the following non diagonal one:

$$g_{\mu\nu} = \begin{pmatrix} 2 & -1 & 0 \\ -1 & 2 & 0 \\ 0 & 0 & 2 \end{pmatrix} \quad (5.19)$$

The basis vectors  $\mathbf{e}^\mu$  of the dual momentum lattice  $\Lambda_{Hex}^*$  do not coincide with those of the lattice  $\Lambda_{Hex}$ . They are the following ones:

$$\mathbf{e}^1 = \left\{\frac{1}{\sqrt{2}}, \frac{1}{\sqrt{6}}, 0\right\} \quad ; \quad \mathbf{e}^2 = \left\{0, \sqrt{\frac{2}{3}}, 0\right\} \quad ; \quad \mathbf{e}^3 = \left\{0, 0, \frac{1}{\sqrt{2}}\right\} \quad (5.20)$$

so that the space lattice is now a proper subgroup of its dual  $\Lambda_{Hex}^*$ , named also the *momentum-lattice*. In order to understand the structure of the hexagonal lattice one ought to consider first the hexagonal tessellation of a plane that is generated by the first two basis vectors  $\mathbf{w}_{1,2}$ .

To this effect it is convenient to look at fig.4 The space lattice which provides a tiling of the plane by means

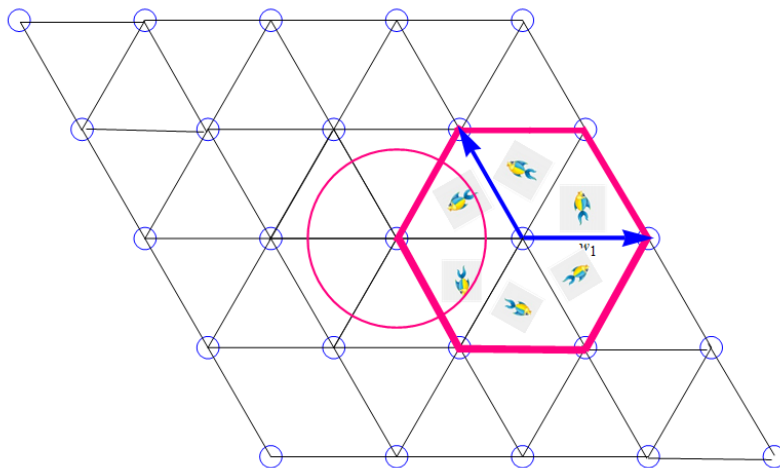


Figure 4: A view of the hexagonal tessellation of the plane. The hexagonal two dimensional lattice coincides with the  $A_2$  root lattice. Indeed the projection on the plane of the two basis vectors  $\mathbf{w}_1$  and  $\mathbf{w}_2$  (the two blue vectors) are the two simple roots of the  $A_2$  Lie algebra. Each point of the lattice can be regarded as the center of a regular hexagon whose vertices are the first nearest neighbors. These hexagons provide a tessellation of the infinite plane.

of regular hexagons coincides with the root lattice of the  $A_2$  Lie algebra its generators being the two simple roots  $\alpha_{1,2}$ .

The plane projection of the dual lattice  $\Lambda_{Hex}^*$  is just the weight lattice of  $A_2$  the plane projection of the basis vectors  $\mathbf{e}_{1,2}$  being just the fundamental weights  $\lambda_{1,2}$ . This is illustrated in the next fig.5. There it is clearly shown that the space lattice is a sublattice of the dual momentum lattice.

The three-dimensional hexagonal lattice is obtained by adjoining an infinite number of equally spaced planes each tiled in the way shown in fig.s 4 and 5. A view of the resulting three dimensional lattices is provided in fig.6.

### 5.2.2 The point group $Dih_6$

The subgroup of the proper rotation group which maps the cubic lattice into itself is the dihedral group  $Dih_6$  whose order is 12. In the next lines we recall its structure.

Abstractly the dihedral  $Dih_6$  group is defined by the following generators and relations:

$$A, B \quad : \quad A^6 = \mathbf{e} \quad ; \quad B^2 = \mathbf{e} \quad ; \quad (BA)^2 = \mathbf{e} \quad (5.21)$$



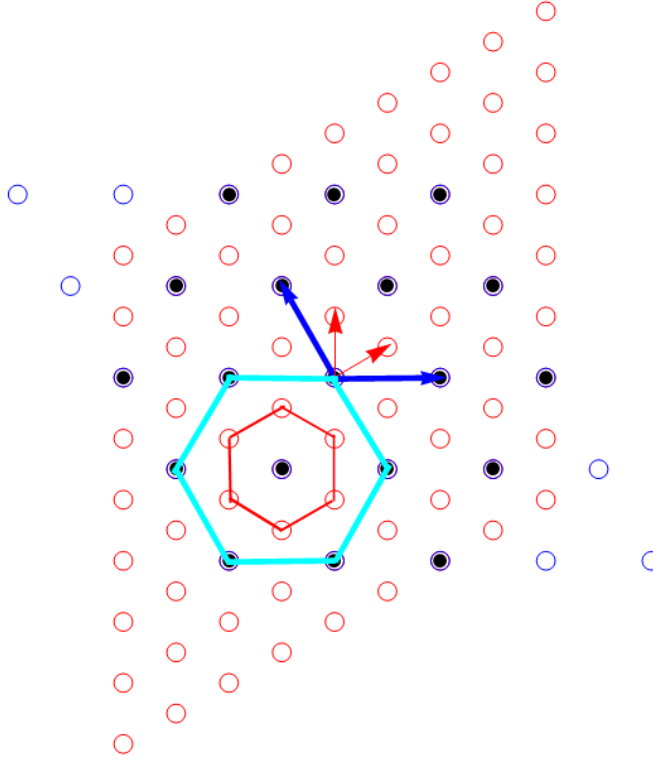


Figure 5: *Illustration of the dual momentum lattice of the hexagonal lattice in the plane. The red circles are the points of the momentum lattice, while the blue ones are the points of the space lattice. In the finite portions of the two lattices that we show in this picture the black points are the common ones. As we see each point of the space-lattice is surrounded by two hexagons; the vertices of the smaller hexagon are moment-lattice points that do not belong to space-lattice, while the vertices of the bigger hexagon are the space-lattice nearest neighbors, as already remarked in the caption of fig.4.*

Explicitly in three dimensions we can take the following matrix-representation for the generators of  $\text{Dih}_6$ :

$$A = \begin{pmatrix} \frac{1}{2} & \frac{\sqrt{3}}{2} & 0 \\ -\frac{\sqrt{3}}{2} & \frac{1}{2} & 0 \\ 0 & 0 & 1 \end{pmatrix} ; \quad B = \begin{pmatrix} -1 & 0 & 0 \\ 0 & 1 & 0 \\ 0 & 0 & -1 \end{pmatrix} \quad (5.22)$$

The group generated by the above generators has 12 elements that can be arranged into 6 conjugacy classes, as it is displayed in table 2: In such a table every group element is uniquely identified by its action on the three-dimensional vector  $\{x, y, z\}$ . The multiplication table of the group  $\text{Dih}_6$  is also omitted for brevity.

### 5.2.3 Irreducible representations of the dihedral group $\text{Dih}_6$ and the character table

The group  $\text{Dih}_6$  has six conjugacy classes. Therefore according to theory we expect six irreducible representations that we name  $D_i$ ,  $i = 1, \dots, 6$ . Let us briefly describe them. The first four representations are

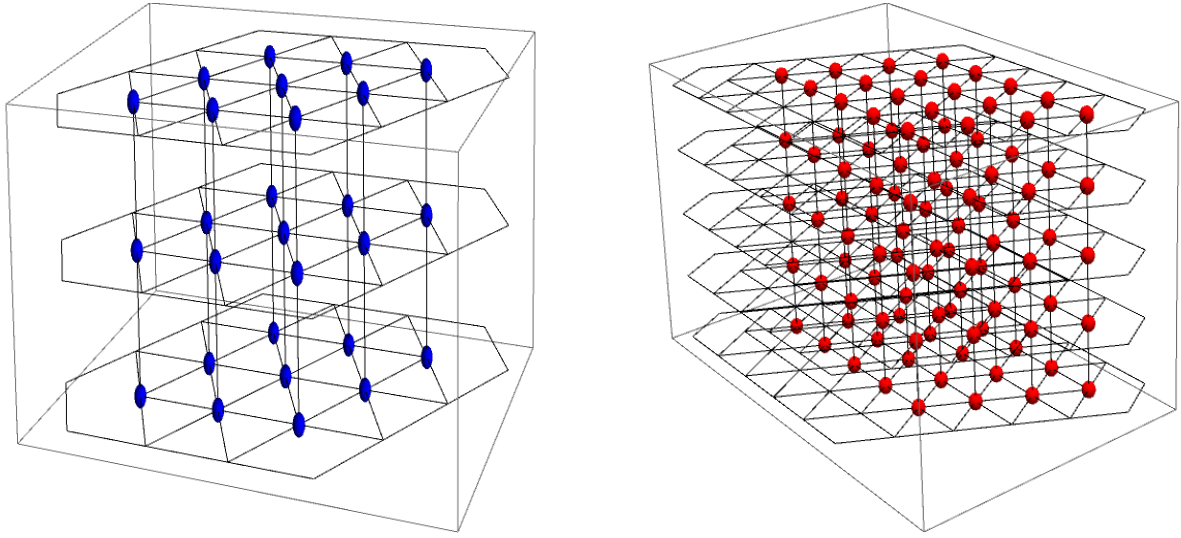


Figure 6: A view of the hexagonal space lattice  $\Lambda_{Hex}$  (blue points on the left) and momentum momentum lattice  $\Lambda_{Hex}^*$  (red points on the right)

$\mathbf{e}$	$1_1 = \{x, y, z\}$
$A$	$2_1 = \{\frac{1}{2}(x + \sqrt{3}y), \frac{1}{2}(y - \sqrt{3}x), z\}$
	$2_2 = \{\frac{1}{2}(x - \sqrt{3}y), \frac{1}{2}(\sqrt{3}x + y), z\}$
$A^2$	$3_1 = \{\frac{1}{2}(\sqrt{3}y - x), \frac{1}{2}(-\sqrt{3}x - y), z\}$
	$3_2 = \{\frac{1}{2}(-x - \sqrt{3}y), \frac{1}{2}(\sqrt{3}x - y), z\}$
$A^3$	$4_1 = \{-x, -y, z\}$
$B$	$5_1 = \{-x, y, -z\}$
	$5_2 = \{\frac{1}{2}(x - \sqrt{3}y), \frac{1}{2}(-\sqrt{3}x - y), -z\}$
	$5_3 = \{\frac{1}{2}(x + \sqrt{3}y), \frac{1}{2}(\sqrt{3}x - y), -z\}$
$BA$	$6_1 = \{\frac{1}{2}(-x - \sqrt{3}y), \frac{1}{2}(y - \sqrt{3}x), -z\}$
	$6_2 = \{x, -y, -z\}$
	$6_3 = \{\frac{1}{2}(\sqrt{3}y - x), \frac{1}{2}(\sqrt{3}x + y), -z\}$

Table 2: Conjugacy Classes of the Dihedral Group  $Dih_6$

one-dimensional.

#### 5.2.4 $D_1$ : the identity representation

The identity representation which exists for all groups is that one where to each element of  $Dih_6$  we associate the number 1

$$\forall \gamma \in O : D_1(\gamma) = 1 \quad (5.23)$$

Obviously the character of such a representation is:

$$\chi_1 = \{1, 1, 1, 1, 1\} \quad (5.24)$$

#### 5.2.5 $D_2$ : the second one-dimensional representation

The representation  $D_2$  is also one-dimensional. It is constructed as follows.

$$\begin{aligned} \forall \gamma \in \{e\} & : D_2(\gamma) = 1 \\ \forall \gamma \in \{A\} & : D_2(\gamma) = -1 \\ \forall \gamma \in \{A^2\} & : D_2(\gamma) = 1 \\ \forall \gamma \in \{A^3\} & : D_2(\gamma) = -1 \\ \forall \gamma \in \{B\} & : D_2(\gamma) = 1 \\ \forall \gamma \in \{BA\} & : D_2(\gamma) = -1 \end{aligned} \quad (5.25)$$

Clearly the corresponding character vector is the following one.

$$\chi_2 = \{1, -1, 1, -1, 1, -1\} \quad (5.26)$$

Said in another way, this is the representation where  $A = -1$  and  $B = 1$ .

#### 5.2.6 $D_3$ : the third one-dimensional representation

The representation  $D_3$  is also one-dimensional. It is constructed as follows.

$$\begin{aligned} \forall \gamma \in \{e\} & : D_2(\gamma) = 1 \\ \forall \gamma \in \{A\} & : D_2(\gamma) = -1 \\ \forall \gamma \in \{A^2\} & : D_2(\gamma) = 1 \\ \forall \gamma \in \{A^3\} & : D_2(\gamma) = -1 \\ \forall \gamma \in \{B\} & : D_2(\gamma) = -1 \\ \forall \gamma \in \{BA\} & : D_2(\gamma) = 1 \end{aligned} \quad (5.27)$$

Clearly the corresponding character vector is the following one.

$$\chi_3 = \{1, -1, 1, -1, -1, 1\} \quad (5.28)$$

Said in another way, this is the representation where  $A = -1$  and  $B = -1$ .

### 5.2.7 $D_4$ : the fourth one-dimensional representation

The representation  $D_4$  is also one-dimensional. It is constructed as follows.

$$\begin{aligned}
\forall \gamma \in \{\mathbf{e}\} & : D_2(\gamma) = 1 \\
\forall \gamma \in \{A\} & : D_2(\gamma) = 1 \\
\forall \gamma \in \{A^2\} & : D_2(\gamma) = 1 \\
\forall \gamma \in \{A^3\} & : D_2(\gamma) = 1 \\
\forall \gamma \in \{B\} & : D_2(\gamma) = -1 \\
\forall \gamma \in \{BA\} & : D_2(\gamma) = -1
\end{aligned} \tag{5.29}$$

Clearly the corresponding character vector is the following one.

$$\chi_4 = \{1, 1, 1, 1, -1, -1\} \tag{5.30}$$

Said in another way, this is the representation where  $A = 1$  and  $B = -1$ .

### 5.2.8 $D_5$ : the first two-dimensional representation

The representation  $D_5$  is two-dimensional and it corresponds to a homomorphism:

$$D_5 : \text{Dih}_6 \rightarrow \text{SL}(2, \mathbb{C}) \tag{5.31}$$

which associates to each element of the dihedral group a  $2 \times 2$  complex valued matrix of determinant one. The homomorphism is completely specified by giving the two matrices representing the two generators:

$$D_5(A) = \begin{pmatrix} e^{\frac{i\pi}{3}} & 0 \\ 0 & e^{-\frac{i\pi}{3}} \end{pmatrix} ; \quad D_5(B) = \begin{pmatrix} 0 & 1 \\ 1 & 0 \end{pmatrix} \tag{5.32}$$

The character vector of  $D_5$  is easily calculated from the above information and we have:

$$\chi_5 = \{2, 1, -1, -2, 0, 0\} \tag{5.33}$$

### 5.2.9 $D_6$ : the second two-dimensional representation

The representation  $D_6$  is also two-dimensional and it corresponds to a homomorphism:

$$D_6 : \text{Dih}_6 \rightarrow \text{SL}(2, \mathbb{C}) \tag{5.34}$$

which associates to each element of the dihedral group a  $2 \times 2$  complex valued matrix of determinant one. The homomorphism is completely specified by giving the two matrices representing the two generators:

$$D_6(A) = \begin{pmatrix} e^{\frac{2i\pi}{3}} & 0 \\ 0 & e^{-\frac{2i\pi}{3}} \end{pmatrix} ; \quad D_6(B) = \begin{pmatrix} 0 & 1 \\ 1 & 0 \end{pmatrix} \tag{5.35}$$

The character vector of  $D_6$  is easily calculated from the above information and we have:

$$\chi_6 = \{2, -1, -1, 2, 0, 0\} \quad (5.36)$$

The character table of the  $Dih_6$  group is summarized in table 3.

Class Irrep	$\{e, 1\}$	$\{A, 2\}$	$\{A^2, 2\}$	$\{A^3, 1\}$	$\{B, 3\}$	$\{BA, 3\}$
$D_1, \chi_1 =$	1	1	1	1	1	1
$D_2, \chi_2 =$	1	-1	1	-1	1	-1
$D_3, \chi_3 =$	1	-1	1	-1	-1	1
$D_4, \chi_4 =$	1	1	1	1	-1	-1
$D_5, \chi_5 =$	2	1	-1	-2	0	0
$D_6, \chi_6 =$	2	-1	-1	2	0	0

Table 3: The character table of the dihedral group  $Dih_6$

### 5.3 Extensions of the Point Group with translations and the Universal Classifying Group

We come now to what constitutes the main mathematical point of [1], namely the extension of the point group with appropriate discrete subgroups of the compactified translation group  $U(1)^3$ . This issue bears on a classical topic dating back to the XIX century, which was developed by crystallographers and in particular by the great russian mathematician Fyodorov [43]. We refer here to the issue of space groups which historically resulted into the classification of the 230 crystallographic groups, well known in the chemical literature, for which an international system of notations and conventions was established that is available in numerous encyclopedic tables and books. Although in [1] one key-point of the logic that leads to the classification of space groups, was utilized, yet the pursued goal happened to be slightly different. Indeed what was aimed at was not the identification of the various space groups, rather the construction of what was christened in [1] the *Universal Classifying Group*, namely a single large group which contains all the existing *space groups* as subgroups. It was advocated in [1] that such *Universal Classifying Group* is the one appropriate to organize the eigenfunctions of the  $\star_g$ -operator into irreducible representations and eventually to uncover the available hidden symmetries of all Arnold-Beltrami flows.

#### 5.3.1 Group extensions

The idea of space groups is naturally related with the notion of group-extensions. Here we analyze how it arises. The covering manifold of the  $T^3$  torus is  $\mathbb{R}^3$  which can be regarded as the following coset manifold:

$$\mathbb{R}^3 \simeq \frac{\mathbb{E}^3}{SO(3)} \quad ; \quad \mathbb{E}^3 \equiv ISO(3) \doteq \mathcal{T}^3 \ltimes SO(3) \quad (5.37)$$

where  $\mathcal{T}^3$  is the three dimensional translation group acting on  $\mathbb{R}^3$  in the standard way:

$$\forall \mathbf{t} \in \mathcal{T}^3, \forall \mathbf{x} \in \mathbb{R}^3 \quad | \quad \mathbf{t} : \mathbf{x} \rightarrow \mathbf{x} + \mathbf{t} \quad (5.38)$$

and the Euclidian group  $\mathbb{E}^3$  is the semi-direct product of the translation group  $\mathcal{T}^3$  with the proper rotation group  $\text{SO}(3)$ .

In an abstract notation the semi-direct product of two groups  $T$  and  $G_0$ , where  $T$  is abelian and supports an action of  $G_0$  which is not necessarily abelian:

$$\forall \gamma \in G_0 \quad \text{and} \quad \forall t \in T \quad \gamma : T \longrightarrow T \quad ; \quad \gamma \circ t \in T \quad (5.39)$$

can be presented as it follows. As a set the semidirect product:

$$G = T \times G_0 \quad (5.40)$$

is the cartesian product  $T \times G_0$  and the product law  $\bullet$  on the set of pairs of elements ( $t \in T, \gamma \in G_0$ ) is the following one:

$$(t, \alpha) \bullet (w, \beta) = (t + \alpha \circ w, \alpha \cdot \beta) \quad (5.41)$$

where the product operation for the abelian group  $T$  has been denoted with  $+$ , (the inverse is  $-$ ) and the neutral element is  $0$ , while for the group  $G_0$  the product operation is denoted by  $\cdot$  and the neutral element is denoted by  $\mathbf{1}$ . As a consequence of the definition of direct product the original abelian group  $T$  is a normal subgroup of  $G$ :

$$T \triangleleft G \quad (5.42)$$

The direct product construction is an example of the realization of the following exact sequence of four maps  $\mu_i$ :

$$0 \xrightarrow[\mu_1]{\iota} T \xrightarrow[\mu_2]{\iota} G \xrightarrow[\mu_3]{\pi} G_0 \xrightarrow[\mu_4]{\pi} \mathbf{1} \quad (5.43)$$

The first map is the injection map of the neutral element of  $T$  into the group it pertains to. The second map is the injection map of the abstract group  $T$  as a normal subgroup in some group  $G$ , the third map is the projection onto the quotient  $G_0 \equiv \frac{G}{T}$ , the fourth map is the projection of the entire  $G_0$  onto its neutral element  $\mathbf{1}$ . The exactness property of the sequence:

$$\ker(\mu_i) = \text{Im}(\mu_{i+1}) \quad (5.44)$$

is evident from the description. Any time we succeed in realizing the middle term  $G$  in such an exact sequence as that in eq. (5.43) we say that  $G$  is a **group extension** of  $T$  by means of the group  $G_0$  which is supposed to have an automorphic action on  $T$ . The direct product is just one example of the realizations of such group extensions but it is not the only one.

### 5.3.2 The exact sequence for space groups and the inhomogeneous group $\mathfrak{I}p_\Lambda$

In modern mathematical language the space groups of crystallography emerge just in the way described above. We choose a crystallographic lattice  $\Lambda$  and a finite point group  $\mathfrak{P} \subset \text{SO}(3)$  that is the maximal one  $\mathfrak{P}_\Lambda^{max}$  leaving  $\Lambda$  invariant or one of its subgroups and we write the exact sequence

$$0 \xrightarrow{\iota} \Lambda \xrightarrow{\iota} \mathfrak{G} \xrightarrow{\pi} \mathfrak{P} \xrightarrow{\pi} \mathbf{1} \quad (5.45)$$

where  $\mathfrak{S}$  is the space group. One possible construction of the exact sequence is the already mentioned semi-direct product:

$$\mathfrak{S}_\times = \Lambda \ltimes \mathfrak{P} \quad (5.46)$$

which we can reproduce quite conveniently through the use of  $4 \times 4$  matrices of the following type:

$$\forall (\mathbf{t}, \gamma) \in \mathfrak{S}_\times \rightarrow D_\times [(\mathbf{t}, \gamma)] = \left( \begin{array}{c|c} \hat{\gamma} & \mathbf{t} \\ \hline 0 & 1 \end{array} \right) \quad (5.47)$$

where by  $\hat{\gamma}$  we mean the  $3 \times 3$  matrix realization of the abstract group element  $\gamma$  in the defining representation of  $\mathfrak{P} \subset \text{SO}(3)$ . Let us see how we can realize the exact sequence (5.45) in a more general way.

We begin by observing that harmonic analysis on  $\mathbb{R}^3$  is a complicated matter of functional analysis since  $\mathcal{T}^3$  is a non-compact group and its unitary irreducible representations are infinite-dimensional. The landscape changes drastically when we compactify our manifold from  $\mathbb{R}^3$  to the three torus  $\text{T}^3$ . Compactification is obtained taking the quotient of  $\mathbb{R}^3$  with respect to the lattice  $\Lambda \subset \mathcal{T}^3$ . As a result of this quotient the manifold becomes  $\mathbb{S}^1 \times \mathbb{S}^1 \times \mathbb{S}^1$  but also the isometry group is reduced. Instead of  $\text{SO}(3)$  as rotation group we are left with its discrete subgroup  $\mathfrak{P}_\Lambda^{max} \subset \text{SO}(3)$  which maps the lattice  $\Lambda$  into itself (the maximal point group or a subgroup thereof  $\mathfrak{P}_\Lambda \subset \mathfrak{P}_\Lambda^{max} \subset \text{SO}(3)$ ) and instead of the translation subgroup  $\mathcal{T}^3$  we are left with the quotient group:

$$\mathfrak{T}_\Lambda^3 \equiv \frac{\mathcal{T}^3}{\Lambda} \simeq \text{U}(1) \times \text{U}(1) \times \text{U}(1) \quad (5.48)$$

In this way we obtain a new group which replaces the Euclidian group and which is the semidirect product of  $\mathfrak{T}_\Lambda^3$  with the point group  $\mathfrak{P}_\Lambda$ :

$$\mathfrak{I}\mathfrak{p}_\Lambda \equiv \mathfrak{T}_\Lambda^3 \ltimes \mathfrak{P}_\Lambda \quad (5.49)$$

The group  $\mathfrak{I}\mathfrak{p}_\Lambda$  that can be named the **Inhomogeneous Point Group** is an exact symmetry of Beltrami equation (4.9) and its action is naturally defined on the parameter space of any of its solutions  $\mathbf{V}(\mathbf{x}|\mathbf{F})$  that we can obtain by means of the algorithm described in section 4.4. To appreciate this point let us state that every component of the vector field  $\mathbf{V}(\mathbf{x}|\mathbf{F})$  associated with a  $\mathfrak{P}_\Lambda$  point-orbit  $\mathcal{O}$  is a linear combinations of the functions  $\cos[2\pi \mathbf{k}_i \cdot \mathbf{x}]$  and  $\sin[2\pi \mathbf{k}_i \cdot \mathbf{x}]$ , where  $\mathbf{k}_i \in \mathcal{O}$  are all the momentum vectors contained in the orbit. Consider next the same functions in a translated point of the three torus  $\mathbf{x}' = \mathbf{x} + \mathbf{c}$  where  $\mathbf{c} = \{\xi_1, \xi_2, \xi_3\}$  is a representative of an equivalence class  $\mathfrak{c}$  of constant vectors defined modulo the lattice:

$$\mathfrak{c} = \mathbf{c} + \mathbf{t} \quad ; \quad \forall \mathbf{t} \in \Lambda \quad (5.50)$$

The above equivalence classes are the elements of the quotient group  $\mathfrak{T}_\Lambda^3$ . Using standard trigonometric identities  $\cos[2\pi \mathbf{k}_i \cdot \mathbf{x} + 2\pi \mathbf{k}_i \cdot \mathbf{c}]$  can be reexpressed as a linear combination of the  $\cos[2\pi \mathbf{k}_i \cdot \mathbf{x}]$  and  $\sin[2\pi \mathbf{k}_i \cdot \mathbf{x}]$  functions with coefficients that depend on trigonometric functions of  $\mathbf{c}$ . The same is true of  $\sin[2\pi \mathbf{k}_i \cdot \mathbf{x} + 2\pi \mathbf{k}_i \cdot \mathbf{c}]$ . Note also that because of the periodicity of the trigonometric functions, the shift in their argument by a lattice translation is not-effective so that one deals only with the equivalence classes (5.50). It follows that for each element  $\mathfrak{c} \in \mathfrak{T}_\Lambda^3$  we obtain a matrix representation  $\mathcal{M}_\mathfrak{c}$  realized on the  $F$  parameters and defined by the following equation:

$$\mathbf{V}(\mathbf{x} + \mathbf{c}|\mathbf{F}) = \mathbf{V}(\mathbf{x}|\mathcal{M}_\mathfrak{c}\mathbf{F}) \quad (5.51)$$

As we already noted in eq.(4.44), for any group element  $\gamma \in \mathfrak{P}_\Lambda$  we also have a matrix representation induced

on the parameter space by the same mechanism:

$$\forall \gamma \in \mathfrak{P}_\Lambda : \quad \gamma^{-1} \cdot \mathbf{V}(\gamma \cdot \mathbf{x} | \mathbf{F}) = \mathbf{V}(\mathbf{x} | \mathfrak{R}[\gamma] \cdot \mathbf{F}) \quad (5.52)$$

Combining eq.s(5.51) and (5.52) we obtain a matrix realization of the entire group  $\mathfrak{G}_\Lambda$  in the following way:

$$\mathbf{V}(\gamma \cdot \mathbf{x} + \mathbf{c} | \mathbf{F}) = \gamma \cdot \mathbf{V}(\mathbf{x} | \mathfrak{R}[\gamma] \cdot \mathcal{M}_c \cdot \mathbf{F}) \quad (5.53)$$

$\Downarrow$

$$\forall (\gamma, \mathbf{c}) \in \mathfrak{I}\mathfrak{p}_\Lambda \rightarrow D[(\gamma, \mathbf{c})] = \mathfrak{R}[\gamma] \cdot \mathcal{M}_c \quad (5.54)$$

Actually the construction of Beltrami vector fields in the lowest lying point-orbit, which usually yields a faithful matrix representation of all group elements, can be regarded as an automatic way of taking the quotient (5.48) and the resulting representation can be considered the defining representation of the group  $\mathfrak{I}\mathfrak{p}_\Lambda$ .

The next point in the logic which leads to space groups is the following observation.  $\mathfrak{I}\mathfrak{p}_\Lambda$  is an unusual mixture of a discrete group (the point group) with a continuous one (the translation subgroup  $\mathfrak{T}_\Lambda^3$ ). This latter is rather trivial, since its action corresponds to shifting the origin of coordinates in three-dimensional space and, from the point of view of the first order differential system that defines trajectories (see eq.(2.14)), it simply corresponds to varying the integration constants. Yet there are in  $\mathfrak{I}\mathfrak{p}_\Lambda$  some discrete subgroups which can be isomorphic to the point group  $\mathfrak{P}_\Lambda$ , or to one of its subgroups  $\mathfrak{H}_\Lambda \subset \mathfrak{P}_\Lambda$ , without being their conjugate in  $\mathfrak{I}\mathfrak{p}_\Lambda$ . Such groups cannot be disposed of by shifting the origin of coordinates and consequently they can encode non-trivial hidden symmetries of the dynamical system (2.14).

The precise mathematical way of thinking is encoded in the already presented exact sequence (5.45). Given the point group  $\mathfrak{P}_\Lambda$  and its semidirect product extension with translations reduced to the unit cell  $\mathcal{T}_{unit}^3 \simeq U(1) \times U(1) \times U(1)$ , namely  $\mathfrak{G}_\Lambda$ , the original point group can be identified as the quotient group:

$$\mathfrak{P}_\Lambda \simeq \frac{\mathfrak{I}\mathfrak{p}_\Lambda}{\mathcal{T}_{unit}^3} \quad (5.55)$$

since  $\mathcal{T}_{unit}^3$  is a normal subgroup:

$$\mathcal{T}_{unit}^3 \triangleleft \mathfrak{I}\mathfrak{p}_\Lambda \quad (5.56)$$

We would like to construct the entire equivalence class of elements in  $\mathfrak{I}\mathfrak{p}_\Lambda$  for each element  $\gamma \in \mathfrak{P}_\Lambda$ . Choosing representatives in these classes we can realize the various group extensions  $\mathfrak{S}$  that can occupy the middle point in the exact sequence (5.45).

This is the mission accomplished by crystallographers the result of the mission being the classification of space groups. It suffices to realize a generalized copy of each generator of the point group and by means of multiplication we obtain the equivalence classes of each point group element.

This leads to the so named Frobenius congruences [44][45]. Let us outline this construction.

### 5.3.3 Frobenius congruences

Following classical approaches we use the already introduced  $4 \times 4$  matrix representation of the group  $\mathfrak{I}\mathfrak{p}_\Lambda$ . Performing the matrix product of two elements, in the translation block one has to take into account equivalence



modulo lattice  $\Lambda$ , namely

$$\left( \begin{array}{c|c} \gamma_1 & \mathbf{c}_1 \\ \hline 0 & 1 \end{array} \right) \cdot \left( \begin{array}{c|c} \gamma_2 & \mathbf{c}_2 \\ \hline 0 & 1 \end{array} \right) = \left( \begin{array}{c|c} \gamma_1 \cdot \gamma_2 & \gamma_1 \mathbf{c}_2 + \mathbf{c}_1 + \Lambda \\ \hline 0 & 1 \end{array} \right) \quad (5.57)$$

Utilizing this notation the next step consists of introducing translation deformations of the generators of the point group  $\mathfrak{P}_\Lambda$  searching for deformations that cannot be eliminated by conjugation with elements of the normal subgroup  $\mathfrak{T}^3 \triangleleft \mathfrak{Jp}_\Lambda$ . We go through the steps of such a construction both in the case of the maximal point group for the cubic lattice  $\mathfrak{P}_{cubic}^{max} = O_{24}$ , denoting with  $O_{24}$  the octahedral group, and in the case of the maximal point group for the alternative hexagonal lattice  $\mathfrak{P}_{hexag}^{max} = Dih_6$ .

### 5.3.4 Frobenius congruences for the Octahedral Group $O_{24}$

The octahedral group is abstractly defined by the presentation displayed in eq.(5.4). As a first step we parameterize the candidate deformations of the two generators  $T$  and  $S$  in the following way:

$$\hat{T} = \left( \begin{array}{ccc|c} 0 & 1 & 0 & \tau_1 \\ 0 & 0 & 1 & \tau_2 \\ 1 & 0 & 0 & \tau_3 \\ \hline 0 & 0 & 0 & 1 \end{array} \right) ; \quad \hat{S} = \left( \begin{array}{ccc|c} 0 & 0 & 1 & \sigma_1 \\ 0 & -1 & 0 & \sigma_2 \\ 1 & 0 & 0 & \sigma_3 \\ \hline 0 & 0 & 0 & 1 \end{array} \right) \quad (5.58)$$

which should be compared with eq.(5.6). Next we try impose on the deformed generators the defining relations of  $O_{24}$ . By explicit calculation we find:

$$\hat{T}^3 = \left( \begin{array}{ccc|c} 1 & 0 & 0 & \tau_1 + \tau_2 + \tau_3 \\ 0 & 1 & 0 & \tau_1 + \tau_2 + \tau_3 \\ 0 & 0 & 1 & \tau_1 + \tau_2 + \tau_3 \\ \hline 0 & 0 & 0 & 1 \end{array} \right) ; \quad \hat{S}^2 = \left( \begin{array}{ccc|c} 1 & 0 & 0 & \sigma_1 + \sigma_3 \\ 0 & 1 & 0 & 0 \\ 0 & 0 & 1 & \sigma_1 + \sigma_3 \\ \hline 0 & 0 & 0 & 1 \end{array} \right) ; \quad (\hat{S}\hat{T})^4 = \left( \begin{array}{ccc|c} 1 & 0 & 0 & 4\sigma_1 + 4\tau_3 \\ 0 & 1 & 0 & 0 \\ 0 & 0 & 1 & 0 \\ \hline 0 & 0 & 0 & 1 \end{array} \right)$$

so that we obtain the conditions:

$$\tau_1 + \tau_2 + \tau_3 \in \mathbb{Z} ; \quad \sigma_1 + \sigma_3 \in \mathbb{Z} ; \quad 4\sigma_1 + 4\tau_3 \in \mathbb{Z} \quad (5.59)$$

which are the Frobenius congruences for the present case. Next we consider the effect of conjugation with the most general translation element of the group  $\mathfrak{T}^3 \triangleleft \mathfrak{Jp}_{cubic}$ . Just for convenience we parameterize the translation subgroup as follows:

$$\mathfrak{t} = \left( \begin{array}{ccc|c} 1 & 0 & 0 & a + c \\ 0 & 1 & 0 & b \\ 0 & 0 & 1 & a - c \\ \hline 0 & 0 & 0 & 1 \end{array} \right) \quad (5.60)$$

and we get:

$$\mathfrak{t}\hat{T}\mathfrak{t}^{-1} = \left( \begin{array}{ccc|c} 0 & 1 & 0 & a - b + c + \tau_1 \\ 0 & 0 & 1 & -a + b + c + \tau_2 \\ 1 & 0 & 0 & \tau_3 - 2c \\ \hline 0 & 0 & 0 & 1 \end{array} \right) ; \quad \mathfrak{t}\hat{S}\mathfrak{t}^{-1} = \left( \begin{array}{ccc|c} 0 & 0 & 1 & 2c + \sigma_1 \\ 0 & -1 & 0 & 2b + \sigma_2 \\ 1 & 0 & 0 & \sigma_3 - 2c \\ \hline 0 & 0 & 0 & 1 \end{array} \right) \quad (5.61)$$

This shows that by using the parameters  $b, c$  we can always put  $\sigma_1 = \sigma_2 = 0$ , while using the parameter  $a$  we can put  $\tau_1 = 0$  (this is obviously only one possible gauge choice, yet it is the most convenient) so that Frobenius congruences reduce to:

$$\tau_2 + \tau_3 \in \mathbb{Z} ; \quad \sigma_3 \in \mathbb{Z} ; \quad 4\tau_3 \in \mathbb{Z} \quad (5.62)$$

Eq.(5.62) is of great momentum. It tells us that any non trivial subgroup  $\hat{\mathfrak{P}} \subset \mathfrak{I}\mathfrak{p}_{cubic}$  which is isomorphic to the point group  $O_{24}$ , but not conjugate to it contains point group elements extended with rational translations of the form  $\mathfrak{c} = \left\{ \frac{n_1}{4}, \frac{n_2}{4}, \frac{n_3}{4} \right\}$  with  $n_i \in \mathbb{Z}$ .

**The example of the group  $GS_{24}$**  An example is provided by the group later named  $GS_{24}$  which will repeatedly appear in our later discussions of Beltrami solutions. In the direct product realization of the point group  $\mathfrak{P} = O_{24}$  the generators  $T$  and  $S$  were specified in eq.s (5.4) and (5.6). In view of the Frobenius congruences let us set:

$$\hat{T} = \left( \begin{array}{cccc} 0 & 0 & 1 & 0 \\ 1 & 0 & 0 & \frac{1}{2} \\ 0 & 1 & 0 & \frac{1}{2} \\ 0 & 0 & 0 & 1 \end{array} \right) ; \quad \hat{S} = \left( \begin{array}{ccc|c} 0 & 0 & 1 & \frac{3}{2} \\ 0 & -1 & 0 & \frac{1}{2} \\ 1 & 0 & 0 & \frac{1}{2} \\ \hline 0 & 0 & 0 & 1 \end{array} \right) \quad (5.63)$$

By an immediate calculation we obtain:

$$\hat{T}^3 = \left( \begin{array}{cccc} 1 & 0 & 0 & 1 \\ 0 & 1 & 0 & 1 \\ 0 & 0 & 1 & 1 \\ 0 & 0 & 0 & 1 \end{array} \right) ; \quad \hat{S}^2 = \left( \begin{array}{cccc} 1 & 0 & 0 & 2 \\ 0 & 1 & 0 & 0 \\ 0 & 0 & 1 & 2 \\ 0 & 0 & 0 & 1 \end{array} \right) ; \quad (\hat{S} \cdot \hat{T})^4 = \left( \begin{array}{cccc} 1 & 0 & 0 & 0 \\ 0 & 1 & 0 & 0 \\ 0 & 0 & 1 & 2 \\ 0 & 0 & 0 & 1 \end{array} \right) \quad (5.64)$$

The above equation is interpreted by stating that:

$$\hat{T}^3 \in \Lambda \subset \mathfrak{S}_{GS} ; \quad \hat{S}^2 \in \Lambda \subset \mathfrak{S}_{GS} ; \quad (\hat{S} \cdot \hat{T})^4 \in \Lambda \subset \mathfrak{S}_{GS} \quad (5.65)$$

where  $\mathfrak{S}_{GS}$  is the space group in the exact sequence:

$$0 \xrightarrow{\iota} \Lambda \xrightarrow{\iota} \mathfrak{S}_{GS} \xrightarrow{\pi} GS_{24} \xrightarrow{\pi} \mathbf{1} \quad (5.66)$$

and the lattice normal subgroup is realized within  $\mathfrak{S}_{\text{GS}}$  by all the matrices of the form:

$$\mathfrak{S}_{\text{GS}} \triangleright \Lambda \ni \left( \begin{array}{ccc|c} 1 & 0 & 0 & n_1 \\ 0 & 1 & 0 & n_2 \\ 0 & 0 & 1 & n_3 \\ \hline 0 & 0 & 0 & 1 \end{array} \right) ; \quad n_i \in \mathbb{Z} \quad (5.67)$$

The group  $\text{GS}_{24}$  is defined as the quotient group:

$$\text{GS}_{24} = \frac{\mathfrak{S}_{\text{GS}}}{\Lambda} \sim \text{O}_{24} \sim \text{S}_4 \quad (5.68)$$

and  $\mathfrak{S}_{\text{GS}}$  is a group extension of the lattice group  $\Lambda$  by means of the abstract group octahedral point group  $\text{O}_{24}$ , yet it is not a semidirect product of the normal subgroup  $\Lambda$  with  $\text{O}_{24}$ . Indeed the space group  $\mathfrak{S}_{\text{GS}}$  contains translations that do not belong to the cubic lattice.

**A conceptual bifurcation** Up to this point our way and that of crystallographers was the same: hereafter our paths separate. The crystallographers classify all possible non trivial groups that extend the point group with such translation deformations: indeed looking at the crystallographic tables one realizes that all known space groups for the cubic lattice have translation components of the form  $\mathfrak{c} = \{\frac{n_1}{4}, \frac{n_2}{4}, \frac{n_3}{4}\}$ . On the other hand, we do something much simpler which leads to a quite big group containing all possible Space-Groups as subgroups, together with other subgroups that are not space groups in the crystallographic sense.

### 5.3.5 The Universal Classifying Group for the cubic lattice: $\text{G}_{1536}$

Inspired by the space group construction and by Frobenius congruences we just consider the subgroup of  $\mathfrak{G}_{\text{cubic}}$  where translations are quantized in units of  $\frac{1}{4}$ . In each direction and modulo integers there are just four translations  $0, \frac{1}{4}, \frac{1}{2}, \frac{3}{4}$  so that the translation subgroup reduces to  $\mathbb{Z}_4 \otimes \mathbb{Z}_4 \otimes \mathbb{Z}_4$  that has a total of 64 elements. In this way we single out a discrete subgroup  $\text{G}_{1536} \subset \mathfrak{G}_{\text{cubic}}$  of order  $24 \times 64 = 1536$ , which is simply the semidirect product of the point group  $\text{O}_{24}$  with  $\mathbb{Z}_4 \otimes \mathbb{Z}_4 \otimes \mathbb{Z}_4$ :

$$\mathfrak{G}_{\text{cubic}} \supset \text{G}_{1536} \simeq \text{O}_{24} \ltimes (\mathbb{Z}_4 \otimes \mathbb{Z}_4 \otimes \mathbb{Z}_4) \quad (5.69)$$

We name  $\text{G}_{1536}$  the universal classifying group of the cubic lattice, and its elements can be labeled as follows:

$$\text{G}_{1536} \in \left\{ p_q, \frac{2n_1}{4}, \frac{2n_2}{4}, \frac{2n_3}{4} \right\} \Rightarrow \left\{ \begin{array}{l} p_q \in \text{O}_{24} \\ \left\{ \frac{n_1}{4}, \frac{n_2}{4}, \frac{n_3}{4} \right\} \in \mathbb{Z}_4 \otimes \mathbb{Z}_4 \otimes \mathbb{Z}_4 \end{array} \right. \quad (5.70)$$

where for the elements of the point group we use the labels  $p_q$  established in eq.(5.5) while for the translation part our notation encodes an equivalence class of translation vectors  $\mathfrak{c} = \{\frac{n_1}{4}, \frac{n_2}{4}, \frac{n_3}{4}\}$ . The reason why we use  $\{\frac{2n_1}{4}, \frac{2n_2}{4}, \frac{2n_3}{4}\}$  is simply due to computer convenience. In the quite elaborate MATHEMATICA codes that were utilized in [1] to derive all the results such a notation was internally used and the automatic LaTeX Export of the outputs was provided in this way. In view of eq.(5.54) one can associate an explicit matrix to each group element of  $\text{G}_{1536}$ , starting from the construction of the Beltrami vector field associated with one point orbit of the octahedral group. Then one can consider such matrices the defining representation of the group if the

representation is faithful. In [1] the lowest lying 6-dimensional orbit was used which is indeed faithful. Three matrices are sufficient to characterize completely the defining representation just as any other representation: the matrix representing the generator  $T$ , the matrix representing the generator  $S$  and the matrix representing the translation  $\{\frac{n_1}{4}, \frac{n_2}{4}, \frac{n_3}{4}\}$ . In [1] it was found:

$$\mathfrak{R}^{\text{defi}}[T] = \begin{pmatrix} 0 & 0 & 0 & 0 & 1 & 0 \\ 0 & 0 & 0 & 0 & 0 & 1 \\ 0 & 1 & 0 & 0 & 0 & 0 \\ 1 & 0 & 0 & 0 & 0 & 0 \\ 0 & 0 & 0 & 1 & 0 & 0 \\ 0 & 0 & 1 & 0 & 0 & 0 \end{pmatrix} ; \quad \mathfrak{R}^{\text{defi}}[S] = \begin{pmatrix} 0 & 0 & 0 & 0 & 1 & 0 \\ 0 & 0 & 0 & 0 & 0 & 1 \\ 0 & 1 & 0 & 0 & 0 & 0 \\ 1 & 0 & 0 & 0 & 0 & 0 \\ 0 & 0 & 0 & 1 & 0 & 0 \\ 0 & 0 & 1 & 0 & 0 & 0 \end{pmatrix} \quad (5.71)$$

$$\mathcal{M}_{\{\frac{2n_1}{2}, \frac{2n_2}{2}, \frac{2n_3}{2}\}}^{\text{defi}} = \begin{pmatrix} \cos(\frac{\pi}{2}n_3) & 0 & \sin(\frac{\pi}{2}n_3) & 0 & 0 & 0 \\ 0 & \cos(\frac{\pi}{2}n_2) & 0 & 0 & -\sin(\frac{\pi}{2}n_2) & 0 \\ -\sin(\frac{\pi}{2}n_3) & 0 & \cos(\frac{\pi}{2}n_3) & 0 & 0 & 0 \\ 0 & 0 & 0 & \cos(\frac{\pi}{2}n_1) & 0 & \sin(\frac{\pi}{2}n_1) \\ 0 & \sin(\frac{\pi}{2}n_2) & 0 & 0 & \cos(\frac{\pi}{2}n_2) & 0 \\ 0 & 0 & 0 & -\sin(\frac{\pi}{2}n_1) & 0 & \cos(\frac{\pi}{2}n_1) \end{pmatrix} \quad (5.72)$$

Relying on the above matrices, any of the 1536 group elements obtains an explicit  $6 \times 6$  matrix representation upon use of formula (5.54). As already stressed one can regard that above as the actual definition of the group  $G_{1536}$  which from this point on can be studied intrinsically in terms of pure group theory without any further reference to lattices, Beltrami flows or dynamical systems.

### 5.3.6 Structure of the $G_{1536}$ group and derivation of its irreps

The identity card of a finite group is given by the organization of its elements into conjugacy classes, the list of its irreducible representation and finally its character table. Since ours is not any of the crystallographic groups, no explicit information is available in the literature about its conjugacy classes, its irreps and its character table. Hence the authors of [1] were forced to do everything from scratch by themselves and they could accomplish the task by means of purposely written MATHEMATICA codes. Most of their results were presented in the form of tables in the appendices of [1]. We will reproduce here those that are most relevant to the purposes of the present paper referring the reader to [1] for additional details.

**Conjugacy Classes** The conjugacy classes of  $G_{1536}$  are explicitly presented in appendix A.1 of [1]. There are 37 conjugacy classes whose populations is distributed as follows:

- |                          |                          |                           |
|--------------------------|--------------------------|---------------------------|
| 1) 2 classes of length 1 | 3) 2 classes of length 6 | 5) 7 classes of length 12 |
| 2) 2 classes of length 3 | 4) 1 class of length 8   | 6) 4 classes of length 24 |

7) 13 classes of length 48

8) 2 classes of length 96

9) 4 classes of length 128

It follows that there must be 37 irreducible representations whose construction is a task which was accomplished in [1] utilizing an iterative strategy algorithm available for solvable groups. We refer the reader to [1] for a description of that algorithm.

### 5.3.7 Derivation of $G_{1536}$ irreps

Utilizing the above described algorithm, implemented by means of purposely written MATHEMATICA codes, the authors of [1] were able to derive the explicit form of the 37 irreducible representations of  $G_{1536}$  and its character table. The essential tool is the following chain of normal subgroups:

$$G_{1536} \triangleright G_{768} \triangleright G_{256} \triangleright G_{128} \triangleright G_{64} \quad (5.73)$$

where  $G_{64} \sim \mathbb{Z}_4 \times \mathbb{Z}_4 \times \mathbb{Z}_4$  is abelian and corresponds to the compactified translation group. The above chain leads to the following quotient groups:

$$\frac{G_{1536}}{G_{768}} \sim \mathbb{Z}_2 \quad ; \quad \frac{G_{768}}{G_{256}} \sim \mathbb{Z}_3 \quad ; \quad \frac{G_{256}}{G_{128}} \sim \mathbb{Z}_2 \quad ; \quad \frac{G_{128}}{G_{64}} \sim \mathbb{Z}_2 \quad (5.74)$$

The description of the normal subgroups is given in various sections of the appendix of [1]. The result for the irreducible representations, thoroughly described also in the appendix of [1] is summarized here. The 37 irreps are distributed according to the following pattern:

- a) 4 irreps of dimension 1, namely  $D_1, \dots, D_4$
- b) 2 irreps of dimension 2, namely  $D_5, \dots, D_6$
- c) 12 irreps of dimension 3, namely  $D_6, \dots, D_{18}$
- d) 10 irreps of dimension 6, namely  $D_7, \dots, D_{28}$
- e) 3 irreps of dimension 8, namely  $D_{29}, \dots, D_{31}$
- f) 6 irreps of dimension 12, namely  $D_{32}, \dots, D_{37}$

The character table calculated in [1] is displayed in that paper and we omit it here. We just stress that all such results are incorporated into the **AlmafluidaNSPsystem** of MATHEMATICA codes available through the Wolfram Community site <https://community.wolfram.com/groups/-/m/t/2555905>.

The irreducible representations of the universal classifying group are a fundamental tool in the classification of Arnold-Beltrami vector fields. Indeed by choosing the various point group orbits of momentum vectors in the cubic lattice, according to their classification presented in the next section 5.4, and constructing the corresponding Arnold-Beltrami fields one obtains all of the 37 irreducible representations of  $G_{1536}$ . Each representation appears at least once and some of them appear several times. Considering next the possible subgroups  $H_i \subset G_{1536}$  and the branching rules of  $G_{1536}$  irreps with respect to  $H_i$  one obtains an explicit algorithm to construct Arnold-Beltrami vector fields with prescribed invariance space groups  $H_i$ . It suffices to select the identity representation of the subgroup in the branching rules. *These are the hidden symmetries of the Beltrami flows.* As we have discussed in the introduction these hidden symmetries extend to the exact Navier-Stokes time dependent solutions.

## 5.4 Classification of the 48 sublattices of the momentum lattice and the irreps of $G_{1536}$

Let us now analyze the action of the octahedral group on the cubic lattice. We define the orbits as the sets of vectors  $\mathbf{k} \in \Lambda$  that can be mapped one into the other by the action of some element of the point group, namely of  $O_{24}$ :

$$\mathbf{k}_1 \in \mathcal{O} \quad \text{and} \quad \mathbf{k}_2 \in \mathcal{O} \quad \Rightarrow \quad \exists \gamma \in O_{24} / \gamma \cdot \mathbf{k}_1 = \mathbf{k}_2 \quad (5.75)$$

In the case of the cubic lattice there are four type of orbits

### 5.4.1 Orbits of length 6

Each of these orbits is of the following form:

$$\mathcal{O}_6 = \left\{ \{0, 0, -n\}, \{0, 0, n\}, \{0, -n, 0\}, \{0, n, 0\}, \{-n, 0, 0\}, \{n, 0, 0\} \right\} \quad (5.76)$$

where  $n \in \mathbb{Z}$  is any integer number. The six vectors belonging to this orbit can be seen as the vertices of a regular octahedron (see fig.7)

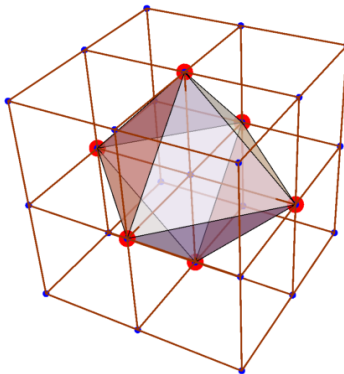


Figure 7: *The length 6 orbit of the octahedral group acting on the cubic lattice corresponds to the lattice points marked in red that can be viewed as the six vertices of a regular octahedron.*

### 5.4.2 Orbits of length 8

Each of these orbits is of the following form

$$\mathcal{O}_8 = \left\{ \begin{array}{llll} \{-n, -n, -n\}, & \{-n, -n, n\}, & \{-n, n, -n\}, & \{-n, n, n\}, \\ \{n, -n, -n\}, & \{n, -n, n\}, & \{n, n, -n\}, & \{n, n, n\} \end{array} \right\} \quad (5.77)$$

where  $n \in \mathbb{Z}$  is any integer number. The 8 vectors belonging to this orbit can be seen as the vertices of a cube (see fig.8)

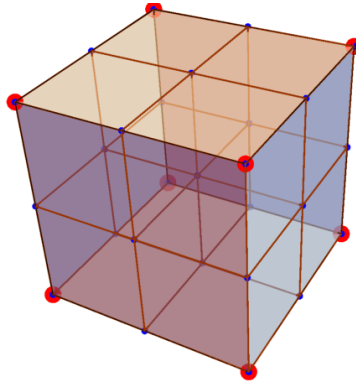


Figure 8: *The length 8 orbit of the octahedral group acting on the cubic lattice corresponds to the lattice points marked in red that can be viewed as the 8 vertices of a cube.*

### 5.4.3 Orbits of length 12

Each of these orbits is of the following form:

$$\mathcal{O}_{12} = \left\{ \begin{array}{cccc} \{0, -n, -n\}, & \{0, -n, n\}, & \{0, n, -n\}, & \{0, n, n\}, \\ \{-n, 0, -n\}, & \{-n, 0, n\}, & \{-n, -n, 0\}, & \{-n, n, 0\}, \\ \{n, 0, -n\}, & \{n, 0, n\}, & \{n, -n, 0\}, & \{n, n, 0\} \end{array} \right\} \quad (5.78)$$

where  $n \in \mathbb{Z}$  is any integer number. The 12 vectors belonging to this orbit can be seen as the middle points of the edges of a cube (see fig.9)

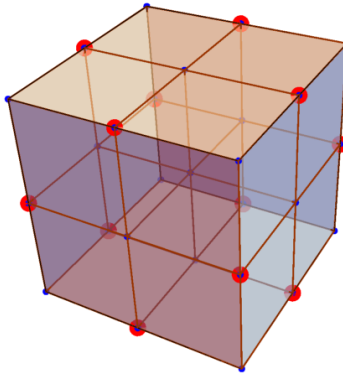


Figure 9: *The length 12 orbit of the octahedral group acting on the cubic lattice corresponds to the lattice points marked in red that can be viewed as the middle points of the edges of a cube.*

#### 5.4.4 Orbits of length 24

Each of these orbits is of the following form:

$$\mathcal{O}_{24} = \left\{ \begin{array}{cccc} \{-p, -q, r\}, & \{-p, q, -r\}, & \{-p, -r, -q\}, & \{-p, r, q\}, \\ \{p, -q, -r\}, & \{p, q, r\}, & \{p, -r, q\}, & \{p, r, -q\}, \\ \{-q, -p, -r\}, & \{-q, p, r\}, & \{-q, -r, p\}, & \{-q, r, -p\}, \\ \{q, -p, r\}, & \{q, p, -r\}, & \{q, -r, -p\}, & \{q, r, p\}, \\ \{-r, -p, q\}, & \{-r, p, -q\}, & \{-r, -q, -p\}, & \{-r, q, p\}, \\ \{r, -p, -q\}, & \{r, p, q\}, & \{r, -q, p\}, & \{r, q, -p\}, \end{array} \right\} \quad (5.79)$$

where  $\{p, q, r\} \in \mathbb{Z}$  is any triplet of integer numbers that are not all three equal in absolute value.

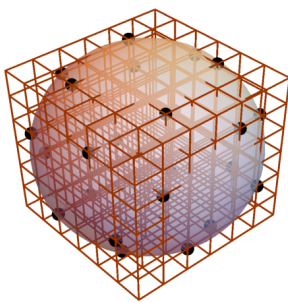


Figure 10: A possible length 24 orbit of the octahedral group acting on the cubic lattice corresponds to the lattice points marked in black. In this case the orbit is generated by the vector  $\{1, 2, 3\}$  and all the orbit points belong to the intersection of the cubic lattice  $\Lambda_{cubic}$  with a sphere of radius  $r = \sqrt{14}$ .

#### 5.4.5 Classification of the 48 types of orbits

The first observation is that the group  $G_{1536}$  has a finite number of irreducible representations so that the number of different types of Arnold-Beltrami vector fields has also got to be finite, namely as many as the 37 irreps, times the number of different ways to obtain them from orbits of length 6,8,12 or 24. The second observation is the key role of the number 4 introduced by Frobenius congruences which was already the clue to the definition of  $G_{1536}$ . What we should expect is that the various orbits should be defined with integers modulo 4 in other words that we should just consider the possible octahedral orbits on a lattice with coefficients in  $\mathbb{Z}_4$  rather than  $\mathbb{Z}$ . The easy guess, which is confirmed by computer calculations, is that the pattern of  $G_{1536}$  representations obtained from the construction of Arnold-Beltrami vector fields according to the algorithm of section 4.4 depends only on the equivalence classes of momentum orbits modulo 4. Hence we have a finite number of such orbits and a finite number of Arnold-Beltrami vector fields which we presently describe. Let us stress that an embryo of the exhaustive classification of orbits we are going to present was introduced by Arnold in his paper [12]. Arnold's one was only an embryo of the complete classification for the following two reasons:



1. The type of momenta orbits were partitioned according to *odd* and *even* (namely according to  $\mathbb{Z}_2$ , rather than  $\mathbb{Z}_4$ )
2. The classifying group was taken to be the crystallographic  $\text{GS}_{24}$ , as defined in the appendices of [1] and already discussed in eq.(5.63) and following lines.

Let us then present the complete classification of point orbits in the momentum lattice. First we subdivide the momenta into five groups:

- A)** Momenta of type  $\{a, 0, 0\}$  which generate  $\text{O}_{24}$  orbits of length 6 and representations of the universal group  $\text{G}_{1536}$  also of dimensions 6.
- B)** Momenta of type  $\{a, a, a\}$  which generate  $\text{O}_{24}$  orbits of length 8 and representations of the universal group  $\text{G}_{1536}$  also of dimensions 8.
- C)** Momenta of type  $\{a, a, 0\}$  which generate  $\text{O}_{24}$  orbits of length 12 and representations of the universal group  $\text{G}_{1536}$  also of dimensions 12.
- D)** Momenta of type  $\{a, a, b\}$  which generate  $\text{O}_{24}$  orbits of length 24 and representations of the universal group  $\text{G}_{1536}$  also of dimensions 24.
- E)** Momenta of type  $\{a, b, c\}$  which generate  $\text{O}_{24}$  orbits of length 24 and representations of the universal group  $\text{G}_{1536}$  of dimensions 48.

The reason why in the cases A) . . . D) the dimension of the representation  $\mathfrak{R}(\text{G}_{1536})$  coincides with the dimension  $|\mathcal{O}|$  of the orbit is simple. For each momentum in the orbit ( $\forall \mathbf{k}_i \in \mathcal{O}$ ) also its negative appears in the same orbit ( $-\mathbf{k}_i \in \mathcal{O}$ ), hence the number of arguments  $\Theta_i \equiv 2\pi \mathbf{k}_i \cdot \mathbf{x}$  of the independent trigonometric functions  $\sin(\Theta_i)$  and  $\cos(\Theta_i)$  is  $\frac{1}{2} \times 2|\mathcal{O}| = |\mathcal{O}|$  since  $\sin(\pm\Theta_i) = \pm \sin(\Theta_i)$  and  $\cos(\pm\Theta_i) = \cos(\Theta_i)$ .

In case E), instead, the negatives of all the members of the orbit  $\mathcal{O}$  are not in  $\mathcal{O}$ . The number of independent trigonometric functions is therefore 48 and such is the dimension of the representation  $\mathfrak{R}(\text{G}_{1536})$ .

In each of the five groups one still has to reduce the entries to  $\mathbb{Z}_4$ , namely to consider their equivalence class mod 4. Each different choice of the pattern of  $\mathbb{Z}_4$  classes appearing in an orbit leads to a different decomposition of the representation into irreducible representation of  $\text{G}_{1536}$ . A simple consideration of the combinatorics leads to the conclusion that there are in total 48 cases to be considered. The very significant result is that all of the 37 irreducible representations of  $\text{G}_{1536}$  appear at least once in the list of these decompositions. Hence for all the *irreps* of this group one can find a corresponding Beltrami field and for some *irreps* such a Beltrami field admits a few inequivalent realizations. The list of the 48 distinct types of momenta is the following one:

- |  |  |  |
|--|--|--|
| 1. $\mathbf{k} = \{0, 0, 1 + 4\rho\}$              | 7. $\mathbf{k} = \{3 + 4\mu, 3 + 4\mu, 3 + 4\mu\}$ | 13. $\mathbf{k} = \{1 + 4\mu, 1 + 4\mu, 2 + 4\rho\}$ |
| 2. $\mathbf{k} = \{0, 0, 2 + 4\rho\}$              | 8. $\mathbf{k} = \{4 + 4\mu, 4 + 4\mu, 4 + 4\mu\}$ | 14. $\mathbf{k} = \{1 + 4\mu, 1 + 4\mu, 3 + 4\rho\}$ |
| 3. $\mathbf{k} = \{0, 0, 3 + 4\rho\}$              | 9. $\mathbf{k} = \{0, 1 + 4\nu, 1 + 4\nu\}$        | 15. $\mathbf{k} = \{1 + 4\mu, 1 + 4\mu, 4 + 4\rho\}$ |
| 4. $\mathbf{k} = \{0, 0, 4 + 4\rho\}$              | 10. $\mathbf{k} = \{0, 2 + 4\nu, 2 + 4\nu\}$       | 16. $\mathbf{k} = \{1 + 4\mu, 1 + 4\mu, 5 + 4\rho\}$ |
| 5. $\mathbf{k} = \{1 + 4\mu, 1 + 4\mu, 1 + 4\mu\}$ | 11. $\mathbf{k} = \{0, 3 + 4\nu, 3 + 4\nu\}$       | 17. $\mathbf{k} = \{1 + 4\mu, 2 + 4\mu, 2 + 4\rho\}$ |
| 6. $\mathbf{k} = \{2 + 4\mu, 2 + 4\mu, 2 + 4\mu\}$ | 12. $\mathbf{k} = \{0, 4 + 4\nu, 4 + 4\nu\}$       | 18. $\mathbf{k} = \{2 + 4\mu, 2 + 4\mu, 6 + 4\rho\}$ |

- |  |   |   |
|--|---|---|
| 19. $\mathbf{k} = \{2 + 4\mu, 2 + 4\mu, 3 + 4\rho\}$ | 29. $\mathbf{k} = \{4 + 4\mu, 8 + 4\nu, 12 + 4\rho\}$ | 39. $\mathbf{k} = \{1 + 4\mu, 3 + 4\nu, 5 + 4\rho\}$  |
| 20. $\mathbf{k} = \{2 + 4\mu, 2 + 4\mu, 4 + 4\rho\}$ | 30. $\mathbf{k} = \{1 + 4\mu, 4 + 4\nu, 8 + 4\rho\}$  | 40. $\mathbf{k} = \{1 + 4\mu, 2 + 4\nu, 6 + 4\rho\}$  |
| 21. $\mathbf{k} = \{1 + 4\mu, 3 + 4\mu, 3 + 4\rho\}$ | 31. $\mathbf{k} = \{2 + 4\mu, 4 + 4\nu, 8 + 4\rho\}$  | 41. $\mathbf{k} = \{1 + 4\mu, 2 + 4\nu, 3 + 4\rho\}$  |
| 22. $\mathbf{k} = \{2 + 4\mu, 3 + 4\mu, 3 + 4\rho\}$ | 32. $\mathbf{k} = \{3 + 4\mu, 4 + 4\nu, 8 + 4\rho\}$  | 42. $\mathbf{k} = \{1 + 4\mu, 3 + 4\nu, 7 + 4\rho\}$  |
| 23. $\mathbf{k} = \{3 + 4\mu, 3 + 4\mu, 7 + 4\rho\}$ | 33. $\mathbf{k} = \{1 + 4\mu, 2 + 4\nu, 4 + 4\rho\}$  | 43. $\mathbf{k} = \{2 + 4\mu, 6 + 4\nu, 10 + 4\rho\}$ |
| 24. $\mathbf{k} = \{1 + 4\mu, 4 + 4\mu, 4 + 4\rho\}$ | 34. $\mathbf{k} = \{1 + 4\mu, 3 + 4\nu, 4 + 4\rho\}$  | 44. $\mathbf{k} = \{2 + 4\mu, 3 + 4\nu, 6 + 4\rho\}$  |
| 25. $\mathbf{k} = \{2 + 4\mu, 4 + 4\mu, 4 + 4\rho\}$ | 35. $\mathbf{k} = \{2 + 4\mu, 4 + 4\nu, 6 + 4\rho\}$  | 45. $\mathbf{k} = \{2 + 4\mu, 3 + 4\nu, 7 + 4\rho\}$  |
| 26. $\mathbf{k} = \{3 + 4\mu, 4 + 4\mu, 4 + 4\rho\}$ | 36. $\mathbf{k} = \{2 + 4\mu, 3 + 4\nu, 4 + 4\rho\}$  | 46. $\mathbf{k} = \{3 + 4\mu, 7 + 4\nu, 11 + 4\rho\}$ |
| 27. $\mathbf{k} = \{4 + 4\mu, 4 + 4\mu, 8 + 4\rho\}$ | 37. $\mathbf{k} = \{1 + 4\mu, 5 + 4\nu, 9 + 4\rho\}$  | 47. $\mathbf{k} = \{1 + 4\mu, 4 + 4\nu, 5 + 4\rho\}$  |
| 28. $\mathbf{k} = \{3 + 4\mu, 3 + 4\mu, 4 + 4\rho\}$ | 38. $\mathbf{k} = \{1 + 4\mu, 2 + 4\nu, 5 + 4\rho\}$  | 48. $\mathbf{k} = \{3 + 4\mu, 4 + 4\nu, 7 + 4\rho\}$  |

where  $\mu, \nu, \rho \in \mathbb{Z}$ . The simplest and lowest lying representative of each of the 48 classes of equivalent momenta is obtained choosing  $\mu = \nu = 0$ .

#### 5.4.6 The 48 orbits type and the irreps of the Universal Classifying Group

In this subsection, quoting the results obtained in [1] for each of the 48 classes enumerated above we provide the decomposition of the corresponding Beltrami vector field parameter space into  $G_{1536}$  irreducible representations. These results are the outcome of extensive MATHEMATICA calculations that were performed with purposely written codes. As already stressed the most relevant point is that all the 37 irreps of the Classifying Group are reproduced: this is the main reason for its name.

#### 5.4.7 Classes of momentum vectors yielding orbits of length 6: $\{\mathbf{a}, 0, 0\}$

**Class of the momentum vector =  $\{0, 0, 1 + 4\rho\}$**

**Dimension of the  $G_{1536}$  representation = 6**

**Orbit =  $D_{23}[G_{1536}, 6]$**

**Class of the momentum vector =  $\{0, 0, 2 + 4\rho\}$**

**Dimension of the  $G_{1536}$  representation = 6**

**Orbit =  $D_{19}[G_{1536}, 6]$**

**Class of the momentum vector =  $\{0, 0, 3 + 4\rho\}$**

**Dimension of the  $G_{1536}$  representation = 6**

**Orbit =  $D_{24}[G_{1536}, 6]$**

**Class of the momentum vector =  $\{0, 0, 4 + 4\rho\}$**

**Dimension of the  $G_{1536}$  representation = 6**

**Orbit =  $D_7[G_{1536}, 3] + D_8[G_{1536}, 3]$**

5.4.8 Classes of momentum vectors yielding orbits of length 8:  $\{a,a,a\}$

Class of the momentum vector =  $\{1 + 4\mu, 1 + 4\mu, 1 + 4\mu\}$

Dimension of the  $G_{1536}$  representation = 8

Orbit =  $D_{30}[G_{1536}, 8]$

Class of the momentum vector =  $\{2 + 4\mu, 2 + 4\mu, 2 + 4\mu\}$

Dimension of the  $G_{1536}$  representation = 8

Orbit =  $D_6[G_{1536}, 2] + D_{17}[G_{1536}, 3] + D_{18}[G_{1536}, 3]$

Class of the momentum vector =  $\{3 + 4\mu, 3 + 4\mu, 3 + 4\mu\}$

Dimension of the  $G_{1536}$  representation = 8

Orbit =  $D_{31}[G_{1536}, 8]$

Class of the momentum vector =  $\{4 + 4\mu, 4 + 4\mu, 4 + 4\mu\}$

Dimension of the  $G_{1536}$  representation = 8

Orbit =  $D_5[G_{1536}, 2] + D_7[G_{1536}, 3] + D_8[G_{1536}, 3]$

5.4.9 Classes of momentum vectors yielding orbits of length 12:  $\{0,a,a\}$

Class of the momentum vector =  $\{0, 1 + 4\nu, 1 + 4\nu\}$

Dimension of the  $G_{1536}$  representation = 12

Orbit =  $D_{32}[G_{1536}, 12]$

Class of the momentum vector =  $\{0, 2 + 4\nu, 2 + 4\nu\}$

Dimension of the  $G_{1536}$  representation = 12

Orbit =  $D_{13}[G_{1536}, 3] + D_{15}[G_{1536}, 3] + D_{20}[G_{1536}, 6]$

Class of the momentum vector =  $\{0, 3 + 4\nu, 3 + 4\nu\}$

Dimension of the  $G_{1536}$  representation = 12

Orbit =  $D_{32}[G_{1536}, 12]$

Class of the momentum vector =  $\{0, 4 + 4\nu, 4 + 4\nu\}$

Dimension of the  $G_{1536}$  representation = 12

Orbit =  $D_2[G_{1536}, 1] + D_5[G_{1536}, 2] + D_7[G_{1536}, 3] + 2D_8[G_{1536}, 3]$

5.4.10 Classes of momentum vectors yielding orbits of length 24:  $\{a,a,b\}$

Class of the momentum vector =  $\{1 + 4\mu, 1 + 4\mu, 2 + 4\rho\}$

Dimension of the  $G_{1536}$  representation = 24

Orbit =  $D_{34}[G_{1536}, 12] + D_{35}[G_{1536}, 12]$

Class of the momentum vector =  $\{1 + 4\mu, 1 + 4\mu, 3 + 4\rho\}$

Dimension of the  $G_{1536}$  representation = 24

Orbit =  $D_{29}[G_{1536}, 8] + D_{30}[G_{1536}, 8] + D_{31}[G_{1536}, 8]$

Class of the momentum vector =  $\{1 + 4\mu, 1 + 4\mu, 4 + 4\rho\}$

Dimension of the  $G_{1536}$  representation = 24

Orbit =  $D_{32}[G_{1536}, 12] + D_{33}[G_{1536}, 12]$

Class of the momentum vector =  $\{1 + 4\mu, 1 + 4\mu, 5 + 4\rho\}$   
 Dimension of the  $G_{1536}$  representation = 24  
 Orbit =  $D_{29}[G_{1536}, 8] + D_{30}[G_{1536}, 8] + D_{31}[G_{1536}, 8]$   
 Class of the momentum vector =  $\{1 + 4\mu, 2 + 4\mu, 2 + 4\rho\}$   
 Dimension of the  $G_{1536}$  representation = 24  
 Orbit =  $D_{25}[G_{1536}, 6] + D_{26}[G_{1536}, 6] + D_{27}[G_{1536}, 6] + D_{28}[G_{1536}, 6]$   
 Class of the momentum vector =  $\{2 + 4\mu, 2 + 4\mu, 6 + 4\rho\}$   
 Dimension of the  $G_{1536}$  representation = 24  
 Orbit =  $D_3[G_{1536}, 1] + D_4[G_{1536}, 1] + 2D_6[G_{1536}, 2] + 3D_{17}[G_{1536}, 3] + 3D_{18}[G_{1536}, 3]$   
 Class of the momentum vector =  $\{2 + 4\mu, 2 + 4\mu, 3 + 4\rho\}$   
 Dimension of the  $G_{1536}$  representation = 24  
 Orbit =  $D_{25}[G_{1536}, 6] + D_{26}[G_{1536}, 6] + D_{27}[G_{1536}, 6] + D_{28}[G_{1536}, 6]$   
 Class of the momentum vector =  $\{2 + 4\mu, 2 + 4\mu, 4 + 4\rho\}$   
 Dimension of the  $G_{1536}$  representation = 24  
 Orbit =  $D_{13}[G_{1536}, 3] + D_{14}[G_{1536}, 3] + D_{15}[G_{1536}, 3] + D_{16}[G_{1536}, 3] + 2D_{20}[G_{1536}, 6]$   
 Class of the momentum vector =  $\{1 + 4\mu, 3 + 4\mu, 3 + 4\rho\}$   
 Dimension of the  $G_{1536}$  representation = 24  
 Orbit =  $D_{29}[G_{1536}, 8] + D_{30}[G_{1536}, 8] + D_{31}[G_{1536}, 8]$   
 Class of the momentum vector =  $\{2 + 4\mu, 3 + 4\mu, 3 + 4\rho\}$   
 Dimension of the  $G_{1536}$  representation = 24  
 Orbit =  $D_{34}[G_{1536}, 12] + D_{35}[G_{1536}, 12]$   
 Class of the momentum vector =  $\{3 + 4\mu, 3 + 4\mu, 7 + 4\rho\}$   
 Dimension of the  $G_{1536}$  representation = 24  
 Orbit =  $D_{29}[G_{1536}, 8] + D_{30}[G_{1536}, 8] + D_{31}[G_{1536}, 8]$   
 Class of the momentum vector =  $\{1 + 4\mu, 4 + 4\mu, 4 + 4\rho\}$   
 Dimension of the  $G_{1536}$  representation = 24  
 Orbit =  $D_{21}[G_{1536}, 6] + D_{22}[G_{1536}, 6] + D_{23}[G_{1536}, 6] + D_{24}[G_{1536}, 6]$   
 Class of the momentum vector =  $\{2 + 4\mu, 4 + 4\mu, 4 + 4\rho\}$   
 Dimension of the  $G_{1536}$  representation = 24  
 Orbit =  $D_9[G_{1536}, 3] + D_{10}[G_{1536}, 3] + D_{11}[G_{1536}, 3] + D_{12}[G_{1536}, 3] + 2D_{19}[G_{1536}, 6]$   
 Class of the momentum vector =  $\{3 + 4\mu, 4 + 4\mu, 4 + 4\rho\}$   
 Dimension of the  $G_{1536}$  representation = 24  
 Orbit =  $D_{21}[G_{1536}, 6] + D_{22}[G_{1536}, 6] + D_{23}[G_{1536}, 6] + D_{24}[G_{1536}, 6]$   
 Class of the momentum vector =  $\{4 + 4\mu, 4 + 4\mu, 8 + 4\rho\}$   
 Dimension of the  $G_{1536}$  representation = 24  
 Orbit =  $D_1[G_{1536}, 1] + D_2[G_{1536}, 1] + 2D_5[G_{1536}, 2] + 3D_7[G_{1536}, 3] + 3D_8[G_{1536}, 3]$   
 Class of the momentum vector =  $\{3 + 4\mu, 3 + 4\mu, 4 + 4\rho\}$   
 Dimension of the  $G_{1536}$  representation = 24  
 Orbit =  $D_{32}[G_{1536}, 12] + D_{33}[G_{1536}, 12]$

5.4.11 Classes of momentum vectors yielding point orbits of length 24 and  $G_{1536}$  representations of dimensions 48: {a,b,c}

Class of the momentum vector =  $\{4 + 4\mu, 8 + 4\nu, 12 + 4\rho\}$

Dimension of the  $G_{1536}$  representation = 48

Orbit =  $2D_1[G_{1536}, 1] + 2D_2[G_{1536}, 1] + 4D_5[G_{1536}, 2] + 6D_7[G_{1536}, 3] + 6D_8[G_{1536}, 3]$

Class of the momentum vector =  $\{1 + 4\mu, 4 + 4\nu, 8 + 4\rho\}$

Dimension of the  $G_{1536}$  representation = 48

Orbit =  $2D_{21}[G_{1536}, 6] + 2D_{22}[G_{1536}, 6] + 2D_{23}[G_{1536}, 6] + 2D_{24}[G_{1536}, 6]$

Class of the momentum vector =  $\{2 + 4\mu, 4 + 4\nu, 8 + 4\rho\}$

Dimension of the  $G_{1536}$  representation = 48

Orbit =  $2D_9[G_{1536}, 3] + 2D_{10}[G_{1536}, 3] + 2D_{11}[G_{1536}, 3] + 2D_{12}[G_{1536}, 3] + 4D_{19}[G_{1536}, 6]$

Class of the momentum vector =  $\{3 + 4\mu, 4 + 4\nu, 8 + 4\rho\}$

Dimension of the  $G_{1536}$  representation = 48

Orbit =  $2D_{21}[G_{1536}, 6] + 2D_{22}[G_{1536}, 6] + 2D_{23}[G_{1536}, 6] + 2D_{24}[G_{1536}, 6]$

Class of the momentum vector =  $\{1 + 4\mu, 2 + 4\nu, 4 + 4\rho\}$

Dimension of the  $G_{1536}$  representation = 48

Orbit =  $2D_{36}[G_{1536}, 12] + 2D_{37}[G_{1536}, 12]$

Class of the momentum vector =  $\{1 + 4\mu, 3 + 4\nu, 4 + 4\rho\}$

Dimension of the  $G_{1536}$  representation = 48

Orbit =  $2D_{32}[G_{1536}, 12] + 2D_{33}[G_{1536}, 12]$

Class of the momentum vector =  $\{2 + 4\mu, 4 + 4\nu, 6 + 4\rho\}$

Dimension of the  $G_{1536}$  representation = 48

Orbit =  $2D_{13}[G_{1536}, 3] + 2D_{14}[G_{1536}, 3] + 2D_{15}[G_{1536}, 3] + 2D_{16}[G_{1536}, 3] + 4D_{20}[G_{1536}, 6]$

Class of the momentum vector =  $\{2 + 4\mu, 3 + 4\nu, 4 + 4\rho\}$

Dimension of the  $G_{1536}$  representation = 48

Orbit =  $2D_{36}[G_{1536}, 12] + 2D_{37}[G_{1536}, 12]$

Class of the momentum vector =  $\{1 + 4\mu, 5 + 4\nu, 9 + 4\rho\}$

Dimension of the  $G_{1536}$  representation = 48

Orbit =  $2D_{29}[G_{1536}, 8] + 2D_{30}[G_{1536}, 8] + 2D_{31}[G_{1536}, 8]$

Class of the momentum vector =  $\{1 + 4\mu, 2 + 4\nu, 5 + 4\rho\}$

Dimension of the  $G_{1536}$  representation = 48

Orbit =  $2D_{34}[G_{1536}, 12] + 2D_{35}[G_{1536}, 12]$

Class of the momentum vector =  $\{1 + 4\mu, 3 + 4\nu, 5 + 4\rho\}$

Dimension of the  $G_{1536}$  representation = 48

Orbit =  $2D_{29}[G_{1536}, 8] + 2D_{30}[G_{1536}, 8] + 2D_{31}[G_{1536}, 8]$

Class of the momentum vector =  $\{1 + 4\mu, 2 + 4\nu, 6 + 4\rho\}$

Dimension of the  $G_{1536}$  representation = 48

Orbit =  $2D_{25}[G_{1536}, 6] + 2D_{26}[G_{1536}, 6] + 2D_{27}[G_{1536}, 6] + 2D_{28}[G_{1536}, 6]$

Class of the momentum vector =  $\{1 + 4\mu, 2 + 4\nu, 3 + 4\rho\}$

Dimension of the  $G_{1536}$  representation = 48

Orbit =  $2D_{34}[G_{1536}, 12] + 2D_{35}[G_{1536}, 12]$

Class of the momentum vector =  $\{1 + 4\mu, 3 + 4\nu, 7 + 4\rho\}$

Dimension of the  $G_{1536}$  representation = 48

Orbit =  $2D_{29}[\mathbf{G}_{1536}, 8] + 2D_{30}[\mathbf{G}_{1536}, 8] + 2D_{31}[\mathbf{G}_{1536}, 8]$   
Class of the momentum vector =  $\{2 + 4\mu, 6 + 4\nu, 10 + 4\rho\}$   
Dimension of the  $\mathbf{G}_{1536}$  representation = 48  
Orbit =  $2D_3[\mathbf{G}_{1536}, 1] + 2D_4[\mathbf{G}_{1536}, 1] + 4D_6[\mathbf{G}_{1536}, 2] + 6D_{17}[\mathbf{G}_{1536}, 3] + 6D_{18}[\mathbf{G}_{1536}, 3]$   
Class of the momentum vector =  $\{2 + 4\mu, 3 + 4\nu, 6 + 4\rho\}$   
Dimension of the  $\mathbf{G}_{1536}$  representation = 48  
Orbit =  $2D_{25}[\mathbf{G}_{1536}, 6] + 2D_{26}[\mathbf{G}_{1536}, 6] + 2D_{27}[\mathbf{G}_{1536}, 6] + 2D_{28}[\mathbf{G}_{1536}, 6]$   
Class of the momentum vector =  $\{2 + 4\mu, 3 + 4\nu, 7 + 4\rho\}$   
Dimension of the  $\mathbf{G}_{1536}$  representation = 48  
Orbit =  $2D_{34}[\mathbf{G}_{1536}, 12] + 2D_{35}[\mathbf{G}_{1536}, 12]$   
Class of the momentum vector =  $\{3 + 4\mu, 7 + 4\nu, 11 + 4\rho\}$   
Dimension of the  $\mathbf{G}_{1536}$  representation = 48  
Orbit =  $2D_{29}[\mathbf{G}_{1536}, 8] + 2D_{30}[\mathbf{G}_{1536}, 8] + 2D_{31}[\mathbf{G}_{1536}, 8]$   
Class of the momentum vector =  $\{1 + 4\mu, 4 + 4\nu, 5 + 4\rho\}$   
Dimension of the  $\mathbf{G}_{1536}$  representation = 48  
Orbit =  $2D_{32}[\mathbf{G}_{1536}, 12] + 2D_{33}[\mathbf{G}_{1536}, 12]$   
Class of the momentum vector =  $\{3 + 4\mu, 4 + 4\nu, 7 + 4\rho\}$   
Dimension of the  $\mathbf{G}_{1536}$  representation = 48  
Orbit =  $2D_{32}[\mathbf{G}_{1536}, 12] + 2D_{33}[\mathbf{G}_{1536}, 12]$

#### 5.4.12 The interpretation of the 48 momentum classes as sublattices of the cubic lattice

The union of the orbits of the 48 vector classes for all values of the integer parameters  $\mu, \nu, \rho$  constitute infinite sublattices of the momentum lattice.

Given the class  $\mathbf{k}^{p,q,r} = \{p + 4\mu, q + 4\nu, r + 4\rho\}$  and the corresponding orbit of each vector in the class  $\mathcal{O}^{(p,q,r)}(\mu, \nu, \rho)$  considering all  $\mu, \nu, \rho \in \mathbb{Z}$  we obtain a sublattice of the original lattice:

$$\Lambda^{p,q,r} \equiv \bigoplus_{\mu, \nu, \rho}^{\infty} \mathcal{O}^{(p,q,r)} \subset \Lambda_{cubic} \quad (5.80)$$

Most of these sublattices are 1 dimensional  $\mathbb{Z} \hookrightarrow \mathbb{Z} \times \mathbb{Z} \times \mathbb{Z}$  some are two dimensional  $\mathbb{Z} \times \mathbb{Z} \hookrightarrow \mathbb{Z} \times \mathbb{Z} \times \mathbb{Z}$  and some are three dimensional  $\mathbb{Z} \times \mathbb{Z} \times \mathbb{Z} \hookrightarrow \mathbb{Z} \times \mathbb{Z} \times \mathbb{Z}$ .

For instance the sublattice  $\Lambda^{0,0,1}$  is formed by all the six dimensional orbits of the vectors of type  $\{0, 0, 1 + 4\mu\}$  with  $\mu \in \mathbb{Z}$ . A picture of the immersion of the points of this sublattice in the full cubic lattice is provided in fig.11. Similarly the sublattice  $\Lambda^{1,1,1}$  is formed by all the eight dimensional orbits of the vectors of type  $\{1 + 4\mu, 1 + 4\mu, 1 + 4\mu\}$  with  $\mu \in \mathbb{Z}$ . A picture of the immersion of the points of this sublattice in the full cubic lattice is provided in fig.12. Finally we display sublattice  $\Lambda^{1,1,2}$  which is formed by all the eight dimensional orbits of the vectors of type  $\{1 + 4\mu, 1 + 4\mu, 2 + 4\nu\}$  with  $\mu, \nu \in \mathbb{Z}$ . A picture of the immersion of the points of this sublattice in the full cubic lattice is provided in fig.13.

### 5.5 The universal classifying group $\mathfrak{U}_{72}$ for the Hexagonal Lattice $\Lambda_{Hex}$

In this section following the same procedure utilized in the cubic case, namely Frobenius congruences, we identify the Universal Classifying Group for the hexagonal lattice with point group  $\mathfrak{P}_{\Lambda_{Hex}} = \text{Dih}_6$  and we discover that it is a group with 72 elements.

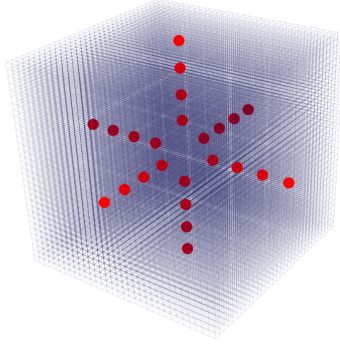


Figure 11: A picture of the immersion of the sublattice  $\Lambda^{0,0,1}$  into the full cubic lattice. The points of  $\Lambda^{0,0,1}$  are painted in red on the background of the grid of the cubic lattice.

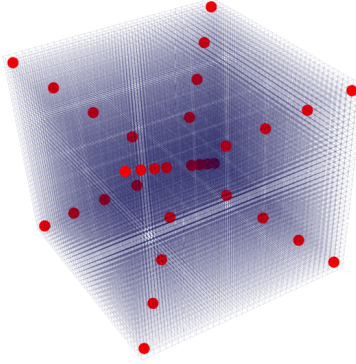


Figure 12: A picture of the immersion of the sublattice  $\Lambda^{1,1,1}$  into the full cubic lattice. The points of  $\Lambda^{1,1,1}$  are painted in red on the background of the grid of the cubic lattice.

### 5.5.1 Frobenius congruences for $\text{Dih}_6$

Utilizing the block triangular representation for the semidirect product we introduce the two candidate generators  $\hat{\mathcal{A}}$  and  $\hat{\mathcal{B}}$  as it follows:

$$\hat{\mathcal{A}} = \left( \begin{array}{ccc|c} \frac{1}{2} & \frac{\sqrt{3}}{2} & 0 & \alpha_1 \\ -\frac{\sqrt{3}}{2} & \frac{1}{2} & 0 & \alpha_2 \\ 0 & 0 & 1 & \alpha_3 \\ \hline 0 & 0 & 0 & 1 \end{array} \right) ; \quad \hat{\mathcal{B}} = \left( \begin{array}{ccc|c} -1 & 0 & 0 & \beta_1 \\ 0 & 1 & 0 & \beta_2 \\ 0 & 0 & -1 & \beta_3 \\ \hline 0 & 0 & 0 & 1 \end{array} \right) \quad (5.81)$$

and we impose the three conditions:

$$\hat{\mathcal{A}}^6 \in \hat{\Lambda} \quad ; \quad \hat{\mathcal{B}}^2 \in \hat{\Lambda} \quad ; \quad (\hat{\mathcal{B}} \cdot \hat{\mathcal{A}})^2 \in \hat{\Lambda} \quad (5.82)$$

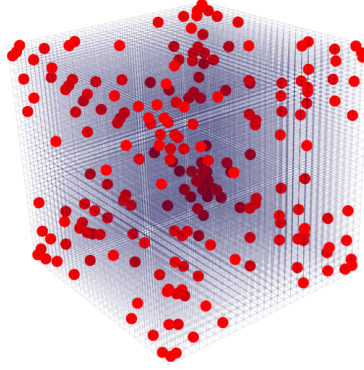


Figure 13: A picture of the immersion of the sublattice  $\Lambda^{1,1,2}$  into the full cubic lattice. The points of  $\Lambda^{1,1,2}$  are painted in red on the background of the grid of the cubic lattice.

where the lattice subgroup is embedded in the inhomogeneous point group  $\mathfrak{I}\mathfrak{p}_{\Lambda_{Hex}}$  as it is specified below:

$$\mathfrak{I}\mathfrak{p}_{\Lambda_{Hex}} \supset \hat{\Lambda} = \left\{ \left( \begin{array}{ccc|c} 1 & 0 & 0 & \sqrt{2}m_1 - \frac{m_2}{\sqrt{2}} \\ 0 & 1 & 0 & \sqrt{\frac{3}{2}}m_2 \\ 0 & 0 & 1 & \sqrt{\frac{3}{2}}m_3 \\ \hline 0 & 0 & 0 & 0 \end{array} \right) \parallel m_{1,2,3} \in \mathbb{Z} \right\} \quad (5.83)$$

By explicit calculation we find:

$$\begin{aligned} \hat{A}^6 &= \begin{pmatrix} 1 & 0 & 0 & 0 \\ 0 & 1 & 0 & 0 \\ 0 & 0 & 1 & 6\alpha_3 \\ 0 & 0 & 0 & 1 \end{pmatrix} ; \quad \hat{B}^2 = \begin{pmatrix} 1 & 0 & 0 & 0 \\ 0 & 1 & 0 & 2\beta_2 \\ 0 & 0 & 1 & 0 \\ \hline 0 & 0 & 0 & 1 \end{pmatrix} \\ (\hat{B} \cdot \hat{A})^2 &= \begin{pmatrix} 1 & 0 & 0 & \frac{1}{2}(-\alpha_1 - \sqrt{3}\alpha_2 + \beta_1 - \sqrt{3}\beta_2) \\ 0 & 1 & 0 & \frac{1}{2}(\sqrt{3}\alpha_1 + 3\alpha_2 - \sqrt{3}\beta_1 + 3\beta_2) \\ 0 & 0 & 1 & 0 \\ \hline 0 & 0 & 0 & 1 \end{pmatrix} \end{aligned} \quad (5.84)$$

Next introducing the generic translation group element

$$T = \begin{pmatrix} 1 & 0 & 0 & t_1 \\ 0 & 1 & 0 & t_2 \\ 0 & 0 & 1 & t_3 \\ \hline 0 & 0 & 0 & 1 \end{pmatrix} ; \quad t_{1,2,3} \in \mathbb{R} \quad (5.85)$$



by conjugating the two generators  $\hat{\mathcal{A}}, \hat{\mathcal{B}}$  we find:

$$T^{-1} \hat{\mathcal{A}} T = \left( \begin{array}{ccc|c} \frac{1}{2} & \frac{\sqrt{3}}{2} & 0 & \frac{1}{2}(2\alpha_1 + t_1 - \sqrt{3}t_2) \\ -\frac{\sqrt{3}}{2} & \frac{1}{2} & 0 & \frac{1}{2}(2\alpha_2 + \sqrt{3}t_1 + t_2) \\ 0 & 0 & 1 & \alpha_3 \\ \hline 0 & 0 & 0 & 1 \end{array} \right); T^{-1} \hat{\mathcal{B}} T = \left( \begin{array}{ccc|c} -1 & 0 & 0 & \beta_1 + 2t_1 \\ 0 & 1 & 0 & \beta_2 \\ 0 & 0 & -1 & \beta_3 + 2t_3 \\ \hline 0 & 0 & 0 & 1 \end{array} \right) \quad (5.86)$$

Hence the parameters  $t_{1,2}$  can be used to set  $\alpha_{1,2} = 0$ , while the parameter  $t_3$  can be utilized to set  $\beta_3 = 0$ . Inserting such a gauge choice in the conditions (5.82), in view of eq.(5.84) and (5.83) we finally get:

$$\hat{\mathcal{A}} = \left( \begin{array}{ccc|c} \frac{1}{2} & \frac{\sqrt{3}}{2} & 0 & 0 \\ -\frac{\sqrt{3}}{2} & \frac{1}{2} & 0 & 0 \\ 0 & 0 & 1 & \frac{1}{2\sqrt{6}} \\ \hline 0 & 0 & 0 & 1 \end{array} \right); \hat{\mathcal{B}} = \left( \begin{array}{ccc|c} -1 & 0 & 0 & 0 \\ 0 & 1 & 0 & 0 \\ 0 & 0 & -1 & 0 \\ \hline 0 & 0 & 0 & 1 \end{array} \right) \quad (5.87)$$

Following the same logic utilized in the cubic case the result that we obtain from eq.(5.87) is that the only fractional translations to be considered are in the  $z$ -direction and that they are of length  $1/6$  of the lattice spacing. Indeed the column vector appearing in the  $\hat{\mathcal{A}}$ -generator, *i.e.*

$$\left\{ 0, 0, \frac{1}{2\sqrt{6}} \right\} = \frac{1}{6} \mathbf{w}_3 \quad (5.88)$$

is the generator of translational  $\mathbb{Z}_6$  subgroup and the Universal Classifying Group for the hexagonal lattice turns out to be:

$$\mathfrak{U}_{72} \equiv \mathbb{Z}_6 \times \text{Dih}_6 \quad (5.89)$$

### 5.5.2 Structure and irreps of $\mathfrak{U}_{72}$

Utilizing the information obtained from Frobenius congruences we know that the abstract structure of the group that we name  $\mathfrak{U}_{72}$  is the following one:

$$\mathfrak{U}_{72} = \mathbb{Z}_2 \times_{\text{semidirect}} (\mathbb{Z}_6 \otimes \mathbb{Z}_6) \quad (5.90)$$

The generators and relations defining this group are as follows. We have just three generators named  $\{\mathcal{A}, \mathcal{B}, \mathcal{T}\}$  that obey the relations:

$$\mathcal{A}^6 = \mathcal{B}^2 = \mathcal{T}^6 = (\mathcal{B}\mathcal{A})^2 = (\mathcal{B}\mathcal{T})^2 = \mathcal{E}; \quad \mathcal{A}\mathcal{T} = \mathcal{T}\mathcal{A} \quad (5.91)$$

In the case of the hexagonal lattice  $\mathcal{A}, \mathcal{B}$  are realized as proper rotations belonging to  $\text{SO}(3)$  and they generate the dihedral group  $\text{Dih}_6$ . The generator  $\mathcal{T}$  is a translation (modulo lattice). However if we suppress the generator  $\mathcal{A}$  we obtain another dihedral group  $\text{Dih}_6 \subset \mathfrak{U}_{72}$  realized partially by rotations, partially by translations. The group  $\mathfrak{U}_{72}$  contains a maximal normal abelian subgroup that we name  $\mathfrak{N}_{36} \simeq \mathbb{Z}_6 \otimes \mathbb{Z}_6$  which is generated by  $\mathcal{A}$  and  $\mathcal{T}$ :

$$\mathfrak{U}_{72} \triangleright \mathfrak{N}_{36} \quad (5.92)$$

This fact is fundamental in order to construct all the irreducible representations of  $\mathfrak{U}_{72}$  with the iterative procedure that can be applied to solvable groups (see section [1]).

### 5.5.3 The auxiliary four dimensional representation of $\mathfrak{U}_{72}$

As we are going to see below, none of the irreducible representation of  $\mathfrak{U}_{72}$  is faithful. In order to study the algebraic structure of  $\mathfrak{U}_{72}$  and its organization in conjugacy classes, we need a faithful representation. The smallest we found is in four dimension.

The auxiliary four dimensional representation is generated as it follows :

$$\mathcal{A} = \begin{pmatrix} \frac{1}{2} & \frac{\sqrt{3}}{2} & 0 & 0 \\ -\frac{\sqrt{3}}{2} & \frac{1}{2} & 0 & 0 \\ 0 & 0 & 1 & 0 \\ 0 & 0 & 0 & 1 \end{pmatrix} ; \quad \mathcal{T} = \begin{pmatrix} 1 & 0 & 0 & 0 \\ 0 & 1 & 0 & 0 \\ 0 & 0 & \frac{1}{2} & \frac{\sqrt{3}}{2} \\ 0 & 0 & -\frac{\sqrt{3}}{2} & \frac{1}{2} \end{pmatrix} ; \quad \mathcal{B} = \begin{pmatrix} 1 & 0 & 0 & 0 \\ 0 & -1 & 0 & 0 \\ 0 & 0 & 1 & 0 \\ 0 & 0 & 0 & -1 \end{pmatrix} \quad (5.93)$$

From the above generators we obtain an explicit form of all the 72 elements that are organized in 24 conjugacy classes as it is displayed in the table below:

Class 1		order of elements = 1		# of elem in class = 1		representative = $\mathcal{E}$
Class 2		order of elements = 2		# of elem in class = 1		representative = $\mathcal{A}^3.\mathcal{T}^3$
Class 3		order of elements = 2		# of elem in class = 1		representative = $\mathcal{A}^3$
Class 4		order of elements = 2		# of elem in class = 1		representative = $\mathcal{T}^3$
Class 5		order of elements = 2		# of elem in class = 9		representative = $\mathcal{B}.\mathcal{A}.\mathcal{T}$
Class 6		order of elements = 2		# of elem in class = 9		representative = $\mathcal{B}.\mathcal{A}$
Class 7		order of elements = 2		# of elem in class = 9		representative = $\mathcal{B}.\mathcal{T}$
Class 8		order of elements = 2		# of elem in class = 9		representative = $\mathcal{B}$
Class 9		order of elements = 3		# of elem in class = 2		representative = $\mathcal{A}^2.\mathcal{T}^2$
Class 10		order of elements = 3		# of elem in class = 2		representative = $\mathcal{A}^2.\mathcal{T}^4$
Class 11		order of elements = 3		# of elem in class = 2		representative = $\mathcal{A}^2$
Class 12		order of elements = 3		# of elem in class = 2		representative = $\mathcal{T}^2$
Class 13		order of elements = 6		# of elem in class = 2		representative = $\mathcal{A}^3.\mathcal{T}^2$
Class 14		order of elements = 6		# of elem in class = 2		representative = $\mathcal{A}^3.\mathcal{T}$
Class 15		order of elements = 6		# of elem in class = 2		representative = $\mathcal{A}^2.\mathcal{T}^3$
Class 16		order of elements = 6		# of elem in class = 2		representative = $\mathcal{A}^2.\mathcal{T}$

Class 17		order of elements = 6		# of elem in class = 2		representative = $\mathcal{A}^2 \cdot \mathcal{T}^5$
Class 18		order of elements = 6		# of elem in class = 2		representative = $\mathcal{A} \cdot \mathcal{T}^3$
Class 19		order of elements = 6		# of elem in class = 2		representative = $\mathcal{A} \cdot \mathcal{T}^2$
Class 20		order of elements = 6		# of elem in class = 2		representative = $\mathcal{A} \cdot \mathcal{T}^4$
Class 21		order of elements = 6		# of elem in class = 2		representative = $\mathcal{A} \cdot \mathcal{T}$
Class 22		order of elements = 6		# of elem in class = 2		representative = $\mathcal{A} \cdot \mathcal{T}^5$
Class 23		order of elements = 6		# of elem in class = 2		representative = $\mathcal{A}$
Class 24		order of elements = 6		# of elem in class = 2		representative = $\mathcal{T}$

#### 5.5.4 Irreducible representations and the character table of $\mathfrak{U}_{72}$

According with general theorems and with the fact that  $\mathfrak{U}_{72}$  is a solvable group we arrive at the conclusion that it has 24 irreps of which 8 are 1-dimensional and 16 are 2-dimensional. These representations were explicitly computed once for all and they are incorporated in the **AlmaFluidaNSPsystem** of MATHEMATICA codes. The character table of 24 irreps is also incorporated in that system and we omit it here.

### 5.6 Classification of orbits of the point group $\text{Dih}_6$ in the momentum lattice

In complete analogy with what it was done for the cubic lattice also in the case of the hexagonal lattice we need to classify the orbits of the point group  $\text{Dih}_6$  in the lattice  $\Lambda_{Hex}^*$ . Here we have six different types of orbits:

#### 5.6.1 Orbits of length 2

These are the simplest orbits and are formed by vectors of the following type:

$$\begin{aligned}
\mathcal{O}_2 &= \{p \lambda_3, -p \lambda_3\} \quad ; \quad p \in \mathbb{Z} \\
&\Downarrow \\
&= \left\{ \left\{ 0, 0, \frac{p}{\sqrt{2}} \right\}, \left\{ 0, 0, -\frac{p}{\sqrt{2}} \right\} \right\} \quad \text{in the orthonormal basis}
\end{aligned} \tag{5.94}$$

that are arranged along the  $z$ -axis. The action of the  $\mathcal{A}$  generator of the dihedral group vanishes on such vectors and they are sensitive only to the  $\mathcal{B}$  generators that flips their orientation.

### 5.6.2 Orbits of length 6

The orbit of length 6 lies in the plane  $z = 0$  and are made by vectors of the following type:

$$\mathcal{O}_6 = \underbrace{\left\{ \begin{array}{l} \{0, -p, 0\} \\ \{0, p, 0\} \\ \{-p, 0, 0\} \\ \{-p, p, 0\} \\ \{p, -p, 0\} \\ \{p, 0, 0\} \end{array} \right\}}_{\text{in the } \lambda_i \text{ basis}} = \underbrace{\left\{ \begin{array}{l} \{0, -\sqrt{\frac{2}{3}}p, 0\} \\ \{0, \sqrt{\frac{2}{3}}p, 0\} \\ \{-\frac{p}{\sqrt{2}}, -\frac{p}{\sqrt{6}}, 0\} \\ \{-\frac{p}{\sqrt{2}}, \frac{p}{\sqrt{6}}, 0\} \\ \{\frac{p}{\sqrt{2}}, -\frac{p}{\sqrt{6}}, 0\} \\ \{\frac{p}{\sqrt{2}}, \frac{p}{\sqrt{6}}, 0\} \end{array} \right\}}_{\text{in the orthonormal basis}} ; \quad p \in \mathbb{Z} \quad (5.95)$$

See fig.14.

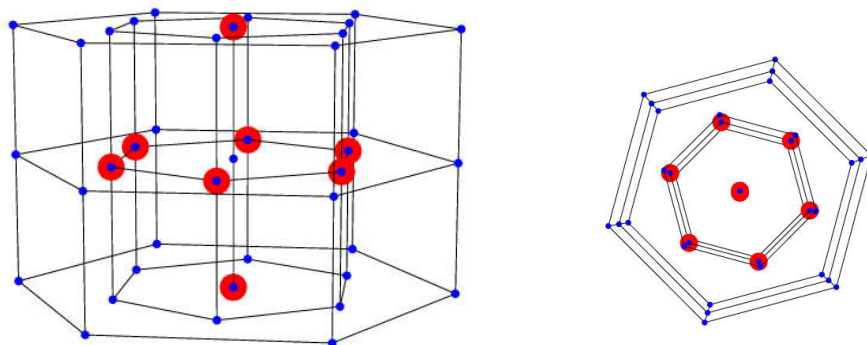


Figure 14: *In this picture we mark with a big circle the points in the hexagonal momentum lattice  $\Lambda_{Hex}^*$  that constitute the lowest lying orbits of length 2 and 6. The orbit of length 2 is given by the two marked antipodal points along the vertical  $z$ -axis, while the orbit of length 6 is given by six vertices of the regular hexagon lying in the horizontal plane  $z = 0$ . In the picture on the left we have a view of the lattice from the front, in the picture on the right we have a view from above. The blue points belong to the space lattice, the red points belong to the dual momentum lattice.*

### 5.6.3 Orbits of length 12 of type 1

The orbits of length 12 and type 1 lie in the  $z = 0$  plane and are of the following form:

$$\mathcal{O}_{12|1} = \underbrace{\left\{ \begin{array}{l} \{-p, -q, 0\} \\ \{-p, p+q, 0\} \\ \{p, -p-q, 0\} \\ \{p, q, 0\} \\ \{-q, -p, 0\} \\ \{-q, p+q, 0\} \\ \{q, -p-q, 0\} \\ \{q, p, 0\} \\ \{-p-q, p, 0\} \\ \{-p-q, q, 0\} \\ \{p+q, -q, 0\} \\ \{p+q, -p, 0\} \end{array} \right\}}_{\text{in the } \lambda_i \text{ basis}} = \underbrace{\left\{ \begin{array}{l} \left\{ -\frac{p}{\sqrt{2}}, -\frac{p+2q}{\sqrt{6}}, 0 \right\} \\ \left\{ -\frac{p}{\sqrt{2}}, \frac{p+2q}{\sqrt{6}}, 0 \right\} \\ \left\{ \frac{p}{\sqrt{2}}, -\frac{p+2q}{\sqrt{6}}, 0 \right\} \\ \left\{ \frac{p}{\sqrt{2}}, \frac{p+2q}{\sqrt{6}}, 0 \right\} \\ \left\{ -\frac{q}{\sqrt{2}}, -\frac{2p+q}{\sqrt{6}}, 0 \right\} \\ \left\{ -\frac{q}{\sqrt{2}}, \frac{2p+q}{\sqrt{6}}, 0 \right\} \\ \left\{ \frac{q}{\sqrt{2}}, -\frac{2p+q}{\sqrt{6}}, 0 \right\} \\ \left\{ \frac{q}{\sqrt{2}}, \frac{2p+q}{\sqrt{6}}, 0 \right\} \\ \left\{ -\frac{p+q}{\sqrt{2}}, \frac{p-q}{\sqrt{6}}, 0 \right\} \\ \left\{ -\frac{p+q}{\sqrt{2}}, \frac{q-p}{\sqrt{6}}, 0 \right\} \\ \left\{ \frac{p+q}{\sqrt{2}}, \frac{p-q}{\sqrt{6}}, 0 \right\} \\ \left\{ \frac{p+q}{\sqrt{2}}, \frac{q-p}{\sqrt{6}}, 0 \right\} \end{array} \right\}}_{\text{in the orthonormal basis}} ; \quad p, q \in \mathbb{Z} \quad (5.96)$$

### 5.6.4 Orbits of length 12 of type 2

The orbits of length 12 and type 2 are the most generic ones that depend on three integers  $p, q, r$  with no relation among them capable of nullify some of the orthonormal components of the vectors belonging to the orbit. Explicitly we find:

$$\mathcal{O}_{12|2} = \underbrace{\left\{ \begin{array}{l} \{-p, -q, r\} \\ \{-p, p+q, -r\} \\ \{p, -p-q, -r\} \\ \{p, q, r\} \\ \{-q, -p, -r\} \\ \{-q, p+q, r\} \\ \{q, -p-q, r\} \\ \{q, p, -r\} \\ \{-p-q, p, r\} \\ \{-p-q, q, -r\} \\ \{p+q, -q, -r\} \\ \{p+q, -p, r\} \end{array} \right\}}_{\text{in the } \lambda_i \text{ basis}} = \underbrace{\left\{ \begin{array}{l} \left\{ -\frac{p}{\sqrt{2}}, -\frac{p+2q}{\sqrt{6}}, \frac{r}{\sqrt{2}} \right\} \\ \left\{ -\frac{p}{\sqrt{2}}, \frac{p+2q}{\sqrt{6}}, -\frac{r}{\sqrt{2}} \right\} \\ \left\{ \frac{p}{\sqrt{2}}, -\frac{p+2q}{\sqrt{6}}, -\frac{r}{\sqrt{2}} \right\} \\ \left\{ \frac{p}{\sqrt{2}}, \frac{p+2q}{\sqrt{6}}, \frac{r}{\sqrt{2}} \right\} \\ \left\{ -\frac{q}{\sqrt{2}}, -\frac{2p+q}{\sqrt{6}}, -\frac{r}{\sqrt{2}} \right\} \\ \left\{ -\frac{q}{\sqrt{2}}, \frac{2p+q}{\sqrt{6}}, \frac{r}{\sqrt{2}} \right\} \\ \left\{ \frac{q}{\sqrt{2}}, -\frac{2p+q}{\sqrt{6}}, \frac{r}{\sqrt{2}} \right\} \\ \left\{ \frac{q}{\sqrt{2}}, \frac{2p+q}{\sqrt{6}}, -\frac{r}{\sqrt{2}} \right\} \\ \left\{ -\frac{p+q}{\sqrt{2}}, \frac{p-q}{\sqrt{6}}, \frac{r}{\sqrt{2}} \right\} \\ \left\{ -\frac{p+q}{\sqrt{2}}, \frac{q-p}{\sqrt{6}}, -\frac{r}{\sqrt{2}} \right\} \\ \left\{ \frac{p+q}{\sqrt{2}}, \frac{p-q}{\sqrt{6}}, -\frac{r}{\sqrt{2}} \right\} \\ \left\{ \frac{p+q}{\sqrt{2}}, \frac{q-p}{\sqrt{6}}, \frac{r}{\sqrt{2}} \right\} \end{array} \right\}}_{\text{in the orthonormal basis}} \quad (5.97)$$

The parameters in the above orbit must satisfy the following conditions:

$$p, q, r \in \mathbb{Z} \quad \text{and} \quad \begin{cases} q \neq -2p \\ q \neq \pm p \end{cases} \quad (5.98)$$

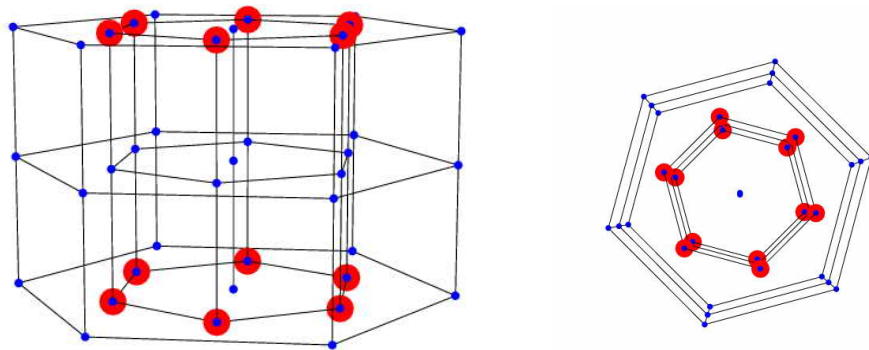


Figure 15: *In this picture we mark with a big circle the points in the hexagonal momentum lattice  $\Lambda_{Hex}^*$  that constitute an orbit of length 12 of type 2,3 or 4. The orbit of length 12 is given by 12 vertices of a polyhedron which has two opposite faces (upper and lower) corresponding to regular hexagons on horizontal planes symmetrical under  $z$ -reflection and 6 rectangular vertical faces. In the picture on the left we have a view of the lattice from the front, in the picture on the right we have a view from above. The blue points belong to the space lattice, the red points belong to the dual momentum lattice. The distinction among type 2,3,4 depends only on the orientation of the hexagonal faces in the lattice.*

### 5.6.5 Orbits of length 12 of type 3

The orbits of length 12 and type 3 correspond to the degeneration of the orbits of type 1 when  $q = -p$ . Explicitly we find:

$$\mathcal{O}_{12|3} = \underbrace{\left\{ \begin{array}{l} \{0, -p, -r\} \\ \{0, -p, r\} \\ \{0, p, -r\} \\ \{0, p, r\} \\ \{-p, 0, -r\} \\ \{-p, 0, r\} \\ \{-p, p, -r\} \\ \{-p, p, r\} \\ \{p, -p, -r\} \\ \{p, -p, r\} \\ \{p, 0, -r\} \\ \{p, 0, r\} \end{array} \right\}}_{\text{in the } \lambda_i \text{ basis}} = \underbrace{\left\{ \begin{array}{l} \{0, -\sqrt{\frac{2}{3}}p, -\frac{r}{\sqrt{2}}\} \\ \{0, -\sqrt{\frac{2}{3}}p, \frac{r}{\sqrt{2}}\} \\ \{0, \sqrt{\frac{2}{3}}p, -\frac{r}{\sqrt{2}}\} \\ \{0, \sqrt{\frac{2}{3}}p, \frac{r}{\sqrt{2}}\} \\ \{-\frac{p}{\sqrt{2}}, -\frac{p}{\sqrt{6}}, -\frac{r}{\sqrt{2}}\} \\ \{-\frac{p}{\sqrt{2}}, -\frac{p}{\sqrt{6}}, \frac{r}{\sqrt{2}}\} \\ \{-\frac{p}{\sqrt{2}}, \frac{p}{\sqrt{6}}, -\frac{r}{\sqrt{2}}\} \\ \{-\frac{p}{\sqrt{2}}, \frac{p}{\sqrt{6}}, \frac{r}{\sqrt{2}}\} \\ \{\frac{p}{\sqrt{2}}, -\frac{p}{\sqrt{6}}, -\frac{r}{\sqrt{2}}\} \\ \{\frac{p}{\sqrt{2}}, -\frac{p}{\sqrt{6}}, \frac{r}{\sqrt{2}}\} \\ \{\frac{p}{\sqrt{2}}, \frac{p}{\sqrt{6}}, -\frac{r}{\sqrt{2}}\} \\ \{\frac{p}{\sqrt{2}}, \frac{p}{\sqrt{6}}, \frac{r}{\sqrt{2}}\} \end{array} \right\}}_{\text{in the orthonormal basis}} ; \quad p, r \in \mathbb{Z} \quad (5.99)$$

### 5.6.6 Orbits of length 12 of type 4

The orbits of length 12 and type 4 correspond to the degeneration of the orbits of type 1 when  $q = -2p$ . Explicitly we find:

$$\mathcal{O}_{12|4} =, \underbrace{\left\{ \begin{array}{l} \{-p, -p, -r\} \\ \{-p, -p, r\} \\ \{-p, 2p, -r\} \\ \{-p, 2p, r\} \\ \{p, -2p, -r\} \\ \{p, -2p, r\} \\ \{p, p, -r\} \\ \{p, p, r\} \\ \{-2p, p, -r\} \\ \{-2p, p, r\} \\ \{2p, -p, -r\} \\ \{2p, -p, r\} \end{array} \right\}}_{\text{in the } \lambda_i \text{ basis}} = \underbrace{\left\{ \begin{array}{l} \{-\frac{p}{\sqrt{2}}, -\sqrt{\frac{3}{2}}p, -\frac{r}{\sqrt{2}}\} \\ \{-\frac{p}{\sqrt{2}}, -\sqrt{\frac{3}{2}}p, \frac{r}{\sqrt{2}}\} \\ \{-\frac{p}{\sqrt{2}}, \sqrt{\frac{3}{2}}p, -\frac{r}{\sqrt{2}}\} \\ \{-\frac{p}{\sqrt{2}}, \sqrt{\frac{3}{2}}p, \frac{r}{\sqrt{2}}\} \\ \{\frac{p}{\sqrt{2}}, -\sqrt{\frac{3}{2}}p, -\frac{r}{\sqrt{2}}\} \\ \{\frac{p}{\sqrt{2}}, -\sqrt{\frac{3}{2}}p, \frac{r}{\sqrt{2}}\} \\ \{\frac{p}{\sqrt{2}}, \sqrt{\frac{3}{2}}p, -\frac{r}{\sqrt{2}}\} \\ \{\frac{p}{\sqrt{2}}, \sqrt{\frac{3}{2}}p, \frac{r}{\sqrt{2}}\} \\ \{-\sqrt{2}p, 0, -\frac{r}{\sqrt{2}}\} \\ \{-\sqrt{2}p, 0, \frac{r}{\sqrt{2}}\} \\ \{\sqrt{2}p, 0, -\frac{r}{\sqrt{2}}\} \\ \{\sqrt{2}p, 0, \frac{r}{\sqrt{2}}\} \end{array} \right\}}_{\text{in the orthonormal basis}} ; \quad p, r \in \mathbb{Z} \quad (5.100)$$

See a picture of orbits of length 12 of type 2,3,4 in fig.15 As we see the shortest orbit of length 2 is actually vertical, namely the associated Beltrami Flows correspond to decoupled systems where only the coordinate  $z(t)$  obeys a non linear differential equation. The other two coordinates form a free system. Similarly the orbits of length 6 and the first orbit of length 12 are all planar. In the corresponding Beltrami Flows there is no dependence on the coordinate  $z$  which forms a free system. Presumably all the Beltrami Flows of this type are integrable. Only the maximal orbits of length 12 of type two, three and four are truly three-dimensional and give rise to systems that might develop chaos.

## 6 Group Theory and $\mathfrak{b}$ -Beltrami fields

### 6.1 The Euler equations in a $\mathfrak{b}$ -three-manifold and the ABC model as a test ground

In view of the geometrical setup discussed in chapter 3.2, in the present one we reconsider Euler equations and Beltrami fields in  $\mathfrak{b}$ -manifolds, following the approach of [3] and focusing in particular on the example of the *ABC*-flows that they used there. Our aim is to bring up to evidence the relation existing between the necessary condition found in [3] for the consistency of Beltrami equation in a particular  $\mathfrak{b}$ -manifold with a particular boundary surface  $\Sigma$  and the group theoretical structure of the ABC-model that was exhaustively presented in [1]. We will argue that such a relation is most likely general and that the possible types of boundary surfaces  $\Sigma$  which can be introduced in Beltrami fields have to be classified in group theoretical terms also in the case of the much more complicated Beltrami flows originated by higher orbits of the point-group in the momentum lattice.



### 6.1.1 The appropriate geometrical rewriting of Euler equations on general three-manifolds

In order to implement our programme we come once again back to Euler equation as written in eq. (2.21) which, in view of the definition of the Bernoulli function given in eq.(2.22) and for steady flows can be stated as follows:

$$i_{\mathbf{U}} \cdot d\Omega^{\mathbf{U}} = -dH_B \quad (6.1)$$

We remind the reader that, geometrically, the one-form  $\Omega^{\mathbf{U}}$  is the *contact form*, the velocity field  $\mathbf{U}$  is its *Reeb-field* and  $H_B$  is indeed the Bernoulli-function. In addition to eq. (6.1) the dynamical system requires, in order to be complete, the divergenceless condition:

$$\nabla \cdot \mathbf{U} \equiv \frac{1}{\sqrt{\det g}} \partial_\ell \left( \sqrt{\det g} U^\ell \right) = 0 \quad (6.2)$$

where  $g_{ij}$  is the metric tensor of the three-manifold. Also equation (6.2) admits an index-free totally geometrical rewriting in terms of the volume three-form defined below:

$$\text{Vol}_g \equiv \frac{1}{3!} \sqrt{\det g} \epsilon_{ijk} dx^i \wedge dx^j \wedge dx^k \quad (6.3)$$

An easy straightforward calculations shows that:

$$d(i_{\mathbf{U}} \cdot \text{Vol}_g) = \nabla \cdot \mathbf{U} \times \text{Vol}_g \quad (6.4)$$

Hence Euler equations reduce to:

$$\begin{aligned} i_{\mathbf{U}} \cdot d\Omega^{\mathbf{U}} &= -dH_B \\ d(i_{\mathbf{U}} \cdot \text{Vol}_g) &= 0 \end{aligned} \quad (6.5)$$

### 6.1.2 The $b$ -deformation of the ABC-model

Next we consider the ABC model vector field as defined in the next section in eq.(6.28) and we try to convert the  $T^3$  torus, obtained by quotienting  $\mathbb{R}^3$  with respect to the cubic lattice, into a  $\mathfrak{b}$ -manifold by choosing, in the covering space  $\mathbb{R}^3$ , the surface  $\Sigma_{x=0} \subset \mathbb{R}^3$  identified by the equation  $x = 0$ . The Beltrami vector becomes parallel to the surface  $\Sigma_{x=0}$  by means of the substitution:

$$\partial_x \longrightarrow x \partial_x \quad (6.6)$$

Hence we have:

$$\begin{aligned} {}^b\mathbf{V}_{ABC} &= (2A \cos[2\pi y] + 2B \cos[2\pi z]) x \partial_x \\ &\quad (2C \cos[2\pi x] - 2B \sin[2\pi z]) \partial_y + (2A \sin[2\pi y] - 2C \sin[2\pi x]) \partial_z \end{aligned} \quad (6.7)$$

According to the principles of  $\mathfrak{b}$ -manifolds summarized in in section 3.2 the metric and the differential forms are accordingly modified. We have:

$$\begin{aligned} {}^b ds^2 &= {}^b g_{ij} dx^i \times dx^j = \left(\frac{dx}{x}\right)^2 + dy^2 + dz^2 \\ {}^b \text{Vol}_g &= \frac{dx}{x} \wedge dy \wedge dz \end{aligned} \quad (6.8)$$

so we easily compute:

$$\begin{aligned} i_{\mathfrak{b}\mathbf{V}_{ABC}} \cdot {}^b \text{Vol}_g &= \frac{2dy \wedge dz (A \cos[2\pi y] + B \cos[(2\pi z])}{x} \\ &\quad - \frac{2dx \wedge dy (C \sin[2\pi x] - A \sin[2\pi y])}{x} - \frac{2dx \wedge dz (C \cos[2\pi x] - B \sin[2\pi z])}{x} \end{aligned} \quad (6.9)$$

and we immediately verify the second of eq.s (6.5)

$$d\left(i_{\mathfrak{b}\mathbf{V}_{ABC}} \cdot {}^b \text{Vol}_g\right) = 0 \quad (6.10)$$

As we know from the discussion in the introduction, the first of eq.s(6.5) is certainly satisfied if the stronger Beltrami equation (2.30) is enforced and before the  $\mathfrak{b}$ -deformation the contact form  $\Omega^{[\mathbf{V}_{ABC}]}$  certainly satisfies it by construction. It is to be seen whether the new  $\mathfrak{b}$ -contact form  ${}^b \Omega^{[\mathbf{V}_{ABC}]}$  still satisfies it. We easily compute:

$$\begin{aligned} {}^b \Omega^{[\mathbf{V}_{ABC}]} &= {}^b g_{ij} {}^b \mathbf{V}_{ABC}^i dx^j = \frac{dx (2A \cos[2\pi y] + 2B \cos[2\pi z])}{x} \\ &\quad + dy (2C \cos[2\pi x] - 2B \sin[2\pi z]) + dz (2A \sin[2\pi y] - 2C \sin[2\pi x]) \end{aligned} \quad (6.11)$$

Taking the Hodge dual of Beltrami equation (2.30) we can equivalently rewrite it as follows:

$$d{}^b \Omega^{[\mathbf{V}_{ABC}]} = \lambda \left( \star_{\mathfrak{b}g} {}^b \Omega^{[\mathbf{V}_{ABC}]} \right) \equiv \lambda \frac{1}{2} \left( i_{\mathfrak{b}\mathbf{V}_{ABC}} \cdot {}^b \text{Vol}_g \right) \quad (6.12)$$

The second member was already calculated, the first is immediately calculated and we find that setting  $\lambda = 2\pi$  which is its original value prior to the deformation, we have:

$$d{}^b \Omega^{[\mathbf{V}_{ABC}]} - \pi \left( i_{\mathfrak{b}\mathbf{V}_{ABC}} \cdot {}^b \text{Vol}_g \right) = -\frac{4\pi C(x-1) (\sin[2\pi x] dx \wedge dy + \cos[2\pi x] dx \wedge dz)}{x} \quad (6.13)$$

As it was done in [3] we have no other way out then choosing  $C = 0$ . Hence we conclude that the complete ABC-model cannot be  $\mathfrak{b}$ -deformed but the AB0-model can. In [3] the boundary surface was posed at  $z = 0$  and the authors reached the same conclusion in the form of the constraint  $A = 0$ . As we argue in the next section these two choices are perfectly equivalent since we can interchange  $A, B, C$  with transformations of the subgroup  $\text{GF}_{192} \subset \text{G}_{1536}$  of which the ABC model constitutes an irreducible three dimensional representation. The important thing is that setting one of the three parameters ABC, equal to zero one obtains a two-parameter

model which constitutes an irreducible representation of a subgroup  $G_{128}^{(AB0)} \subset G_{1536}$ <sup>8</sup>. Inside  $G_{128}^{(AB0)}$  the stabilizer of the two vector  $(A, B)$  is a group of order 16,  $G_{16}^{(AB0)}$  which contains a purely translational subgroup  $G_4^{(AB0)} \sim \mathbb{Z}_4$  made by the quantized translation of  $1/4$  in the  $y$ -direction. This makes the dynamical system actually two-dimensional. It is a remarkable fact that the  $\mathfrak{b}$ -deformation of the chosen type is possible only in presence of this particular hidden symmetry. We come back to this question at the end of the chapter. First we recall from [1] the group-theory behind the ABC models.

## 6.2 Group theoretical interpretation of the ABC flows

From the analysis [1] the following pattern emerged. The Universal Classifying Group  $G_{1536}$  contains at least two<sup>9</sup> isomorphic but not conjugate subgroups of order 192, namely  $G_{192}$  and  $GF_{192}$  in the adopted nomenclature. The classical ABC-flows are obtained from the lowest lying momentum orbit of length 6 which produces an irreducible 6-dimensional representation of the Universal Classifying Group:  $D_{23} [G_{1536}, 6]$ . The vector field is the following one:

$$\mathbf{V}^{(6)}(\mathbf{r}|\mathbf{F}) = \begin{pmatrix} 2 \cos(2\pi z) F_1 + 2 \cos(2\pi y) F_2 + 2 \sin(2\pi z) F_3 - 2 \sin(2\pi y) F_5 \\ -2 \sin(2\pi z) F_1 + 2 \cos(2\pi z) F_3 + 2 \cos(2\pi x) F_4 + 2 \sin(2\pi x) F_6 \\ 2 \sin(2\pi y) F_2 - 2 \sin(2\pi x) F_4 + 2 \cos(2\pi y) F_5 + 2 \cos(2\pi x) F_6 \end{pmatrix} \quad (6.14)$$

where  $F_i$  ( $i = 1, \dots, 6$ ) are real numbers. The three parameter ABC-flow is just the irreducible 3-dimensional representation  $D_{12} [GF_{192}, 3]$  in the split

$$D_{23} [G_{1536}, 6] = D_{12} [GF_{192}, 3] \oplus D_{15} [GF_{192}, 3] \quad (6.15)$$

With respect to the isomorphic but not conjugate subgroup  $G_{192}$  the representation  $D_{23} [G_{1536}, 6]$  remains instead irreducible:

$$D_{23} [G_{1536}, 6] = D_{20} [G_{192}, 6] \quad (6.16)$$

so that there is no proper way of reducing the six parameters to three.

Indeed, as shown in [1], we have the following chain of inclusions:

$$G_{1536} \supset GF_{192} \supset GS_{24} \quad (6.17)$$

that is parallel to the other one:

$$G_{1536} \supset G_{192} \supset O_{24} \quad (6.18)$$

$G_{192}$  being another subgroup, isomorphic to  $GF_{192}$ , but not conjugate to it in  $G_{1536}$ . (see appendices A.6 and A.7 of [1] for the detailed description of these two subgroups of the Universal Classifying Group  $G_{1536}$  of the

---

<sup>8</sup>The subgroups  $G_{128}^{(OBC)}$  and  $G_{128}^{(ABC)}$  are obviously conjugate in  $G_{1536}$  to  $G_{128}^{(AB0)}$  and therefore isomorphic to this latter and among themselves

<sup>9</sup>It is known that there are 4 different Space-Groups  $\Gamma_{24}^I$  ( $I = 1, \dots, 4$ ) of order 24, isomorphic to the point group  $O_{24}$  but not conjugate one to the other under the action of the continuous translation group. One of them is the point group itself  $\Gamma_{24}^1 = O_{24}$  which is a subgroup of the first of the two groups of order 192 identified in [1]:  $O_{24} \subset G_{192}$ . Another of the four mentioned groups is  $\Gamma_{24}^2 = GS_{24}$  which is a subgroup of the second group of order 192 identified by the authors of [1]:  $GS_{24} \subset GF_{192}$ . It remains to see whether  $\Gamma_{24}^3$  and  $\Gamma_{24}^4$  are contained in the two already identified subgroups  $G_{192}$  and  $GF_{192}$  or if there exists other two such non conjugate subgroups of order 192 that respectively contain  $\Gamma_{24}^3$  and  $\Gamma_{24}^4$ . The answer was not worked out in [1]. Extensive but lengthy calculations could resolve the issue.

cubic lattice). Since  $G_{192}$  and  $GF_{192}$  are isomorphic they have the same irreps and the same character table. Yet, since they are not conjugate, the branching rules of the same  $G_{1536}$  irrep with respect to the former or the latter subgroup can be different. In the case of the representation  $D_{23} [G_{1536}, 6]$ , which is that produced by the fundamental orbit of order six, we have (see appendix D of [1]):

$$D_{23} [G_{1536}, 6] = \begin{cases} D_{20} [G_{192}, 6] & = D_4 [O_{24}, 3] \oplus D_5 [O_{24}, 3] \\ D_{12} [GF_{192}, 3] \oplus D_{15} [GF_{192}, 3] & = D_1 [GS_{24}, 1] \oplus D_3 [GS_{24}, 2] \oplus D_4 [GS_{24}, 3] \end{cases} \quad (6.19)$$

where in the second line we have used the branching rules:

$$D_{12} [GF_{192}, 3] = D_1 [GS_{24}, 1] \oplus D_3 [GS_{24}, 2] \quad (6.20)$$

$$D_{15} [GF_{192}, 3] = D_4 [GS_{24}, 3] \quad (6.21)$$

that, in view of the isomorphism, are identical with:

$$D_{12} [G_{192}, 3] = D_1 [O_{24}, 1] \oplus D_3 [O_{24}, 2] \quad (6.22)$$

$$D_{15} [G_{192}, 3] = D_4 [O_{24}, 3] \quad (6.23)$$

Eq.(6.19) has far reaching consequences. While there are no Beltrami vector fields obtained from this orbit that are invariant with respect to the octahedral point group  $O_{24}$ , there exists such an invariant Beltrami flow with respect to the isomorphic  $GS_{24}$ : it corresponds to the  $D_1 [GS_{24}, 1]$  irrep in the second line of (6.19). Furthermore while the six parameter space  $\mathbf{F}$  is irreducible with respect to the action of the group  $G_{192}$  (the irrep  $D_{20} [G_{192}, 6]$ ) it splits into two three-dimensional subspaces with respect to  $GF_{192}$ . This is the origin of the ABC-flows. Indeed the ABC Beltrami flows can be identified with the irreducible representation  $D_{12} [GF_{192}, 3]$ . Let us see how. Explicitly we have the following projection operators on the two irreducible representations,  $D_{12}$  and  $D_{15}$ :

$$\Pi^{(12)} [GF_{192}, 3] \mathbf{F} = \{F_1, F_2, 0, F_4, 0, 0\} \quad (6.24)$$

$$\Pi^{(15)} [GF_{192}, 3] \mathbf{F} = \{0, 0, F_3, 0, F_5, F_6\} \quad (6.25)$$

If we set  $F_3 = F_5 = F_6 = 0$  we kill the irreducible representation  $D_{15} [GF_{192}, 3]$  and the residual Beltrami vector field, upon the following identifications:

$$A = F_1 \quad ; \quad B = F_4 \quad ; \quad C = F_2 \quad (6.26)$$

coincides with the time honored ABC flow of eq.(4.8). Indeed inserting the special parameter vector  $\mathbf{F} = \{A, C, 0, B, 0, 0\}$  in eq.(6.14) we obtain:

$$\begin{aligned} \mathbf{V}^{(6)} (\{x, y, z\} \mid \{A, C, 0, B, 0, 0\}) &\equiv \mathbf{V}_{(ABC)}(x, y, z) \\ \mathbf{V}_{(ABC)} \left(x + \frac{3}{4}, y, z - \frac{1}{4}\right) &= \mathcal{V}^{(ABC)}(x, y, z) \end{aligned} \quad (6.27)$$

the vector field  $\mathcal{V}^{(ABC)}(x, y, z)$  being that defined by eq.(4.8).

For future quick reference it is convenient to write explicitly the ABC Beltrami field  $\mathbf{V}^{(ABC)}(x, y, z)$  in the

normalization we utilize in the sequel:

$$\mathbf{V}^{(ABC)}(x, y, z) = \begin{pmatrix} 2A \cos(2\pi y) + 2B \cos(2\pi z) \\ 2C \cos(2\pi x) - 2B \sin(2\pi z) \\ 2A \sin(2\pi y) - 2C \sin(2\pi x) \end{pmatrix} \quad (6.28)$$

The next step is provided by considering the explicit form of the decomposition of the  $D_{12} [\text{GF}_{192}, 3]$  irrep, *i.e.* the ABC flow, into irreducible representations of the subgroup  $\text{GS}_{24}$ . The two invariant subspaces are immediately characterized in terms of the parameters  $A, B, C$ , as it follows:

$$D_1 [\text{GS}_{24}, 1] \Leftrightarrow A = B = C \neq 0 \quad (6.29)$$

$$D_3 [\text{GS}_{24}, 2] \Leftrightarrow A + B + C = 0 \quad (6.30)$$

The most symmetric case  $A : A : A = 1$  simply corresponds to the identity representation of the subgroup  $\text{GS}_{24} \subset \text{GF}_{192}$  which occurs in the splitting of the 3-dimensional representation:

$$D_{12} [\text{GF}_{192}, 3] = D_1 [\text{GS}_{24}, 1] \oplus D_3 [\text{GS}_{24}, 2] \quad (6.31)$$

### 6.2.1 The (A, A, A)-flow invariant under $\text{GS}_{24}$

This information suffices to understand the role of the  $A : A : A = 1$  Beltrami vector field often considered in the literature. It is the unique one invariant under the order 24 group  $\text{GS}_{24}$  isomorphic to the octahedral point group. Explicitly, in our notations, it takes the following form<sup>10</sup>:

$$\mathbf{V}_{(A,A,A)}(\mathbf{r}) = \mathbf{V}_{(A,A,A)}(x, y, z) \equiv 2A \begin{pmatrix} (\cos(2\pi y) + \cos(2\pi z)) \\ (\cos(2\pi x) - \sin(2\pi z)) \\ (\sin(2\pi y) - \sin(2\pi x)) \end{pmatrix} \quad (6.32)$$

This vector field  $\mathbf{V}_{(A,A,A)}(x, y, z)$  is everywhere non singular in the fundamental unit cube (the torus  $\mathbb{T}^3$ ) apart from eight isolated *stagnation points* where it vanishes. They are listed below.

$$\begin{aligned} s_1 &= \left\{ \frac{1}{8}, \frac{1}{8}, \frac{3}{8} \right\} ; & s_2 &= \left\{ \frac{1}{8}, \frac{3}{8}, \frac{1}{8} \right\} \\ s_3 &= \left\{ \frac{3}{8}, \frac{1}{8}, \frac{5}{8} \right\} ; & s_4 &= \left\{ \frac{3}{8}, \frac{3}{8}, \frac{7}{8} \right\} \\ s_5 &= \left\{ \frac{5}{8}, \frac{5}{8}, \frac{7}{8} \right\} ; & s_6 &= \left\{ \frac{5}{8}, \frac{7}{8}, \frac{5}{8} \right\} \\ s_7 &= \left\{ \frac{7}{8}, \frac{5}{8}, \frac{1}{8} \right\} ; & s_8 &= \left\{ \frac{7}{8}, \frac{7}{8}, \frac{3}{8} \right\} \end{aligned} \quad (6.33)$$

A numerical plot of this vector field is displayed in fig. 16.

In order to provide the reader with a visual impression of the dynamics of this flow, in fig.17 we display a set of  $5 \times 5 \times 5 = 125$  streamlines, namely of numerical integrations of the differential system:

$$\frac{d\mathbf{r}}{dt} = \mathbf{V}_{(A,A,A)}(\mathbf{r}) \quad (6.34)$$

---

<sup>10</sup>Observe that here and in the sequel we stick to our conventions for  $x, y, z$ , which differ from those of eq.(4.8) by the already mentioned shift  $\{\frac{3}{4}, 0, -\frac{1}{4}\}$

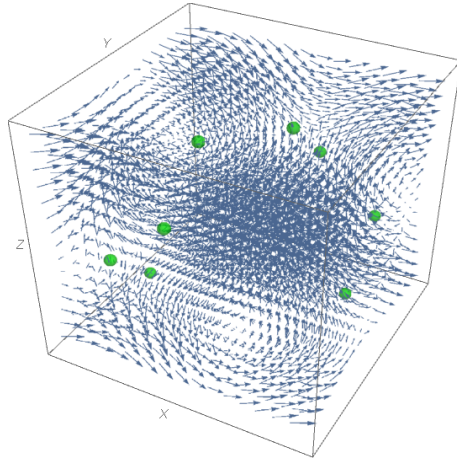


Figure 16: A plot of the  $A : A : A = 1$  Beltrami vector field invariant under the group  $GS_{24}$  with a view of its eight stagnation points of eq.(6.33)

with initial conditions:

$$\mathbf{r}(0) = \mathbf{r}_0 = \left\{ \frac{n_1}{6}, \frac{n_2}{6}, \frac{n_3}{6} \right\} \quad ; \quad n_{1,2,3} = 0, 1, 2, 3, 4, 5 \quad (6.35)$$

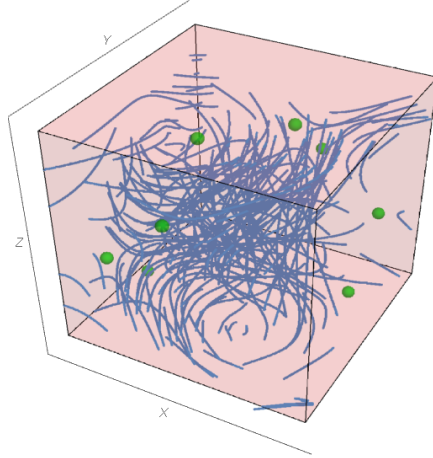


Figure 17: A plot of 216 streamlines of the  $A : A : A = 1$  Beltrami vector field with equally spaced initial conditions. The numerical solutions are smooth in  $\mathbb{R}^3$ . When a branch reaches a boundary of the unit cube it is continued with its image in the cube modulo the appropriate lattice translation. The circles in this figure are the eight stagnation points

### 6.3 Chains of subgroups and the flows $(A, B, 0)$ , $(A, A, 0)$ and $(A, 0, 0)$

In the literature a lot of attention has been given to the special subcases of the ABC-flow where one or two of the parameters vanish or two are equal among themselves and one vanishes. Also these cases can be thoroughly characterized in group theoretical terms and their special features can be traced back to the hidden subgroup structure associated with them.

#### 6.3.1 The $(A, B, 0)$ case and its associated chain of subgroups

First we consider the case where we put to zero one of the three parameters leaving the other two undetermined.

A preliminary important observation is the following. Each of the three parameters is associated in eq.(6.28) with the trigonometric functions of one of the three variables  $x, y, z$ . Hence permuting the variables  $x, y, z$  is equivalent to permute the  $A, B, C$  coefficients. There are also some changes of sign but all these operations are contained in the point group  $O_{24}$  as one can immediately realize looking at eq.(5.5). Hence in the Universal Classifying Group  $G_{1536}$  that contains the point group there are certainly elements that can map the parameter vector  $\{A, B, C\}$  in any other permutation of the same letters. That means that considering the case  $C = 0$  is no loss of generality. The invariance groups that we determine for this case will just be conjugate to the invariance groups appearing in the case  $A = 0$  or in the case  $B = 0$ . So let us make the choice  $C = 0$  which was already done in [1].

**When we put  $C = 0$**  we define a two dimensional subspace of the representation  $D_{12} [GF_{192}, 3]$  which is invariant under some proper subgroup  $H^{(A,B,0)} \subset GF_{192}$ . This group  $H^{(A,B,0)}$  can be calculated and found to be of order 64, yet we do not dwell on it because the subgroup of the classifying group  $G_{1536}$  which leaves the subspace  $(A, 0, 0, B, 0, 0)$  invariant is larger than  $H^{(A,B,0)}$  and it is not contained in  $GF_{192}$ . It has order 128 and we name it  $G_{128}^{(A,B,0)}$ . This short discussion is important because it implies the following: the flows  $(A, B, 0)$  should not be considered just as a particular case of the  $ABC$ -flows rather as a different set of flows, whose properties are encoded in the group  $G_{128}^{(A,B,0)}$ .

The group  $G_{128}^{(A,B,0)}$  is solvable and a chain of normal subgroups can be found, all of index 2 which ends with the abelian  $G_4^{(A,B,0)}$  isomorphic to  $Z_4$ . This latter is nothing else than the group of quantized translation in the  $y$ -direction and its inclusion in the group leaving the space  $(A, 0, 0, B, 0, 0)$  invariant actually means that the differential system must be  $y$ -independent and hence two dimensional. The chain of normal subgroups is displayed here below:

$$\mathbb{Z}_4 \sim G_4^{(A,B,0)} \triangleleft G_8^{(A,B,0)} \triangleleft G_{16}^{(A,B,0)} \triangleleft \begin{cases} G_{32}^{(A,B,0)} \triangleleft G_{64}^{(A,B,0)} \triangleleft G_{128}^{(A,B,0)} \\ G_{32}^{(A,A,0)} \end{cases}$$

(6.36)

and it allows for the construction of irreducible representations of  $G_{128}^{(A,B,0)}$  and all other members of the chain, by means of the induction algorithm. Such a construction we have not done, but all the groups of the chain are listed, with their conjugacy classes in appendix E of [1]. The group  $G_{128}^{(A,B,0)}$  leaves the subspace  $(A, 0, 0, B, 0, 0)$

invariant but still mixes the parameters  $A$  and  $B$  among themselves. The subgroup  $G_{16}^{(A,B,0)} \triangleleft G_{128}^{(A,B,0)}$  instead stabilizes the very vector  $(A, 0, 0, B, 0, 0)$ . This means that any  $(A, B, 0)$ -flow has a hidden symmetry of order 16 provided by the group  $G_{16}^{(A,B,0)}$ . The general form of these Beltrami fields is the following one:

$$\mathbf{V}_{(A,B,0)}(\mathbf{r}) = \mathbf{V}_{(A,B,0)}(x, y, z) \equiv \begin{pmatrix} 2A \cos(2\pi y) + 2B \cos(2\pi z) \\ -2B \sin(2\pi z) \\ 2A \sin(2\pi y) \end{pmatrix} \quad (6.37)$$

In fig.18 we display a plot of the vector field and an example of equally spaced streamlines.

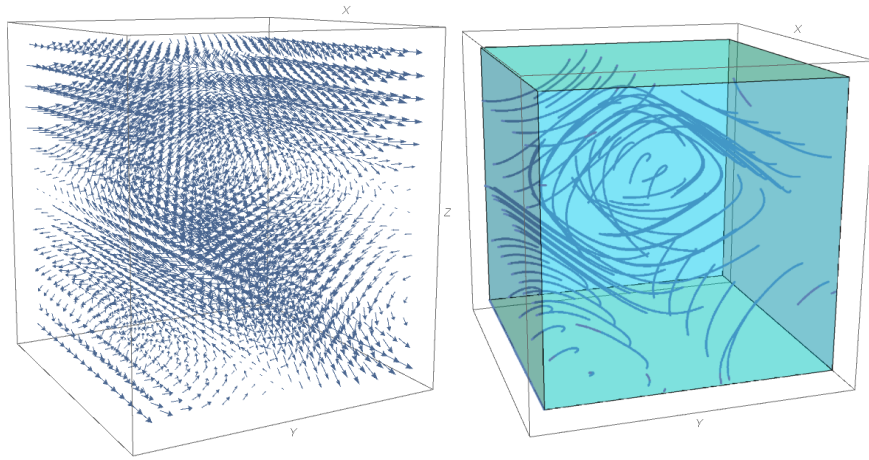


Figure 18: A plot of the Beltrami vector field  $\mathbf{V}_{(A,B,0)}(\mathbf{r})$  (on the left) with  $A = 5$ ,  $B = 7$ . On the right a family of streamlines with equally spaced initial conditions is displayed.

Looking at eq.(6.36) we notice that there is another group of order 32, namely  $G_{32}^{(A,A,0)}$  which contains  $G_{16}^{(A,B,0)}$  but it is not contained neither in  $G_{128}^{(A,B,0)}$  nor in  $GF_{192}$ . This group is the stabilizer of the vector  $(A, 0, 0, A, 0, 0)$  and hence it is the hidden symmetry group of the flows of type  $(A, A, 0)$ . Once again the very fact that  $G_{32}^{(A,A,0)}$  is not contained in  $G_{128}^{(A,B,0)}$  shows that the  $(A, A, 0)$  flow should not be considered as a particular case of the  $(A, B, 0)$ -flows rather as a new type of its own. Let us also stress the difference with the case of the  $(A, A, A)$ -flow. Here the hidden symmetry group  $GS_{24}$  is contained in  $GF_{192}$  and the interpretation of the  $(A, A, A)$ -flow as a particular case of the  $(A, B, C)$ -flows is permitted. Having set:

$$\mathbf{V}_{(A,A,0)}(\mathbf{r}) = \mathbf{V}_{(A,A,0)}(x, y, z) \equiv A \begin{pmatrix} 2A \cos(2\pi y) + 2A \cos(2\pi z) \\ -2A \sin(2\pi z) \\ 2A \sin(2\pi y) \end{pmatrix} \quad (6.38)$$

in fig.19 we display a plot of the vector field  $\mathbf{V}_{(A,A,0)}(\mathbf{r})$  and a family of its streamlines. In the case of this flow there are not isolated stagnation points, rather, because of the  $x$ -independence of the Beltrami vector field,



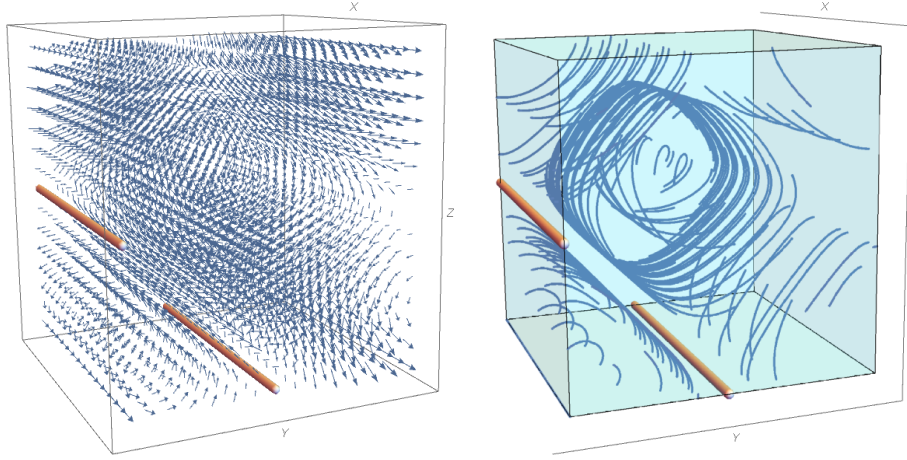


Figure 19: A plot of the *Betrami* vector field  $\mathbf{V}_{(A,A,0)}(\mathbf{r})$  (on the left) where are visible (fat lines) the two stagnation lines of the flow. On the right a family of streamlines with equally spaced initial conditions is displayed.

there are two entire stagnation lines explicitly given below:

$$\text{sl}_1 = \left\{ x, \frac{1}{2}, 0 \right\} \quad ; \quad \text{sl}_2 = \left\{ x, 0, \frac{1}{2} \right\} \quad (6.39)$$

Let us finally come to the case of the flow  $(A, 0, 0)$ . The one-dimensional subspace of vectors of the form  $(A, 0, 0, 0, 0, 0)$  is left invariant by a rather big subgroup of the classifying group which is of order 256. We name it  $G_{256}^{(A,0,0)}$  and its description is given in appendix E of [1]. It is a solvable group with a chain of normal subgroups of index 2 which ends into a subgroup of order 16 isomorphic to  $\mathbb{Z}_4 \times \mathbb{Z}_4$ . This information is summarized in the equation below:

$$\begin{array}{l} \mathbb{Z}_4 \times \mathbb{Z}_4 \sim G_{16}^{(A,0,0)} \triangleleft G_{32}^{(A,0,0)} \triangleleft G_{64}^{(A,0,0)} \triangleleft \circ \\ \mathbb{Z}_4 \sim G_4^{(A,B,0)} \triangleleft G_8^{(A,B,0)} \triangleleft G_{16}^{(A,B,0)} \triangleleft G_{32}^{(A,B,0)} \triangleleft G_{64}^{(A,B,0)} \subset \circ \end{array} \quad \begin{array}{l} \circ \\ \circ \end{array} \quad \begin{array}{l} G_{128}^{(A,0,0)} \triangleleft G_{256}^{(A,0,0)} \\ G_{128}^{(A,0,0)} \triangleleft G_{256}^{(A,0,0)} \end{array} \quad (6.40)$$

The group  $G_{256}^{(A,0,0)}$  leaves the subspace  $(A, 0, 0, 0, 0, 0)$  invariant but occasionally changes the sign of  $A$ . The subgroup  $G_{128}^{(A,0,0)} \subset G_{256}^{(A,0,0)}$  stabilizes the very vector  $(A, 0, 0, 0, 0, 0)$  and therefore it is the hidden symmetry

of the  $(A, 0, 0)$  flows encoded in the planar vector field:

$$\mathbf{V}^{(A,0,0)}(\mathbf{r}) = \mathbf{V}^{(A,0,0)}(x, y, z) \equiv A \begin{pmatrix} \cos(2\pi z) \\ -\sin(2\pi z) \\ 0 \end{pmatrix} \quad (6.41)$$

Looking back at equation (6.40) it is important to note that the group  $G_{128}^{(A,0,0)} \neq G_{128}^{(A,B,0)}$  is different from the homologous group appearing in the group-chain of the  $(A, B, 0)$ -flows. So once again the  $(A, 0, 0)$ -flows cannot be regarded as particular cases of the  $(A, B, 0)$ -flows. Yet the group  $G_{128}^{(A,0,0)}$  contains the entire chain of normal subgroups  $G_{128}^{(A,B,0)}$  starting from  $G_{64}^{(A,B,0)}$ . There is however a very relevant proviso  $G_{64}^{(A,B,0)}$  is a subgroup of  $G_{128}^{(A,0,0)}$  but it is not normal. In fig. 20 we show a plot of the vector field  $\mathbf{V}^{(A,0,0)}(\mathbf{r})$  and a family

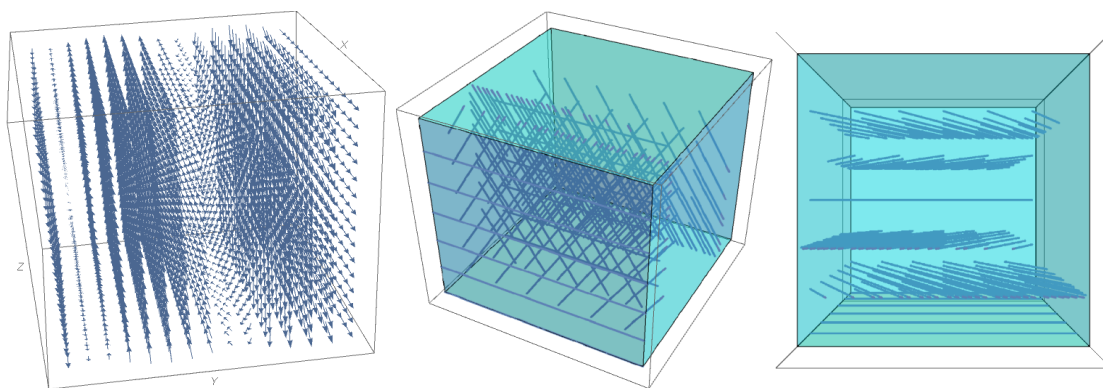


Figure 20: A plot of the Beltrami vector field  $\mathbf{V}^{(A,0,0)}(\mathbf{r})$  (on the left). On the right a family of streamlines with equally spaced initial conditions is displayed. The planar structure of the streamlines, that are all straight lines, is quite visible. In the center a standard viewpoint shot of the streamlines, on the right a view from above.

of its streamlines.

## 6.4 Temporary Conclusion

Comparing the group theoretical analysis of the ABC models with  $b$ -deformations of the simple considered type it becomes obvious that there is a link between the symmetry group of a Beltrami-flow and the surfaces  $\Sigma$  that can be utilized to introduce a  $b$ -deformed manifold able to host the  $b$ -deformation of that Beltrami-flow. At the moment the precise relation between the boundary surface  $\Sigma$  and the symmetry group is by no means clear yet it is evident that it exists and it should be explored. Such exploration requires a study of the possible  $b$ -deformations in the Beltrami flows associated with higher point group orbits in the momentum lattice. It is obviously a research direction that should be pursued. Indeed all other Beltrami flows arising from different instances of the 48 classes of momentum vectors have similar structures. The result of the construction algorithm produces a representation of the Universal Classifying Group that can be either reducible or irreducible. This latter can be split into irreps of either  $G_{192}$  or  $GF_{192}$  and apparently all cases of invariant Beltrami vector fields have invariance groups that are subgroups of one of the two groups  $G_{192}$  or  $GF_{192}$ . It would be interesting to transform this observation into a theorem. At the moment we have not found an

obvious proof.

### 6.4.1 A look at the streamlines of the $b$ -deformed $AB0$ -model

In order to see what the  $b$ -deformations might be good for, we consider plotting the  $\mathfrak{b}$ -deformed field and some of its trajectories. For the sake of possible applications it is much better to work on compact spaces rather than on non compact  $\mathbb{R}^3$ , preserving the periodicity. As it was already remarked in [3] as equation of the boundary, instead of  $x = 0$ , one can choose  $\sin[2\pi x] = 0$ . So instead of eq.s (6.6,6.7), we get

$$\partial_x \longrightarrow \sin[2\pi x] \partial_x \quad (6.42)$$

and:

$$\begin{aligned} {}^{\mathfrak{b}}\mathbf{V}_{ABC} = & (2A \cos[2\pi y] + 2B \cos[2\pi z]) \sin[2\pi x] \partial_x \\ & (2C \cos[2\pi x] - 2B \sin[2\pi z]) \partial_y + (2A \sin[2\pi y] - 2C \sin[2\pi x]) \partial_z \end{aligned} \quad (6.43)$$

and all the other formulae in section 6.1.2 hold true upon the substitution of the denominators  $1/x$  with  $1/\sin[2\pi x]$ . The conclusion remains the same. The  $\mathfrak{b}$ -deformed Beltrami equation holds true if and only if  $C = 0$ . In the next figure 21 we present a picture of  $\mathfrak{b}$ -deformed  $AB0$ -field and family of streamlines with the same parameters  $A = 5, A = 7$  utilized for the un-deformed case in fig. 18.

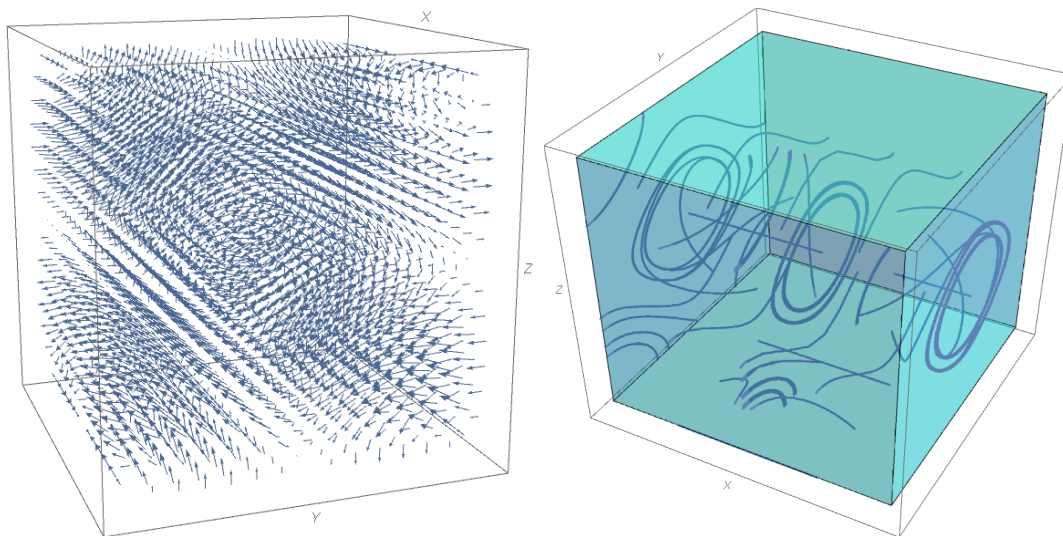


Figure 21: A plot of the Beltrami vector field  ${}^{\mathfrak{b}}\mathbf{V}_{ABC}$  (on the left). On the right a family of streamlines with equally spaced initial conditions is displayed. What it means to be parallel to the boundary becomes clear in this picture: the trajectories that come very close to  $x = 0$  or  $x = 1$  end up swinging on the two faces of the cubic cell.

## 7 The Landscape Conception with Examples

Having clarified the group theoretical foundations of Arnold–Beltrami Flows we come back to the issue of producing exact solutions of the Navier-Stokes equations based on velocity fields that satisfy Beltrami equation. In presence of non-vanishing viscosity we can name such solution **NS-Beltrami generalized steady flows**

### 7.1 Beltrami equation and generalized steady flows

The two pillars on which the solutions we consider reside are provided by the following:

**A)** Implementation of the **generalized steady flow** condition displayed in eq. (2.25)

**B)** Constancy of the Bernoulli hamiltonian function  $H_B$  defined in eq.(2.22)

The pillar B) is easily implemented by setting the pressure field equal to a constant  $h$  minus the squared norm of velocity field:

$$p(\mathbf{x}, t) = h - \frac{1}{2} \| U(\mathbf{x}, t) \|^2 = h - \text{const} \times \frac{\Omega^{[U]} \wedge \star_g \Omega^{[U]}}{\text{Vol}} \quad (7.1)$$

where

$$\text{Vol} \equiv \frac{1}{3!} \det(g) dx \wedge dy \wedge dz \quad (7.2)$$

is the volume 3-form. If the velocity field satisfies Beltrami equation with eigenvalue  $\mu$

$$\star_g d\Omega^{[U]} = \mu \Omega^{[U]} \quad (7.3)$$

then  $\Omega^{[U]}$  is a **contact form** and we get:

$$\Omega^{[U]} \wedge \star_g \Omega^{[U]} = \frac{1}{\mu} \Omega^{[U]} \wedge d\Omega^{[U]} = \lambda(\mathbf{x}, t) \text{Vol} \quad (7.4)$$

So that the physical pressure field (apart from the additive constant  $h$ ) obtains an inspiring geometrical interpretation: indeed it is the nowhere vanishing function  $\lambda(\mathbf{x}, t)$  mentioned in the definition 3.8 of the Reeb field.

As for pillar A) it is sufficient to recall eq.s (2.27,2.28). The essential point is that, as a consequence of Beltrami equation, the contact one-form  $\Omega^{[U]}$ , whose normalized Reeb field is just the velocity field  $U(\mathbf{x}, t)$ , is an eigenstate of the Laplace-Beltrami operator  $\Delta$  with eigenvalue  $\mu^2$

$$\Delta \Omega^{[U]} = \mu^2 \Omega^{[U]} \quad (7.5)$$

Then the implementation of the generalized steady flow condition goes as follows. Consider the finite dimensional vector space provided by the eigenspace pertaining to the eigenvalue  $\mu$ :

$$\mathbf{V}_\mu \ni \Omega^{[u]} \Rightarrow \star_g d\Omega^{[u]} = \mu \Omega^{[u]} \quad ; \quad \Omega^{[u]} = \sum_{i=1}^{N_\mu} F_i \Omega^{[u_i]} \quad (7.6)$$

where  $u_i(\mathbf{x})$  are the normalized Reeb fields of a basis of solutions  $\Omega^{[u_i]}$  and  $F_i$  the free parameters spanning the eigenspace  $\mathbf{V}_\mu$ . The number  $N_\mu$  is the degeneracy of the eigenvalue  $\mu$  namely the dimension of the eigenspace.

Next subdivide the  $\mathbf{V}_\mu$  in two freely chosen subspaces:

$$\mathbf{V}_\mu = \mathbf{V}_\mu^0 \oplus \mathbf{V}_\mu^t \quad ; \quad \dim \mathbf{V}_\mu^0 = M_0 < N_\mu \quad ; \quad \dim \mathbf{V}_\mu^t = N_\mu - M_0 \quad (7.7)$$

Correspondingly the contact form  $\Omega^{[u]}$  and its normalized Reeb field  $u(\mathbf{x})$  will split in two parts:

$$\Omega^{[u]} = \Omega^{[u^0]} + \Omega^{[u^t]} \quad ; \quad \Omega^{[u^0]} \in \mathbf{V}_\mu^0 \quad ; \quad \Omega^{[u^t]} \in \mathbf{V}_\mu^t \quad (7.8)$$

Then setting the driving force as follows:

$$\mathbf{f} = -\nu \mu \Omega^{[u^0]} \quad (7.9)$$

and the contact form (Reeb field) as follows

$$\Omega^{[U]} = \Omega^{[u^0]} + \exp[-\mu^2 t] \Omega^{[u^t]} \quad (7.10)$$

the generalized steady flow condition (2.25) is satisfied and the velocity field

$$U(\mathbf{x}, t) = u^0(\mathbf{x}) + \exp[-\mu^2 t] u^t(\mathbf{x}) \quad (7.11)$$

fulfils the Navier-Stokes equation (2.1).

## 7.2 The landscape conception

It follows from the above discussion that the main issue in order to construct the NS-Beltrami generalized steady flows is the construction of the eigenspaces  $\mathbf{V}_\mu$  and their organization in subspaces according with symmetry principles. This is what leads to the *landscape conception*.

When the manifold  $\mathcal{M}_3$  is the torus defined by eq.(2.3), the construction of the eigenspace  $\mathbf{V}_\mu$  can be performed geometrically, relying on the algorithm explained in section 4.4 and on the orbits of the point group  $\mathfrak{P}_\Lambda$  in the momentum lattice  $\Lambda^*$ . We just need to consider all those orbits for which the squared norm of the momentum vectors  $\mathbf{k}$  is the same. Geometrically this amounts to consider the spherical layers of radius  $r = \sqrt{\mathbf{k}^2}$  defined in section 4.3. This solution of Beltrami equation constitutes a reducible representation of the Universal Classifying Group  $\mathfrak{U}\mathfrak{G}_\Lambda$  of dimension  $N_{\mathbf{k}^2}$

$$\mathrm{SL}_{\mathbf{k}^2} \xrightarrow{\text{Beltrami field}} D[\mathfrak{U}\mathfrak{G}_\Lambda, N_{\mathbf{k}^2}] \quad (7.12)$$

which can be decomposed into irreps

$$D[\mathfrak{U}\mathfrak{G}_\Lambda, N_{\mathbf{k}^2}] = \bigoplus_{i=1}^{\mathfrak{r}} a_i D_i[\mathfrak{U}\mathfrak{G}_\Lambda, n_i] \quad ; \quad \sum_i a_i n_i = N_{\mathbf{k}^2} \quad (7.13)$$

having denoted by  $\mathfrak{r}$  the number of conjugacy classes and hence of irreps of  $\mathfrak{U}\mathfrak{G}_\Lambda$ , by  $n_i$  the dimension of the  $i$ -th irrep and by  $a_i$  its multiplicity. Since  $N_{\mathbf{k}^2} \rightarrow \infty$  when  $\mathbf{k}^2 \rightarrow \infty$  it is obvious that enlarging the landscape the same representations will reappear again and again with increasing multiplicity.

The essential thing is that the Beltrami and anti-Beltrami solutions associated with the same layer decompose exactly in the same way with respect to the Universal Classifying Group  $\mathfrak{U}\mathfrak{G}_\Lambda$ .

The **AlmafluidaNSPsystem** posted in Wolfram Community and available from that site is finalized to:

a) to the construction of a large landscape

- b) to the construction of the Beltrami solution on each chosen spherical layer of that landscape
- c) to the group theoretical analysis of the corresponding representation  $D [\mathfrak{UG}_\Lambda, N_{\mathbf{k}^2}]$  including its further decomposition with respect to subgroups of  $\mathfrak{UG}_\Lambda$ .

### 7.3 Sketches of the cubic and hexagonal landscapes

In this section we flash through a pair of inspiring examples from both instances of main lattice families, the cubic and hexagonal ones.

#### 7.3.1 The cubic landscape

Utilizing the background MATHEMATICA code **UniClasGroupCubicLat** of the **AlmafluidaNSPsystem**, we have constructed a rather large portion of the self-dual cubic lattice  $\Lambda_{cubic}$  containing 117649 lattice points. In this portion of the lattice we found 1057 spherical layers that we analyzed with our computer code. In this way we found a maximally large representation of dimension 792 residing on the largest radius sphere hosted by this lattice region:

$$\text{MaxDim} = \dim D [G_{1536}, 792] = 792 \quad \Leftrightarrow \quad |\mathbf{k}|^2 = 689 \quad (7.14)$$

#### 7.3.2 An example of Chaos from symmetry from the cubic lattice

As an illustration of the Beltrami construction we considered the Beltrami fields associated with a specific layer namely that one where:

$$|\mathbf{k}|^2 = 576 \quad (7.15)$$

We find that the number of points on this layer is 30 that arrange themselves in a point group orbit  $\mathcal{O}_6$  of length 6 plus another one  $\mathcal{O}_{24}$  of length 24. The Beltrami solution corresponding to this layer has therefore eigenvalue  $\mu = 24\pi$  and the reducible representation of the Universal Classifying Group is found to decompose into irreps as follows:

$$D [G_{1536}, 30] = D_1 [G_{1536}, 1] + D_2 [G_{1536}, 1] + 2D_5 [G_{1536}, 2] + 4D_7 [G_{1536}, 3] + 4D_8 [G_{1536}, 3] \quad (7.16)$$

As one sees the considered layer contains one singlet of the maximal possible symmetry group. It is interesting to visualize both the plot of this vector field and some of its trajectories. In fig.22 Next we show the example of just one trajectory and of 27 equally spaced streamlines of this symmetric vector field that we have followed for 50 iterations of numerical integrations. The plots are displayed in fig.23

#### 7.3.3 The hexagonal landscape

As for the hexagonal lattice we have so far constructed a landscape portion portion of the infinite momentum lattice that is shaped as a polyhedron with an hexagonal basis and it is displayed fig.24. This landscape contains 33084 *interior points* and 3888 *points on its boundary*. This distinction has no intrinsic meaning and it simply corresponds to the geometrical shape of the considered lattice portion. We have intersected this polyhedron shaped portion of the lattice with spheres and we have found 544 spherical layers.

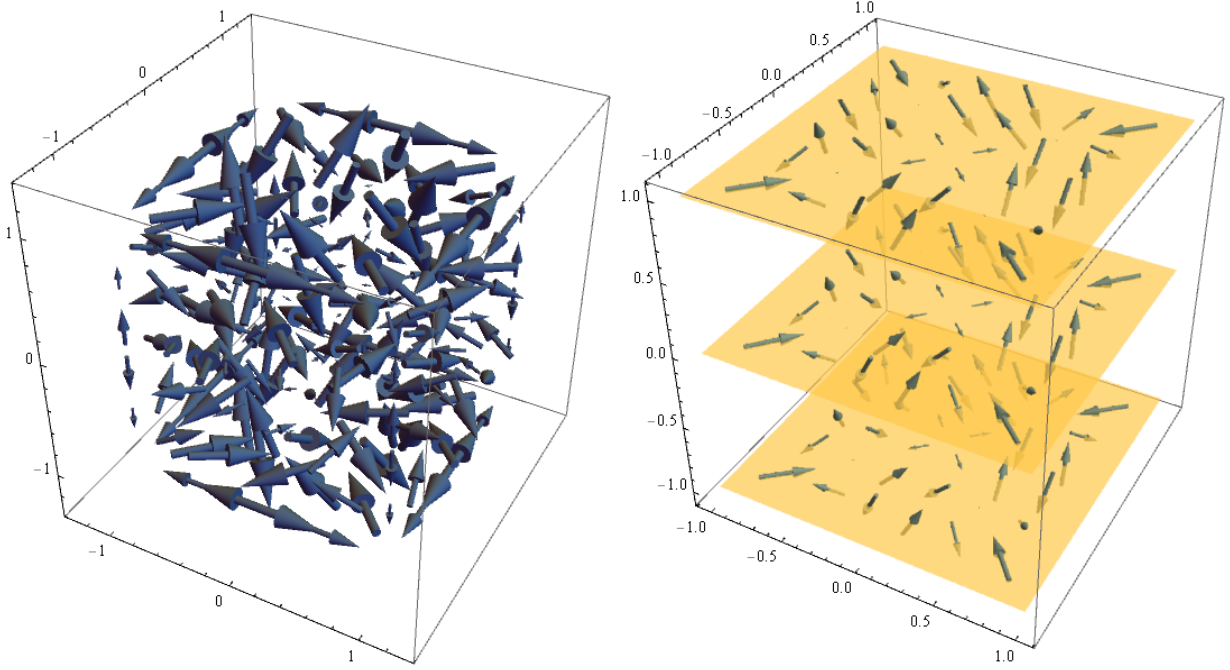


Figure 22: In this figure we show the three dimensional vector plot of the unique Beltrami vector field invariant under the largest symmetry group  $G_{1536}$  that arises in the eigenspace pertaining to the Beltrami eigenvalue  $\mu = 24$  namely on the spherical layer  $\mathbf{k}^2 = 576$ . The high symmetry of the vector field is almost evident at eye-sight.

#### 7.4 An example of chaos from symmetry in the hexagonal landscape

Among the records of this landscape we have considered the spherical layer defined by:

$$\mathbf{k}^2 = \frac{128}{3} \quad (7.17)$$

which contains 90 lattice point. These 90 lattice points intercepted by the sphere of radius  $\sqrt{\frac{128}{3}}$  are organized in the following orbits of the point group  $\text{Dih}_6$ :

$$\begin{aligned} \mathbb{S}_{r^2=\frac{128}{3}} \cap \Lambda_{hexag}^* &= O_1(\{6, 1\}) + O_2(\{12, 3\}) + O_3(\{12, 2\}) + O_4(\{12, 2\}) \\ &+ O_5(\{12, 2\}) + O_6(\{12, 2\}) + O_7(\{12, 2\}) + O_8(\{12, 2\}) \end{aligned} \quad (7.18)$$

and yield a  $90 \times 90$ -dimensional representation of the Universal Classifying Group  $\mathfrak{U}_{72}$  which admits the following decomposition into irreps:

$$\begin{aligned} D[\mathfrak{U}_{72}, 90] &= 2D_1(\mathfrak{U}_{72}, 1) + 2D_3(\mathfrak{U}_{72}, 1) + 3D_5(\mathfrak{U}_{72}, 1) + 3D_7(\mathfrak{U}_{72}, 1) + 5D_{10}(\mathfrak{U}_{72}, 2) \\ &+ 5D_{11}(\mathfrak{U}_{72}, 2) + 5D_{13}(\mathfrak{U}_{72}, 2) + 5D_{15}(\mathfrak{U}_{72}, 2) + 5D_{17}(\mathfrak{U}_{72}, 2) \\ &+ 5D_{19}(\mathfrak{U}_{72}, 2) + 5D_{21}(\mathfrak{U}_{72}, 2) + 5D_{24}(\mathfrak{U}_{72}, 2) \end{aligned} \quad (7.19)$$

As one sees from eq.(7.19) the 90-dimensional parameter space contains a 2-dimensional subspace invariant with respect to the full group  $\mathfrak{U}_{72}$ , corresponding to the identity representation. It is interesting to choose such

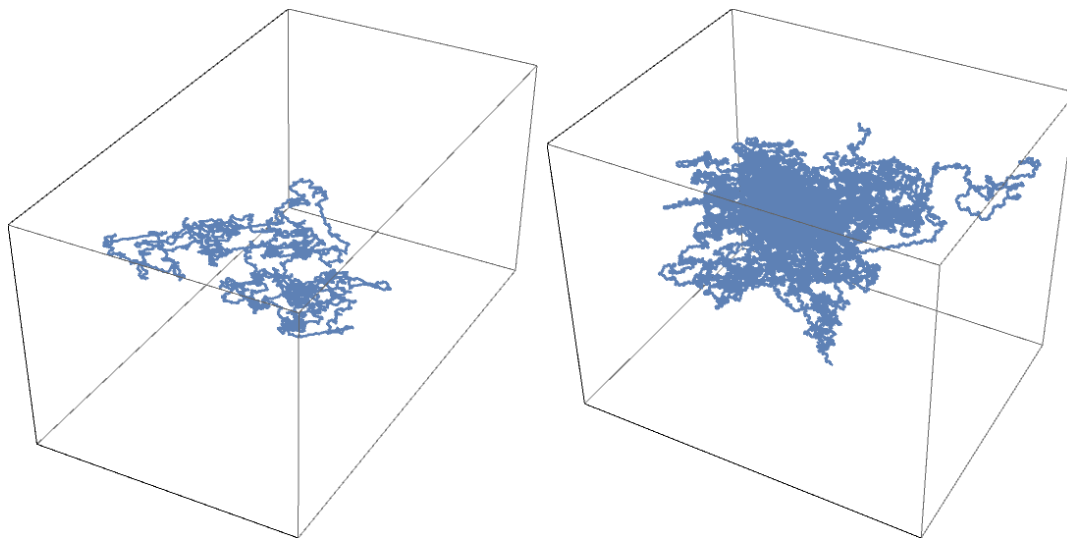


Figure 23: *In the picture on the left we show just one fluid element trajectory starting in a randomly chosen point  $p = \{1/7, 2/9, 5/33\}$ . In the picture on the right we display the plot of 27 streamlines whose starting point are equally spaced over the three dimensions. After 50 integration cycles they make an inextricable pattern. This is the visual manifestation of the contact structure.*

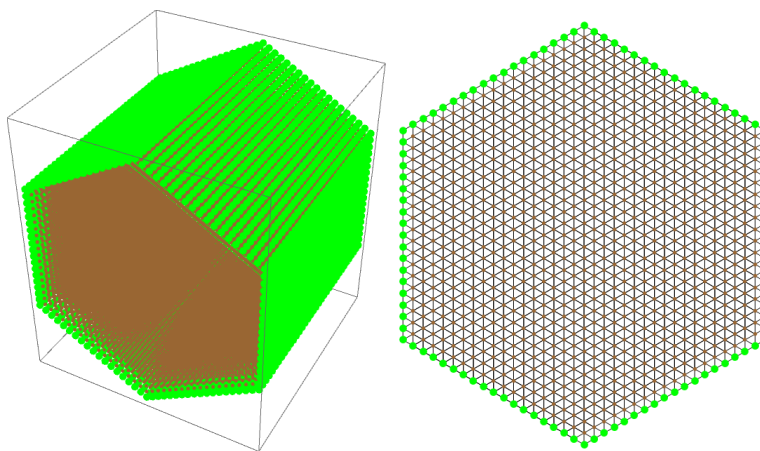


Figure 24: *The portion of considered hexagonal momentum lattice is taken to be a polyhedron with an hexagonal basis that is shown on the right, extended in the  $z$ -direction just as much as it extends in the  $xy$ -plane. The lattice points on the 6 lateral faces of this polyhedron have been displayed in green while the lattice points that are inside the polyhedron have been displayed in brown. There are 3888 points inside the polyhedron and 4800 points on the 6 faces. Note that for visual convenience we have aligned the  $z$ -axis horizontally and the  $y$ -axis vertically.*



an example and consider its properties.

#### 7.4.1 Choice of the $\mathcal{U}_{72}$ invariant subspace

Collecting respectively the coefficients of  $Y_{1,1}$  and  $Y_{1,2}$ , that parameterize the singlet 2-dimensional subspace and using the hexagonal cell coordinates  $u, v, r$  defined by:

$$x = \frac{2u - v}{\sqrt{2}} \quad ; \quad y = \sqrt{\frac{3}{2}}v \quad ; \quad z = \sqrt{2}r \quad (7.20)$$

we obtain two explicit vector fields  $\mathbf{V}^{sing|1,2}(u, v, r)$  of which, due to the massiveness of the formulae, we display only the first, in order to give the reader some feeling of the result structure and quality. Here it is:

$$\begin{aligned} \mathbf{V}_1^{sing|1} = & \frac{1}{8\sqrt{3}} \{ 11 \sin(2\pi(6r + 3u - 7v)) - 28 \sin(2\pi(6r + 4u - 7v)) - 17 \sin(2\pi(6r + 7u - 4v)) \\ & - 17 \sin(2\pi(6r + 7u - 3v)) + 17 \sin(2\pi(6r - 7u + 3v)) - 28 \sin(2\pi(-6r + 4u + 3v)) \\ & - 28 \sin(2\pi(6r + 4u + 3v)) + 17 \sin(2\pi(6r - 7u + 4v)) + 11 \sin(2\pi(-6r + 3u + 4v)) \\ & + 11 \sin(2\pi(6r + 3u + 4v)) + 28 \sin(2\pi(6r - 4u + 7v)) - 11 \sin(2\pi(6r - 3u + 7v)) \\ & - 32 \cos(2\pi(6r + 3u - 7v)) - 16 \cos(2\pi(6r + 4u - 7v)) - 16 \cos(2\pi(6r + 7u - 4v)) \\ & + 16 \cos(2\pi(6r + 7u - 3v)) - 16 \cos(2\pi(6r - 7u + 3v)) - 16 \cos(2\pi(-6r + 4u + 3v)) \\ & + 16 \cos(2\pi(6r + 4u + 3v)) + 16 \cos(2\pi(6r - 7u + 4v)) - 32 \cos(2\pi(-6r + 3u + 4v)) \\ & + 32 \cos(2\pi(6r + 3u + 4v)) + 16 \cos(2\pi(6r - 4u + 7v)) + 32 \cos(2\pi(6r - 3u + 7v)) \} \end{aligned} \quad (7.21)$$

$$\begin{aligned} \mathbf{V}_2^{sing|1} = & \frac{1}{8} ( 15 \sin(2\pi(6r + 3u - 7v)) + 2 \sin(2\pi(6r + 4u - 7v)) + 13 \sin(2\pi(6r + 7u - 4v)) \\ & - 13 \sin(2\pi(6r + 7u - 3v)) + 13 \sin(2\pi(6r - 7u + 3v)) - 2 \sin(2\pi(-6r + 4u + 3v)) \\ & - 2 \sin(2\pi(6r + 4u + 3v)) - 13 \sin(2\pi(6r - 7u + 4v)) \\ & - 15 \sin(2\pi(-6r + 3u + 4v)) - 15 \sin(2\pi(6r + 3u + 4v)) - 2 \sin(2\pi(6r - 4u + 7v)) \\ & - 15 \sin(2\pi(6r - 3u + 7v)) - 16 \cos(2\pi(6r + 4u - 7v)) - 16 \cos(2\pi(6r + 7u - 4v)) \\ & - 16 \cos(2\pi(6r + 7u - 3v)) + 16 \cos(2\pi(6r - 7u + 3v)) + 16 \cos(2\pi(-6r + 4u + 3v)) \\ & - 16 \cos(2\pi(6r + 4u + 3v)) + 16 \cos(2\pi(6r - 7u + 4v)) + 16 \cos(2\pi(6r - 4u + 7v)) \end{aligned} \quad (7.22)$$

$$\begin{aligned}
\mathbf{V}_3^{sing|1} = & \frac{1}{4\sqrt{3}} \{ 11 \sin(2\pi(6r + 3u - 7v)) + 11 \sin(2\pi(6r + 4u - 7v)) + 11 \sin(2\pi(6r + 7u - 4v)) \\
& + 11 \sin(2\pi(6r + 7u - 3v)) + 11 \sin(2\pi(6r - 7u + 3v)) - 11 \sin(2\pi(-6r + 4u + 3v)) \\
& + 11 \sin(2\pi(6r + 4u + 3v)) - 8 \cos(2\pi(6r - 4u + 7v)) + 8 \cos(2\pi(6r - 3u + 7v)) \\
& + 11 \sin(2\pi(6r - 7u + 4v)) - 11 \sin(2\pi(-6r + 3u + 4v)) + 11 \sin(2\pi(6r + 3u + 4v)) \\
& + 11 \sin(2\pi(6r - 4u + 7v)) + 11 \sin(2\pi(6r - 3u + 7v)) + 8 \cos(2\pi(6r + 3u - 7v)) \\
& - 8 \cos(2\pi(6r + 4u - 7v)) + 8 \cos(2\pi(-6r + 4u + 3v)) + 8 \cos(2\pi(6r + 4u + 3v)) \\
& + 8 \cos(2\pi(6r + 7u - 4v)) - 8 \cos(2\pi(6r + 7u - 3v)) - 8 \cos(2\pi(6r - 7u + 3v)) \\
& + 8 \cos(2\pi(6r - 7u + 4v)) - 8 \cos(2\pi(-6r + 3u + 4v)) - 8 \cos(2\pi(6r + 3u + 4v)) \}
\end{aligned} \tag{7.23}$$

In order to perceive what *chaos from symmetry* really means we focus on the above singlet Beltrami vector field and we make a vector plot of it inside the cubic shaped fundamental cell  $u \in [0, 1], v \in [0, 1], r \in [0, 1]$  which can be smoothly mapped into one of the three sectors of the hexagonal cell.

The result for our singlet field is displayed in fig.25.

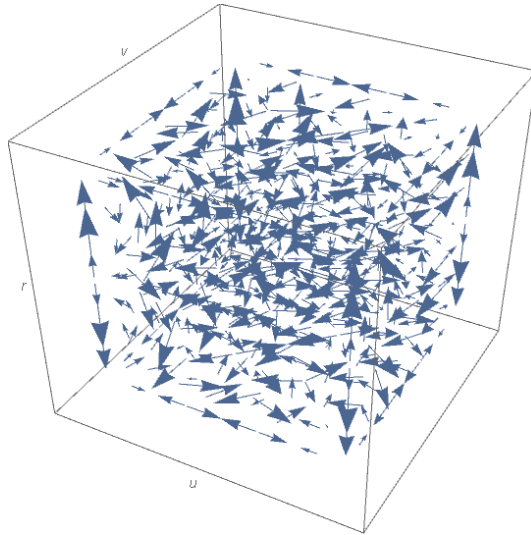


Figure 25: *Plot of the vector field displayed in eq.s (7.21-7.23) which is invariant with respect to the full group  $\mathfrak{A}_{72}$ . The high symmetry of this vector field is visible at eight sight. The pattern repeats itself under rotation and reflections but also under the 1/6 translations in the vertical direction  $r$ .*

Given the high symmetry of the vector plot the capricious chaotic development of the stream-lines follows from the integration of the first order equations. As an exemplification we begin with a single stream line starting at a generic initial point of the hexagonal fundamental cell.

We choose:

$$\{u_0, v_0, r_0\} = \left\{ \frac{2}{7}, \frac{4}{9}, \frac{2}{15} \right\} \tag{7.24}$$

The response elaborated by the computer is the wandering path presented in fig.26.

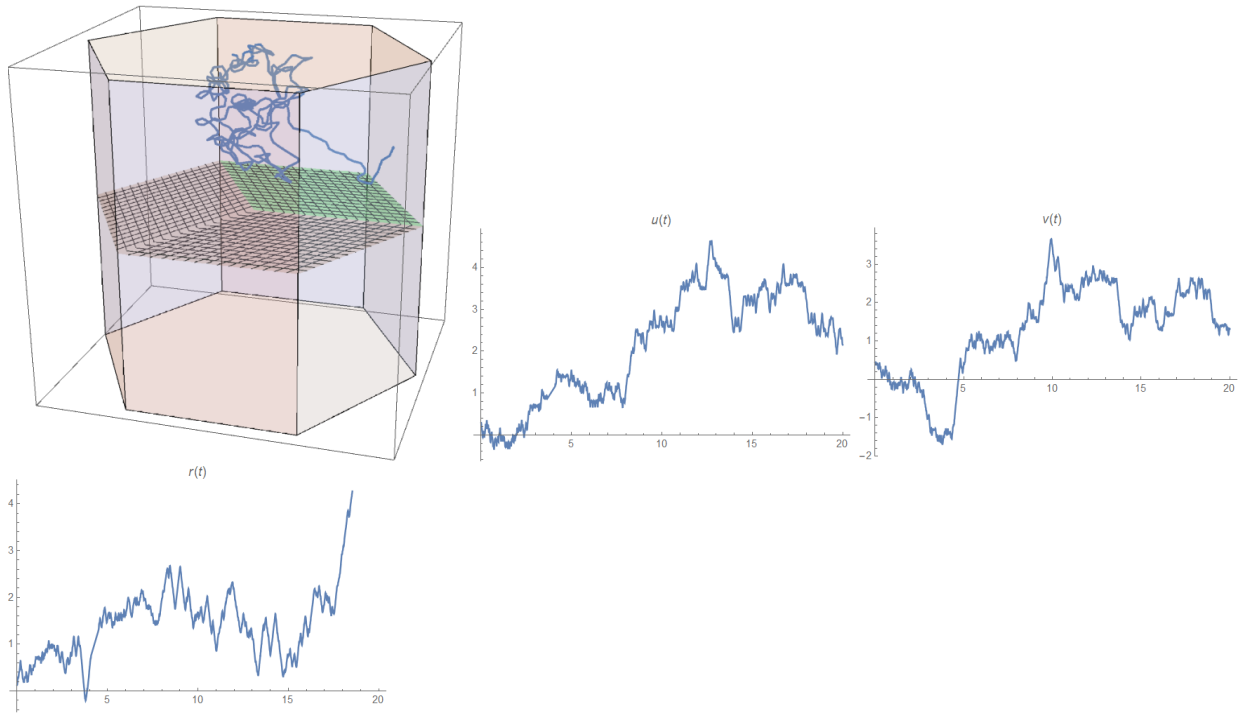


Figure 26: Plot of the single streamline starting at the point (7.24) for the vector field invariant under  $\mathfrak{U}_{72}$  defined in eq.s (7.21-7.23) and displayed in fig. 25. In the first picture we present the three-dimensional path of the fluid element within the hexagonal cell, whose basis is divided in the three sectors, related to each other by a  $2\pi/3$  rotation. In green we have the fundamental sector, image of the square  $u \in [0, 1], v \in [0, 1]$ . The other pictures display the time plots  $u(t), v(t), r(t)$  of the three hexagonal coordinates. The chaotic behavior is fully evident.

Next we proceeded to the calculation of 25 streamlines that have equally spaced starting points in the fundamental planar cell  $u \in [0, 1], v \in [0, 1]$  but after 30 integration steps have already diffused capriciously and chaotically throughout the entire hexagonal cell. The result is what you see in figure 27.

## 7.5 A vertical motion

The main problem one meets in several applications of hydrodynamics is, as we already stressed, that of mixing a chaotic behavior at small scales with an approximate global motion, at larger scales, in one definite direction that we can conventionally assume to be the  $z$ -axis. The superposition is intrinsically forbidden by the non linearity of the NS and Euler equations, yet within the scope of the Beltrami fields and the landscape approach there is a limited superposition freedom: *Beltrami flows having the same eigenvalue parameter  $\lambda$  can be linearly combined*. Hence it is interesting to consider whether in the same spherical layer that contains highly symmetric and hence chaotic flows like that described in the previous section 7.4.1 there are other orbits that provide instead rather orderly flows uniformly directed. The answer is yes and it is also of a general type. All orbits of the point group  $Dih_6$  in the momentum lattice  $\Lambda_{exag}^*$  that are of type  $O(6, 1)$  have the following features:

- a) The orbits is planar at  $z = 0$

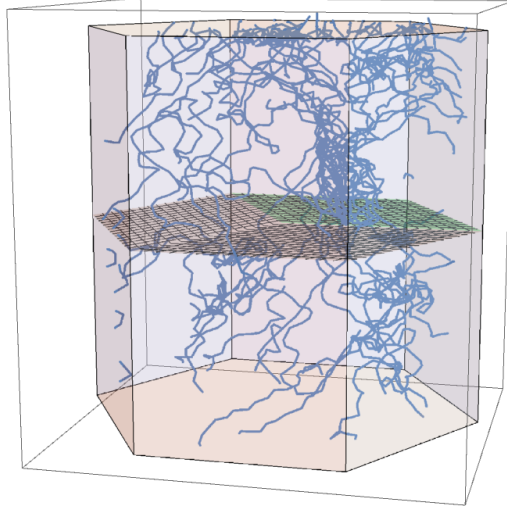


Figure 27: Plot of 25 streamlines, all originating at equally spaced points in the fundamental sector (green parallelogram) of the hexagonal basis for the vector field invariant under  $\mathfrak{U}_{72}$  defined in eq.s (7.21-7.23) and displayed in fig. 25. The chaotic behavior after  $t_{max} = 20$  units of integration time are quite evident.

- b) The Beltrami flow associated with the orbit has a 6 dimensional parameter space that decomposes with respect to the  $\mathfrak{U}_{72}$  group according to the following scheme:

$$D[\mathfrak{U}_{72}, 6] = D_{\alpha}[\mathfrak{U}_{72}, 1] + D_{\beta}[\mathfrak{U}_{72}, 1] + D_{\gamma}[\mathfrak{U}_{72}, 2] + D_{\delta}[\mathfrak{U}_{72}, 2] \quad (7.25)$$

where  $D_{\alpha}, D_{\beta}$  are two different one-dimensional and  $D_{\gamma}, D_{\delta}$  are two different two-dimensional representations.

- c) The restriction of the Beltrami field to the two one-dimensional representations provides an integral model whose streamlines are parallel spirals directed in the  $z$  direction that wind around their central vertical axis with wider or more tight coils.

An example is shown in fig.28

## 8 Conclusions

In the previous sections of the present paper we have outlined and presented the theoretical basis of the mechanism **Chaos from symmetry**, emerging from the use of Beltrami fields as ingredients of exact periodic solutions of the Navier-Stokes equations. When the compact space in which they occur is a three torus, as introduced in eq. (2.3), these exact solutions are governed quite efficiently by Group Theory. This is the fundamental message that is not widely and fully appreciated neither among the differential geometers and dynamical system theorists that give important contributions to the field of mathematical hydrodynamics, nor among the applied scientists doing numerical simulations and working in CFD.

Notwithstanding their long life Navier-Stokes equations have few exact solutions, the existing ones providing already a wide spectrum of qualitatively different behaviors and enucleating the essential point of difficulty that can be summarized as follows.

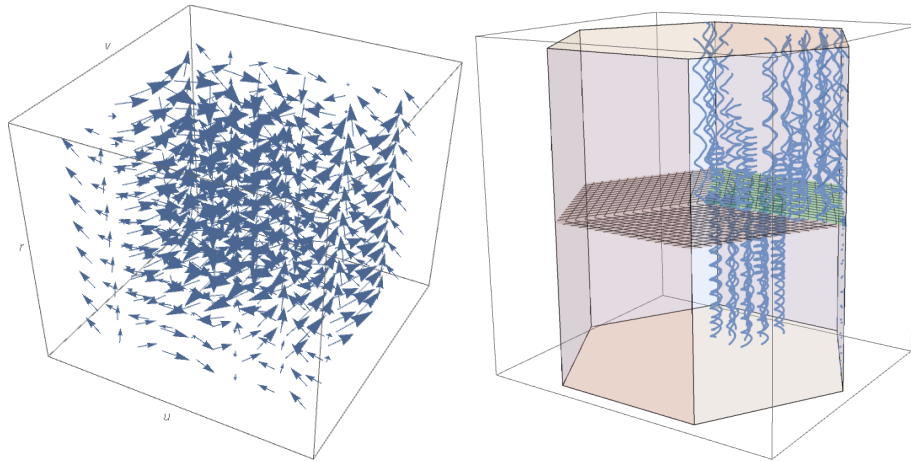


Figure 28: Plot of a Beltrami field from a planar 6 orbit in sided by a plot of 25 of its streamlines, originating from the fundamental planar cell. As one realizes some are uprising spirals, some other descending spirals.

As stressed in the introduction both conceptually and at the level of applications, one would like to consider hydro flows that have at least two scales, a *macro scale* where we observe a directional, reasonably ordered flow and a *micro scale* where the flow is instead chaotic. How to combine the two aspects into exact solutions is the open unsolved problem.

Vladimir Arnold unveiled since the years 70.s of the XXth century the profound topological nature of chaotic behavior [4, 9]. His theorem 2.1 emphasizes the essential role of Beltrami vector fields that are precisely what, after the work of one of us with A.Sorin of 2014-2015 [1], can be precisely classified and constructed in terms of Finite Group Theory. On the other hand Beltrami fields have a natural relation, in the capacity of Reeb fields, with the geometrical conception of *contact structures* on odd-dimensional manifolds. Contact Manifolds in odd-dimensions have symbiotic relations with symplectic manifolds one dimension above and one dimension below and so does their defining contact one-form; all that brings into the field of hydrodynamics the visions and the arguments of differential geometry of symplectic related type. The group-theoretical classification of Beltrami fields therefore reflects into a group-theoretical classification of contact-structures and of their allied even-manifolds. Contact structures are the deep root of chaotic behavior being the geometric obstruction to the existence of a foliation of the ambient manifold  $\mathcal{M}$  in which the fluid moves and foliations being, instead, the essential ingredient of potential or laminar ordered flows.

So the difficulty in reconciling the above mentioned two scale regimes within one and the same exact solution of Navier-Stokes equation is not an occasional one, rather it is a very much conceptual antinomy.

What are the possible strategic way out? Three have emerged that might be combined together:

1. Within the scope of the landscape approach to Beltrami fields one can superimpose motions that look like directional ones on larger scales, although they reveal themselves as winding spirals at smaller scales, with properly chaotic motions at short distances. From the point of view of contact structure Beltrami fields are necessary for chaos yet not viceversa. There are Beltrami fields that give rise to integral systems and coexist on the same spherical layer with really chaos-generating Beltrami fields that typically are the most symmetric ones.
2. Consider the new development of singular contact structures and singular Beltrami fields in so named

$\mathfrak{b}$ -manifolds.

3. Reconsider the results of [2] where it was shown that solutions of Navier Stokes equations display the feature of weakly interacting Beltrami spectra.

As we have shown in the present work the case 2) of the above list that was initiated by the authors of [21, 20, 19, 46, 47, 22, 3, 18] has an unsuspected strong relation with the group theoretical structure of Beltrami fields that requires to be clarified in detail and is potentially very powerful.

Similarly the in depth analysis of the landscape properties in search of algorithmic recipes for the optimal synthesis of over all directional flows with low scale chaotic flows requires appropriate group theoretical investigations and also extensive surveys of the landscape at large. For instance the classification of the 48 momentum classes of the cubic lattice achieved in [1] has not yet been done for the hexagonal lattice. To this effect implementation of the **AlmafluidaNSPsystem** on large powerful computers would be quite appropriate.

That of point 3) is anyhow the master direction to be explored. This was already emphasized in section 4.3, the Beltrami operator is a chiral one and a generic periodic solution of Navier Stokes equations is layer by layer the superposition of a Beltrami and an anti-Beltrami field. This leads to the concept of the Beltrami spectral index. On the other hand the very fact that Beltrami and anti-Beltrami fields have the same group-theoretical structure combined with the fact that the same representations of the Universal Classifying Group reappear on successive layers provides the opportunity of constructing candidate solutions of the Navier Stokes equations in the form of Fourier expansions with prescribed hidden symmetries. Whether the free coefficients can be determined in such a way as to provide exact solutions of the Navier Stokes differential equations is something to be explored. Reversely known exact solutions of the NS equations have to be analyzed from the point of view of hidden symmetries. This is the most promising direction for future work.

## Acknowledgements

The present scientific investigation has been conducted within the framework of the Project *ALMA FLUIDA* partially financed by the Toscana Region as part of the Consultancy Agreement between ITALMATIC Presse e Stampi and the DISAT of Politecnico di Torino. The origin of this investigation is traced back to a previous study of Arnold-Beltrami Flows conducted in 2014-15 by one of us (P.F.), together with his long time collaborator and close friend Alexander Sorin. P.F. would like to express his gratitude to A. Sorin for introducing him to this topic that now finds new life. Last but not least we desire to express our gratitude to our great friend Sauro Additati for envisaging the whole scheme of the project and to the Fredianis, father Adriano and son Roberto, directing ITALMATIC Presse e Stampi, who made this scientific mission not only possible but also very pleasant due to their warm and deep friendship. Last but not least it is a pleasure to express our gratitude to Daniele Marchisio first of all for our amicable relations that we developed during these months since the time when the ALMA FLUIDA project was firstly conceived and constructed together, secondly for his excellent coordination of the Politecnico consultancy still going on.

## References

- [1] P. Fré and A. S. Sorin, “Classification of Arnold-Beltrami flows and their hidden symmetries,” *Phys. Part. Nucl.*, vol. 46, no. 4, pp. 497–632, 2015.
- [2] P. Constantin and A. Majda, “The Beltrami Spectrum for Incompressible Fluids,” *Communications in Mathematical Physics*, vol. 115, p. 864–896, 1988.
- [3] R. Cardona, E. Miranda, and D. Peralta-Salas, “Euler flows and singular geometric structures,” *Philosophical Transactions of the Royal Society A: Mathematical, Physical and Engineering Sciences*, vol. 377, p. 20190034, Sep 2019.
- [4] V. I. Arnold, “Sur la géométrie différentielle des groupes de Lie de dimension infinie et ses applications à l’hydrodynamique des fluides parfaits,” *Ann. Inst. Fourier*, vol. 16, pp. 316–361, 1966.
- [5] S. Childress, “Construction of steady-state hydromagnetic dynamos. i. spatially periodic fields.” Report MF-53, Courant Inst. of Math. Sci., 1967.
- [6] S. Childress, “New solutions of the kinematic dynamo problem,” *J. Math. Phys.*, vol. 11, pp. 3063 – 3076, 1970.
- [7] M. Hénon, “Sur la topologie des lignes de courant dans un cas particulier,” *C. R. Acad. Sci. Paris*, vol. 262, pp. 312 – 314, 1966.
- [8] T. Dombre, U. Frisch, J. Greene, M. Henon, A. Mehr, and A. Soward, “Chaotic streamlines in the abc flows,” *J. Fluid Mech.*, vol. 167, pp. 353 – 391, 1986.
- [9] V. I. Arnold and B. A. Khesin, *Topological Methods in Hydrodynamics*. Springer, 1998.
- [10] O. I. Bogoyavlenskij, “Infinite families of exact periodic solutions to the Navier-Stokes equations,” *Moscow Mathematical Journal*, vol. 3, pp. 1 – 10, 2003.
- [11] O. Bogoyavlenskij and B. Fuchssteiner, “Exact NSE solutions with crystallographic symmetries and no transfer of energy through the spectrum,” *J. Geom. Phys.*, vol. 54, pp. 324 – 338, 2005.
- [12] V. I. Arnold, “On the evolution of a magnetic field under the action of transport and diffusion,” in *VLADIMIR I. ARNOLD: Collected Works, VOLUME II, Hydrodynamics, Bifurcation Theory, and Algebraic Geometry 1965-1972*, Springer-Verlag Berlin Heidelberg, 2014.
- [13] G. E. Marsh, *Force-Free Magnetic Fields: Solutions, Topology and Applications*. World Scientific (Singapore), 1996.
- [14] S. Childress and A. D. Gilbert, *Stretch, twist, fold: the fast dynamo*. Springer-Verlag, 1995.
- [15] S. E. Jones and A. D. Gilbert, “Dynamo action in the ABC flows using symmetries,” *Geophys. Astrophys. Fluid Dyn.*, vol. 108, pp. 83 – 116, 2014.
- [16] J. Etnyre and R. Ghrist, “Contact topology and hydrodynamics: Beltrami fields and the Seifert conjecture,” *Nonlinearity*, vol. 13(2), pp. 441–458, 2000.

- [17] R. Ghrist, “On the contact geometry and topology of ideal fluids,” in *Handbook of Mathematical Fluid Dynamics*, vol. IV, pp. 1 – 38, 2007.
- [18] E. Miranda and C. Oms, “The geometry and topology of contact structures with singularities,” *ArXiv/1806.05638*, 2021.
- [19] R. Cardona and E. Miranda, “On the Volume Elements of a Manifold with Transverse Zeroes,” *Regular and Chaotic Dynamics*, vol. 24, pp. 187 – 197, Mar 2019.
- [20] R. Cardona and E. Miranda, “Integrable systems and closed one forms,” *Journal of Geometry and Physics*, vol. 131, pp. 204–209, Sep 2018.
- [21] V. Guillemin, E. Miranda, and A. R. Pires, “Symplectic and Poisson geometry on b-manifolds,” *Advances in Mathematics*, vol. 264, pp. 864 – 896, Oct 2014.
- [22] J. Pollard and G. P. Alexander, “Singular Contact Geometry and Beltrami Fields in Cholesteric Liquid Crystals,” *ArXiv/1911.10159*, 2019.
- [23] E. Miranda, C. Oms, “The singular Weinstein conjecture”, *ArXiv/2005.09568*, 2020.
- [24] E. Miranda, C. Oms, and D. Peralta-Salas, “On the singular Weinstein conjecture and the existence of escape orbits for b-Beltrami fields,” *Communications in Contemporary Mathematics*, vol. 24, mar 2022.
- [25] P. G. Frè, *Gravity, a Geometrical Course*, vol. Volume 1 and 2. Dordrecht: Springer, 2013.
- [26] R. Cardona, “The topology of Bott integrable fluids,” *ArXiv/2006.16880*, 2020.
- [27] H. Poincaré, “Sur les courbes définies par une équation différentielle,” in *Oeuvres*, vol. 1, 1892.
- [28] I. Bendixson, “Sur les courbes définies par des équations différentielles,” *Acta Mathematica*, vol. 24, pp. 1–88, 1901.
- [29] H. Geiges, “Contact geometry,” *Handbook of Differential Geometry*, 2006.
- [30] C. Wang, “Exact solutions of the unsteady navier-stokes equations,” *Annu. Rev. Fluid. Mech.*, vol. 23, pp. 159–177, 1991.
- [31] F. Englert, “Spontaneous compactification of eleven-dimensional supergravity,” *Physics Letters B*, vol. 119, no. 4-6, pp. 339–342, 1982.
- [32] P. Fré, “Supersymmetric M2-branes with Englert fluxes, and the simple group  $PSL(2, 7)$ ,” *Fortsch. Phys.*, vol. 64, no. 6-7, pp. 425–462, 2016.
- [33] B. L. Cerchiai, P. Fré, and M. Trigiante, “The Role of  $PSL(2, 7)$  in M-theory: M2-Branes, Englert Equation and the Septuples,” *Fortsch. Phys.*, vol. 67, no. 5, p. 1900020, 2019.
- [34] L. Castellani, R. D’Auria, and P. Fré, *Supergravity and superstrings: A Geometric perspective. Vol. 1,2,3*. 1991.
- [35] R. D’Auria and P. Fré, “Universal Bose-Fermi mass-relations in Kaluza-Klein supergravity and harmonic analysis on coset manifolds with Killing spinors,” *Annals of Physics*, vol. 162, no. 2, pp. 372–412, 1985.



- [36] R. D’Auria and P. Fré, “On the fermion mass-spectrum of Kaluza-Klein supergravity,” *Annals of Physics*, vol. 157, no. 1, pp. 1–100, 1984.
- [37] D. Fabbri, P. Fré, L. Gualtieri, and P. Termonia, “M-theory on  $\text{AdS}_4 \times \text{M}^{1,1,1}$ : the complete  $\text{Osp}(2|4) \times \text{SU}(3) \times \text{SU}(2)$  spectrum from harmonic analysis,” *Nuclear Physics B*, vol. 560, no. 1-3, pp. 617–682, 1999. [hep-th/9903036].
- [38] P. Fré, L. Gualtieri, and P. Termonia, “The structure of  $\mathcal{N} = 3$  multiplets in  $\text{AdS}_4$  and the complete  $\text{Osp}(3|4) \times \text{SU}(3)$  spectrum of M-theory on  $\text{AdS}_4 \times \text{N}^{0,1,0}$ ,” *Physics Letters B*, vol. 471, no. 1, pp. 27–38, 1999. [hep-th/9909188].
- [39] L. Gualtieri, *Harmonic analysis and superconformal gauge theories in three dimensions from the AdS/CFT correspondence*. PhD thesis, Department of Physics, University of Torino. Ph. D. thesis e-Print ArXiv: hep-th 0002116.
- [40] V. Arnol’d, Y. Zel’dovich, A. Ruzmaikin, and D. Sokolov, “Magnetic field in a stationary flow with stretching in riemannian space,” *Sov. Phys. 1083, JETP*, vol. 54, pp. 1083–1120, 1981.
- [41] E. Beltrami, “articolo,” in *Opere matematiche*, vol. 4, p. 304, 1889.
- [42] C. Dongho and P. Duboskiy, “Travelling Wave-like solutions of the Navier Stokes and related equations,” *Journal of Mathematical Analysis and Applications*, vol. 204, pp. 930–939, 1996.
- [43] E. Fyodorov, “The symmetry of regular systems of figures,” *Proceedings of the Imperial St. Petersburg Mineralogical Society*, vol. series 2- vol. 28, 1891.
- [44] M. Aroyo, A. Kirov, C. Capillas, J. Perez-Mato, and H. Wondratschek, “Bilbao crystallographic server. ii. representations of crystallographic point groups and space groups,” *Acta Crystallographica Section A: Foundations of Crystallography*, vol. 62, pp. 115 – 128, 2006.
- [45] B. Souvignier, “Group theory applied to crystallography,” 2008. preprint.
- [46] R. Cardona, E. Miranda, D. Peralta-Salas, and F. Presas, “Universality of Euler flows and flexibility of Reeb embeddings,” *ArXiv/1911.01963*, 2020.
- [47] R. Cardona and E. Miranda, “Integrable systems on singular symplectic manifolds: From local to global,” *ArXiv/2007.10314*, 2021.